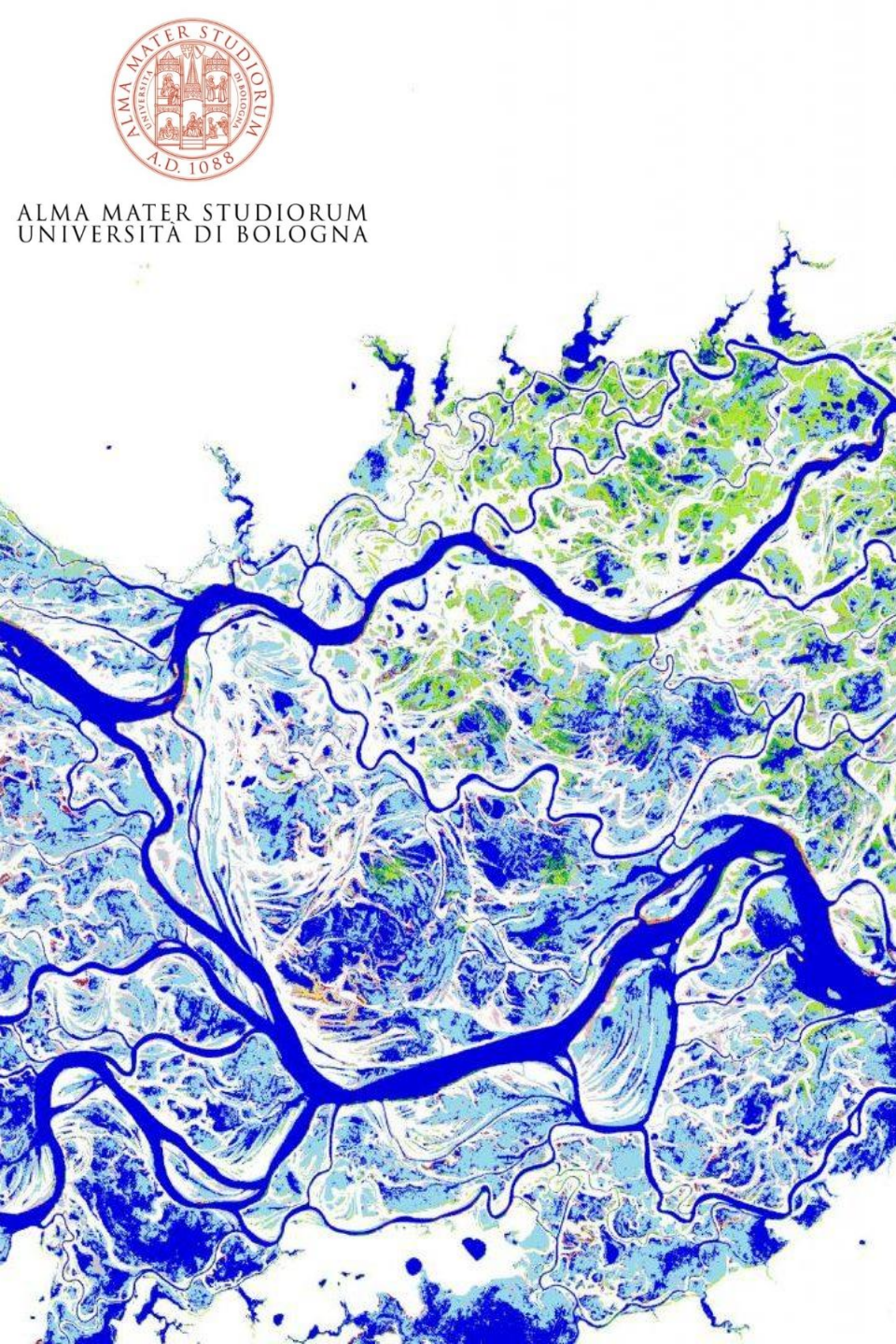


ALMA MATER STUDIORUM  
UNIVERSITÀ DI BOLOGNA

*Doctoral Winter School*  
**DATA RICH HYDROLOGY**  
2019 Edition



# Remote sensing data and tools to foster inland water monitoring and flood modelling

**Alessio Domeneghetti et al. (...many others)**

[alessio.domeneghetti@unibo.it](mailto:alessio.domeneghetti@unibo.it)

**DICAM, University of Bologna, Italy**

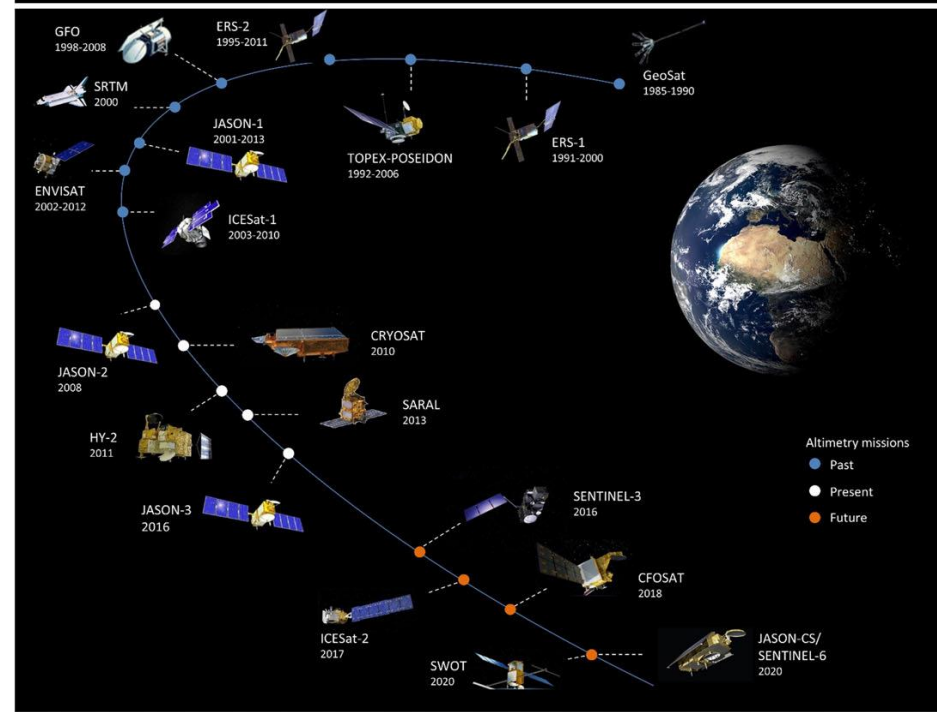
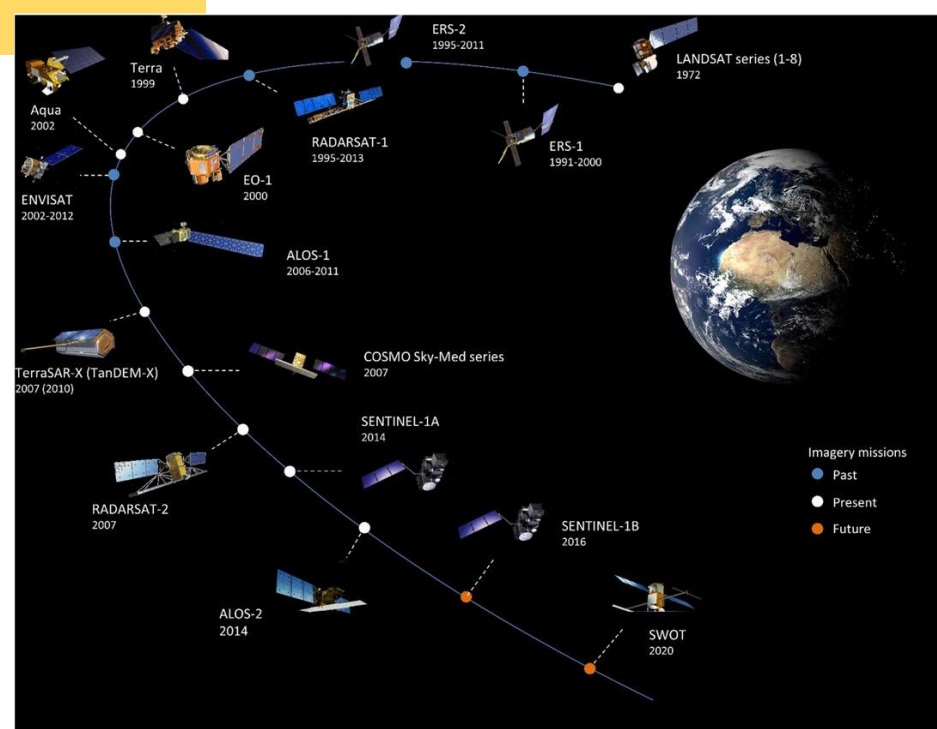
# Remote sensing data and tools to foster...

## → inland water monitoring

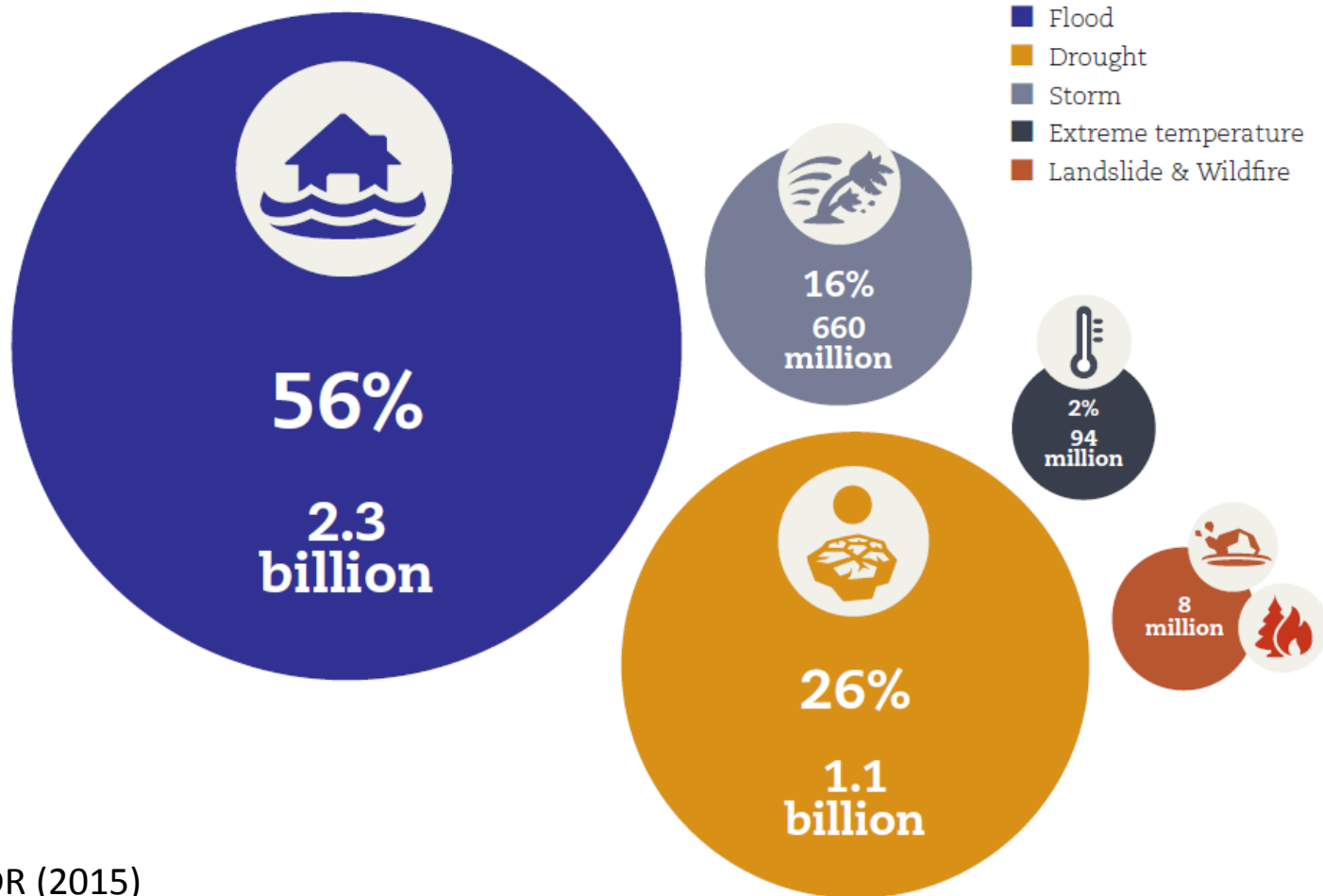
(e.g. satellite altimetry, SWOT)

## → flood modeling

Available data and tools for flood hazard modelling

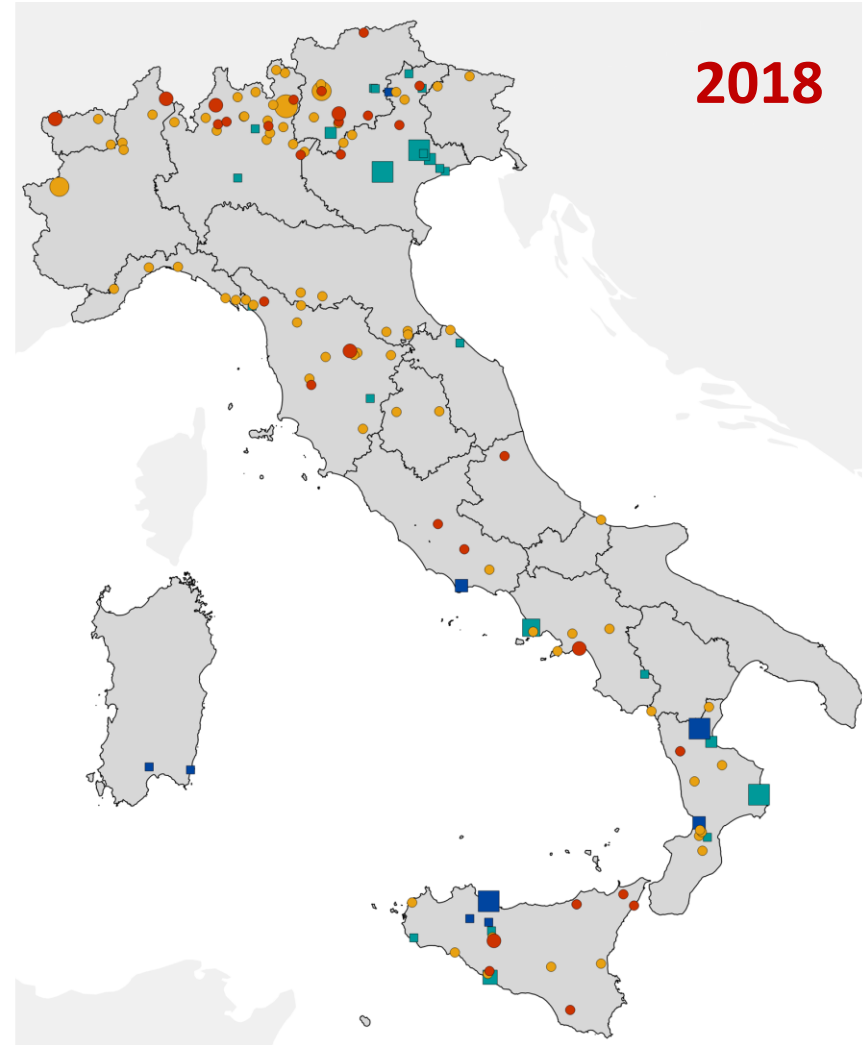
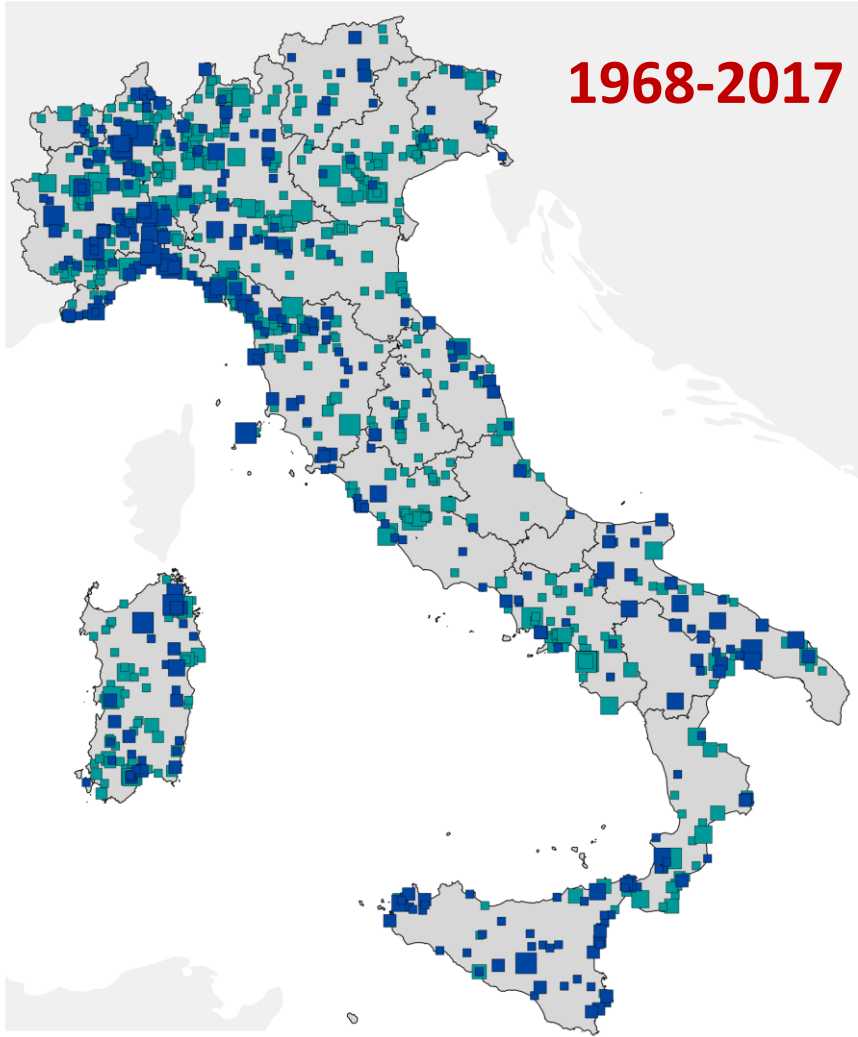


# Number of people affected by weather-related disasters (1995-2015)



UNISDR (2015)  
United Nation Office for Disaster Risk Reduction

# ...in Italy?



Fatality, missing and wounded

Evacuated homeless

- >5
- 4-5
- 2-3
- 1

- >250
- 151-250
- 101-150
- 51-100
- 1-50

**Total number of fatalities due to inundations**

1968-2017 = 592

2018 = 26

Related to landslides

- >5
- 4-5
- 2-3
- 1
- >250
- 151-250
- 101-150
- 51-100
- 1-50



# FLOOD HAZARD MODELING AT DIFFERENT (LARGE) SCALE AND IN POORLY SURVEYED AREAS

## Main challenges

- Monitoring/modeling/predicting floods at the large (regional, continental or global) scale is challenging by nature
- Most hydrodynamic models were not developed for large scale applications
- Boundary data (river data, inflow, water level, floodplain topography, etc.) are lacking in many places or are inaccurate

# Initiatives and concerns for global flood modeling

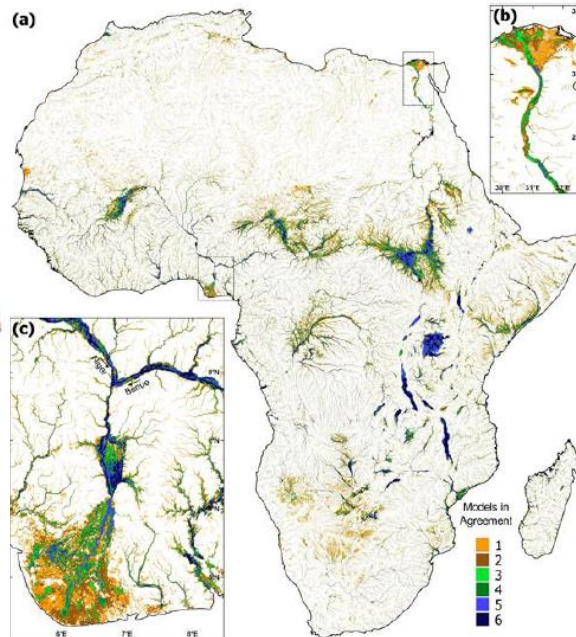
- River network characterization
- Model conditioning (precipitation, river flows, gauged information, etc.)
- Numerical model computationally efficient
- Model calibration and validation
- Topography
- Bathymetry



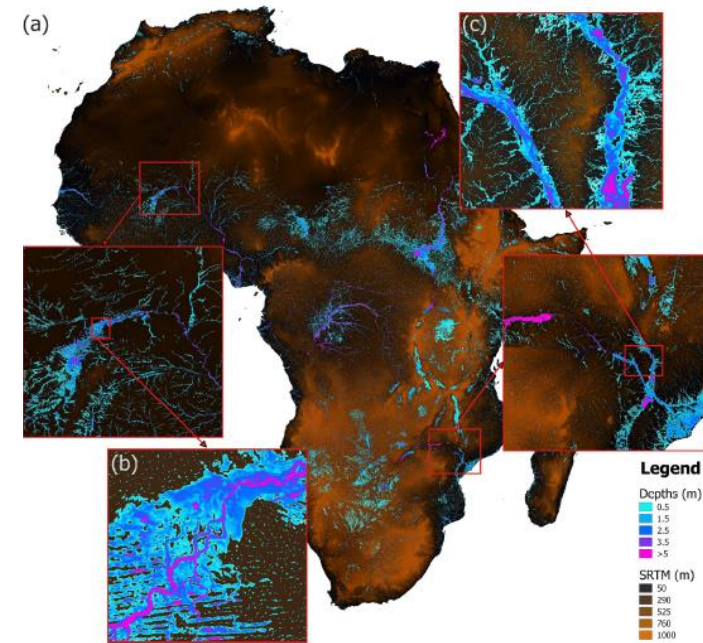
Alfieri et al., 2014 (HP)

Dottori et al., 2016

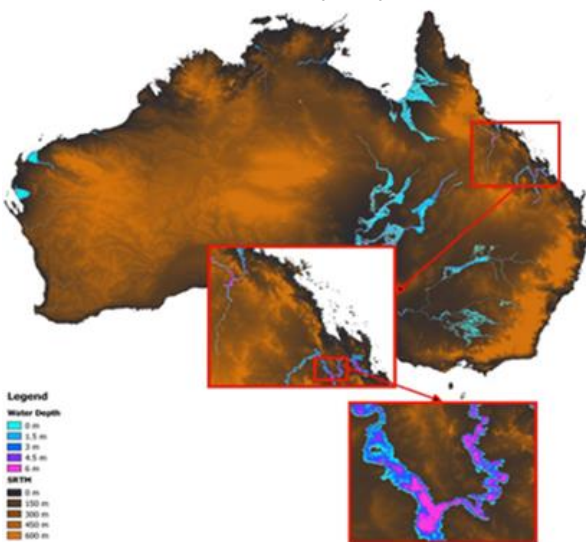
Trigg et al., 2016 (ERL)



Sampson et al., 2015 (WRR)



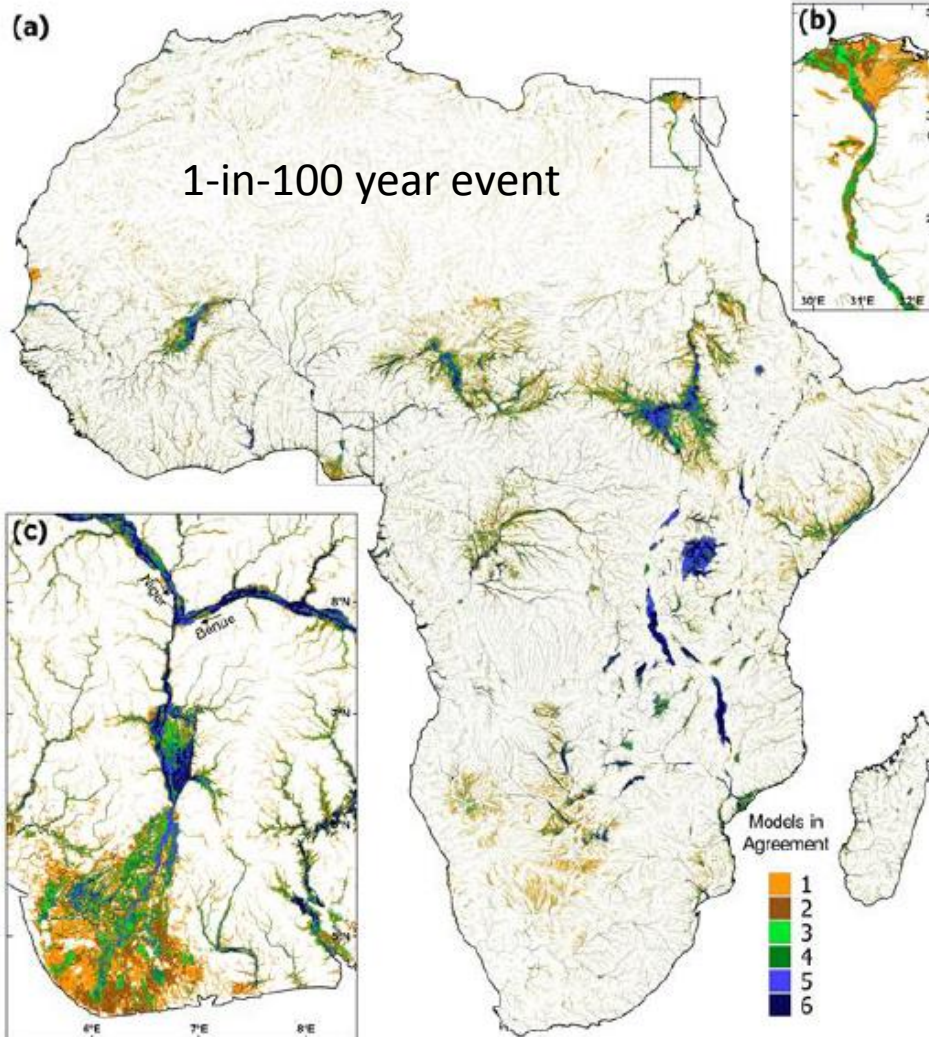
Schumann et al., 2016 (GRL)



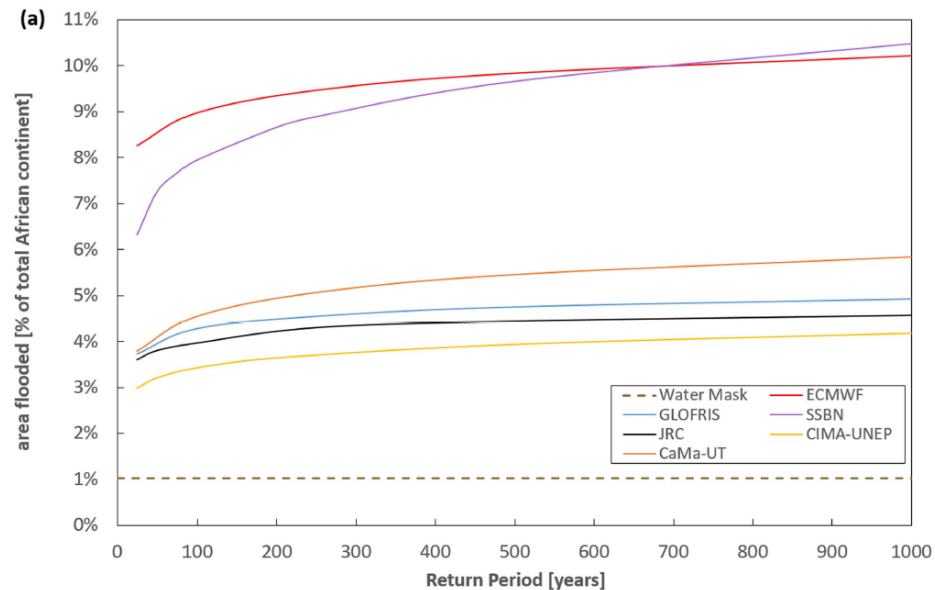
# Initiatives and concerns for global flood modeling

“[...] fluvial (river) flood risk for much of the world is still ‘unmapped’, and even where mapping exists, it often uses different and inconsistent methodologies or datasets across countries and regions.”

Trigg et al., 2016 (ERL)



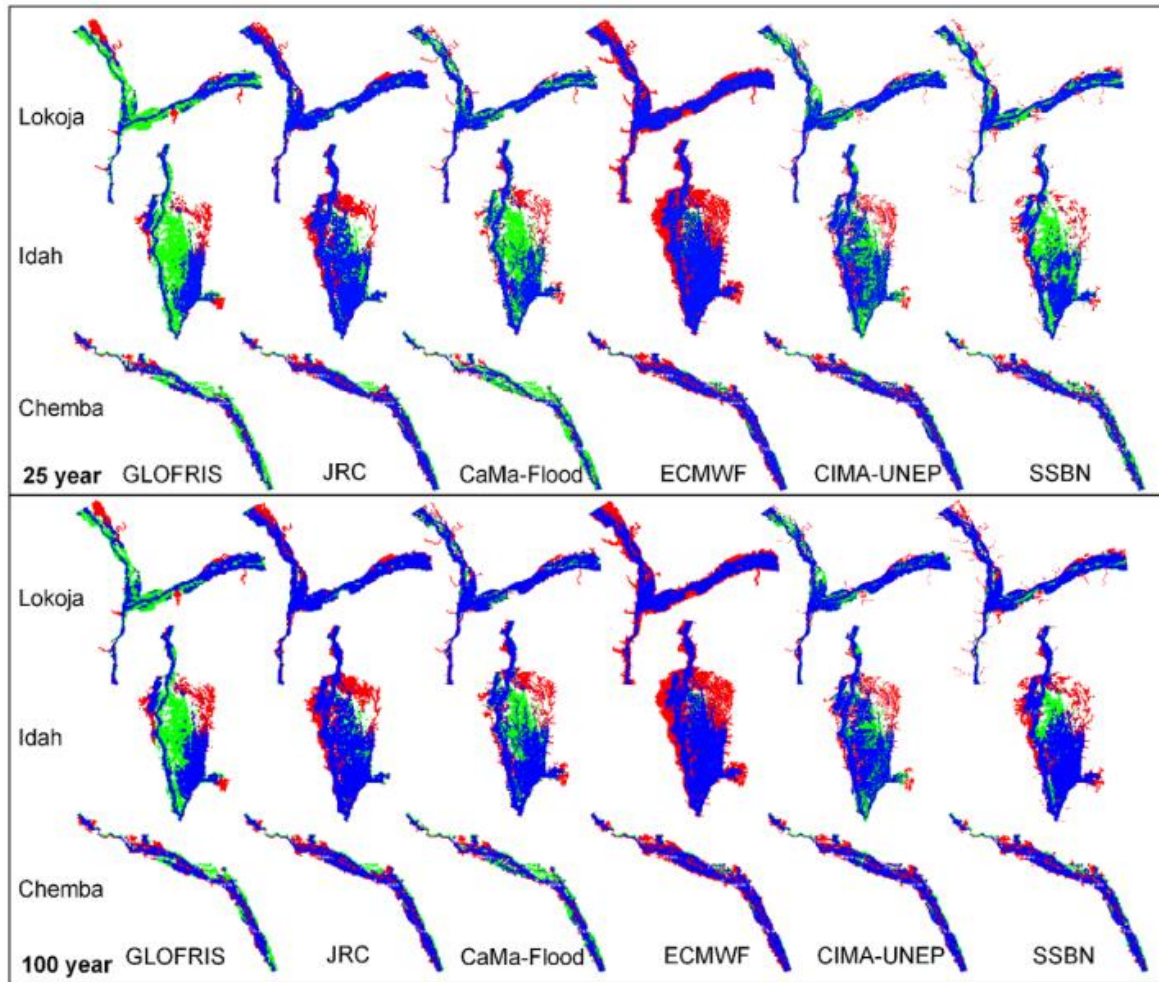
6 models compared in the study were:  
CaMa-Flood, CIMA-UNEP, ECMWF, GLOFRIS, JRC, and SSBN (now Fathom Global).



return periods (25, 100, 250, 500, 1000 y)

Only 30-40% agreement in flood extent

# Initiatives and concerns for global flood modeling



Bernhofen et al., 2018 (ERL)

Events considered for the validation (2) are retrieved from the **Dartmouth Flood Observatory (DFO) archive**. The DFO uses MODIS imagery to capture flood events globally, and stores them online in an open-access Archive (since 2000).

Overlap of individual global flood model extent for return period flows of 25 and 100 years and MODIS observed flood extent



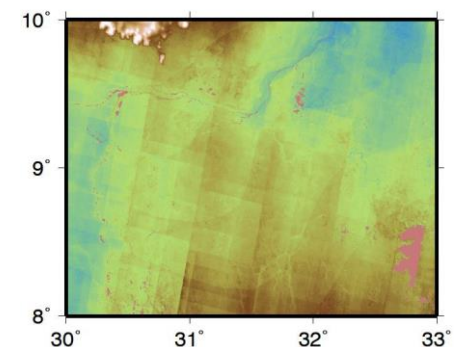
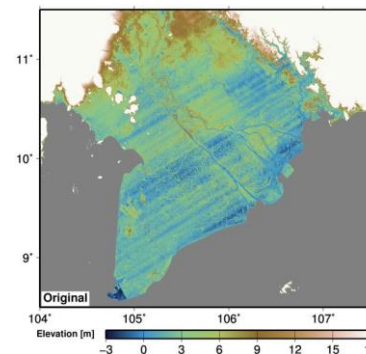
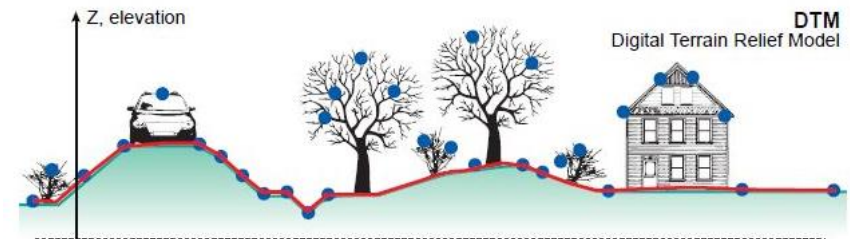
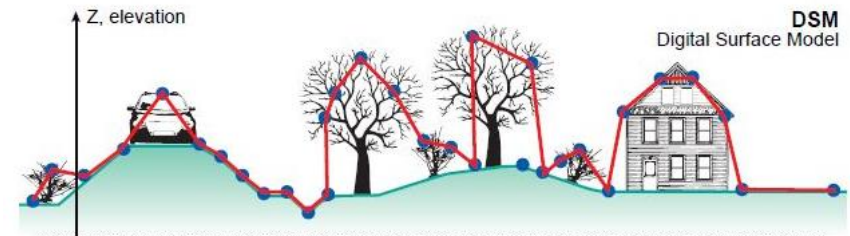
# Global Topography data

Digital Elevation Model (DEM) is a fundamental baseline data for many geosciences analysis (hydrological modeling, flood modeling, land classification, terrain analysis, etc.)

... in most part of the world spaceborne DEM are usually the only source of topographic data

## Error types in spaceborne DEMs

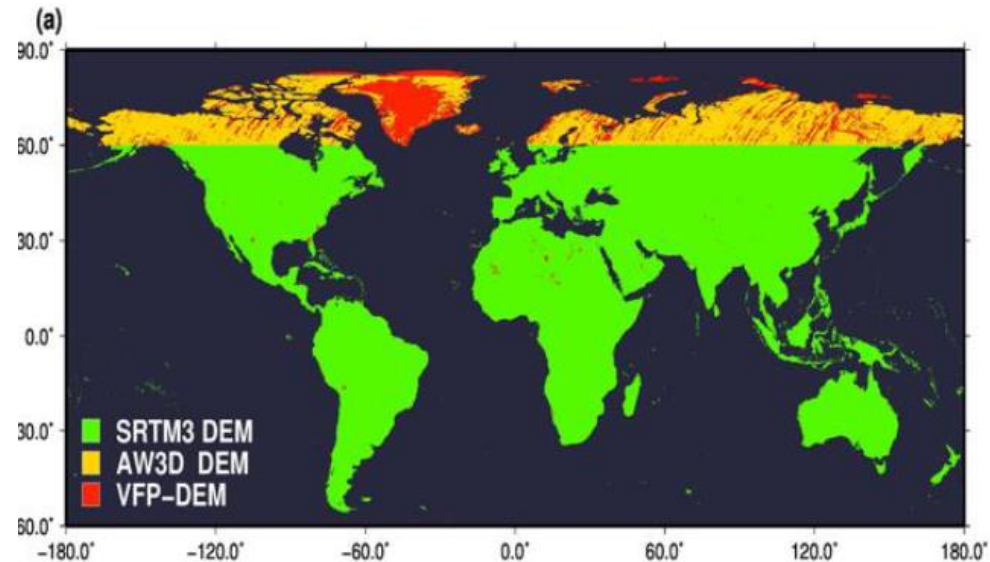
- Vegetation height bias/object bias
- Speckle noise (random noise due terrain reflection)
- Stripe noise (unrealistic terrain undulation)
- Absolute bias (overall shift)



# Global Topography data

## Common Global (semi-Global) DEMs

- **SRTM3 DEM v2.1**  
C-band radar interferometry, 90 m res.  
(Shuttle Radar Topography Mission, 2000)
- **AW3D-30m DEM (above 60N)**  
optical stereoview.
- **Viewfinder Panorama DEM**  
digitized paper map to fill SRTM gap



**Overall vertical error might vary from 4.7 m up to 9 m in different continents [Rodriguez et al., 2006; Beck, 2014; Schumann et al., 2014; Yan et al., 2015].**

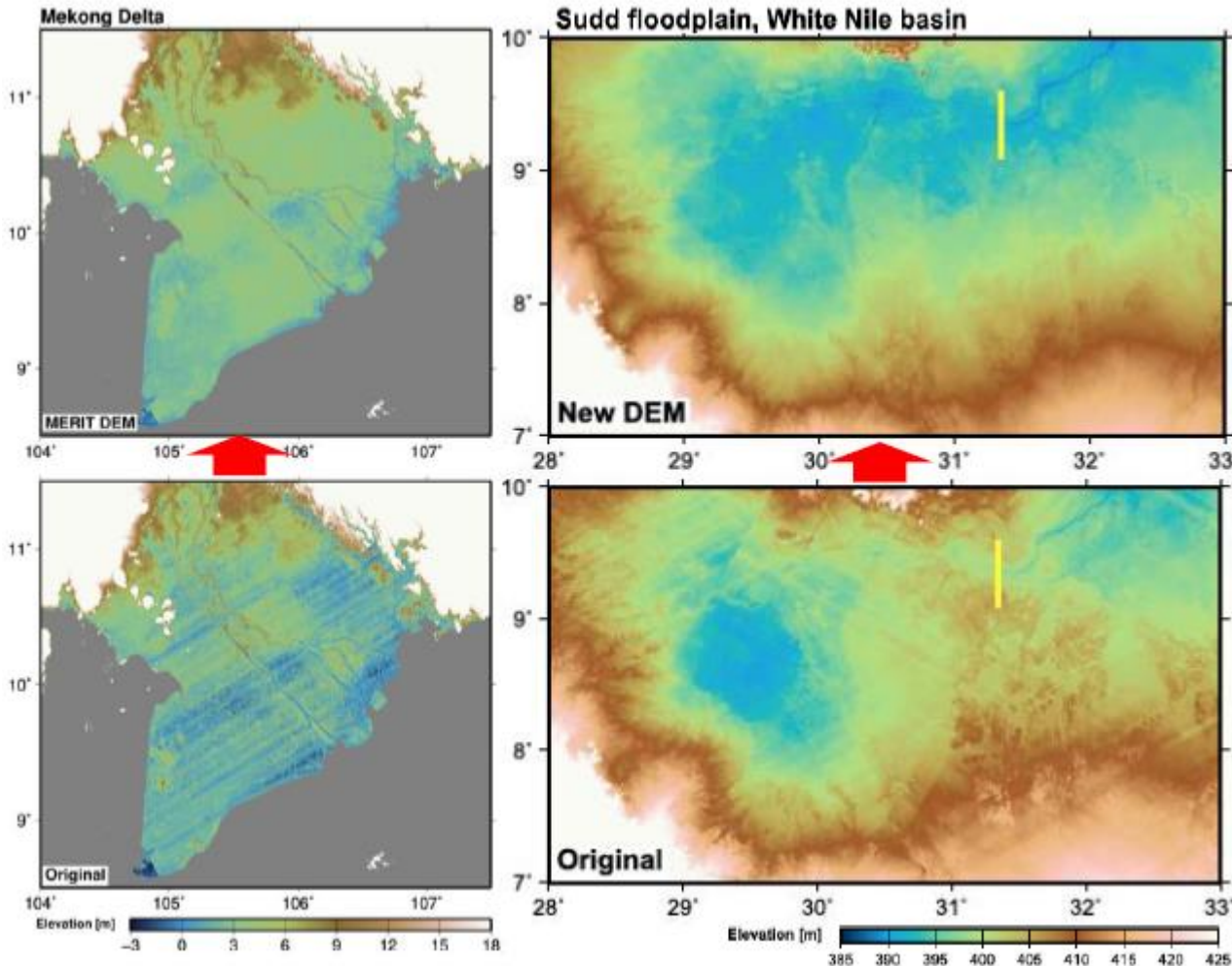
**SRTM DEM**

# Global Topography data



## MERIT DEM (Multi-Error-Removed Improved-Terrain DEM)

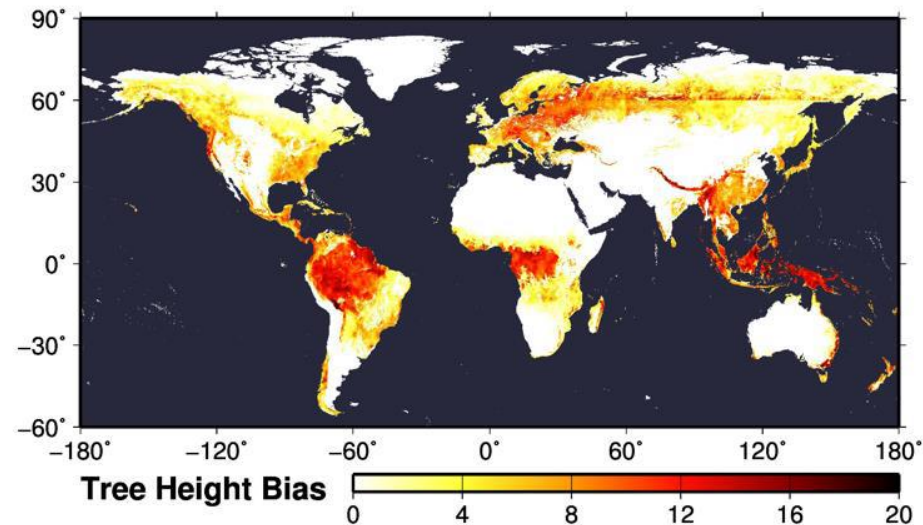
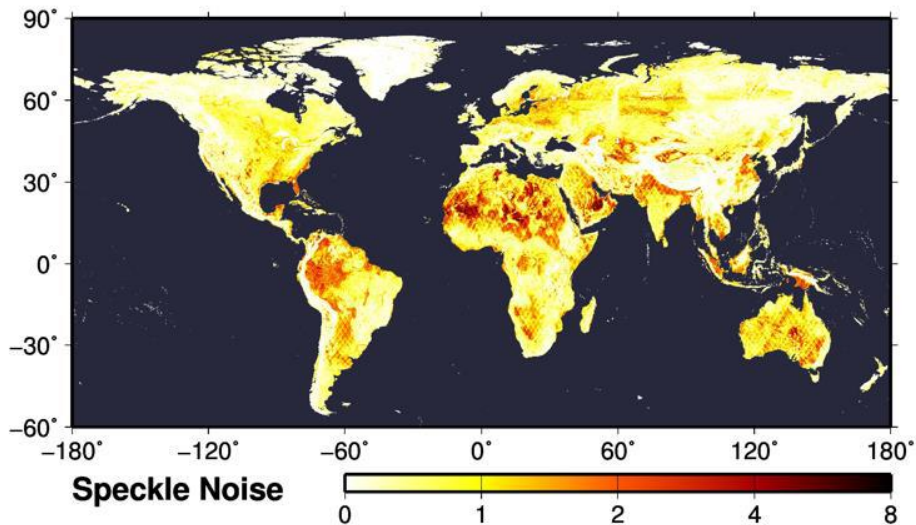
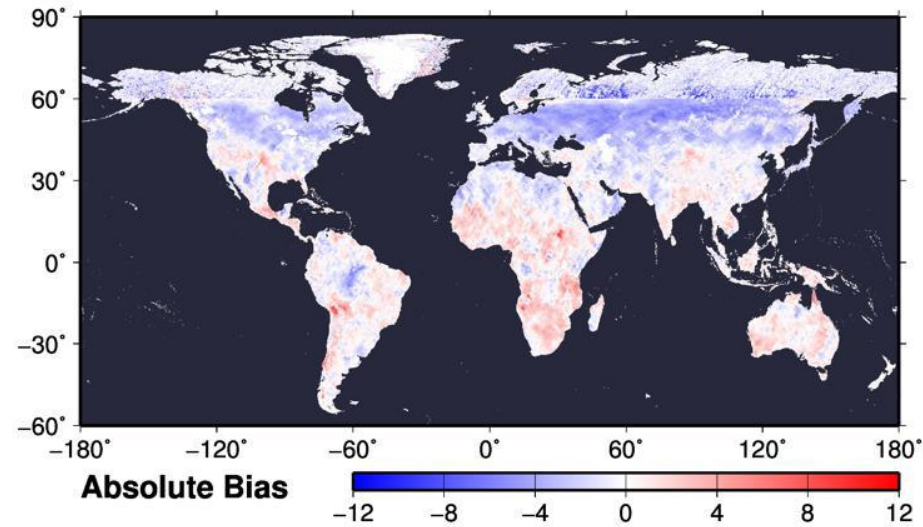
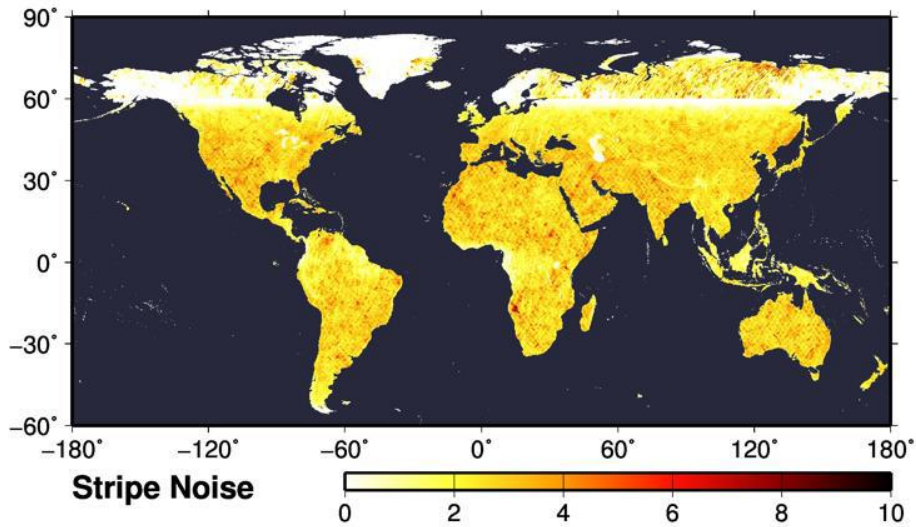
Obtained by applying multi-component error removal to SRTM3 and AW3D



Yamazaki et al., 2017 (GRL)

[http://hydro.iis.u-tokyo.ac.jp/~yamada/MERIT\\_DEM/](http://hydro.iis.u-tokyo.ac.jp/~yamada/MERIT_DEM/)

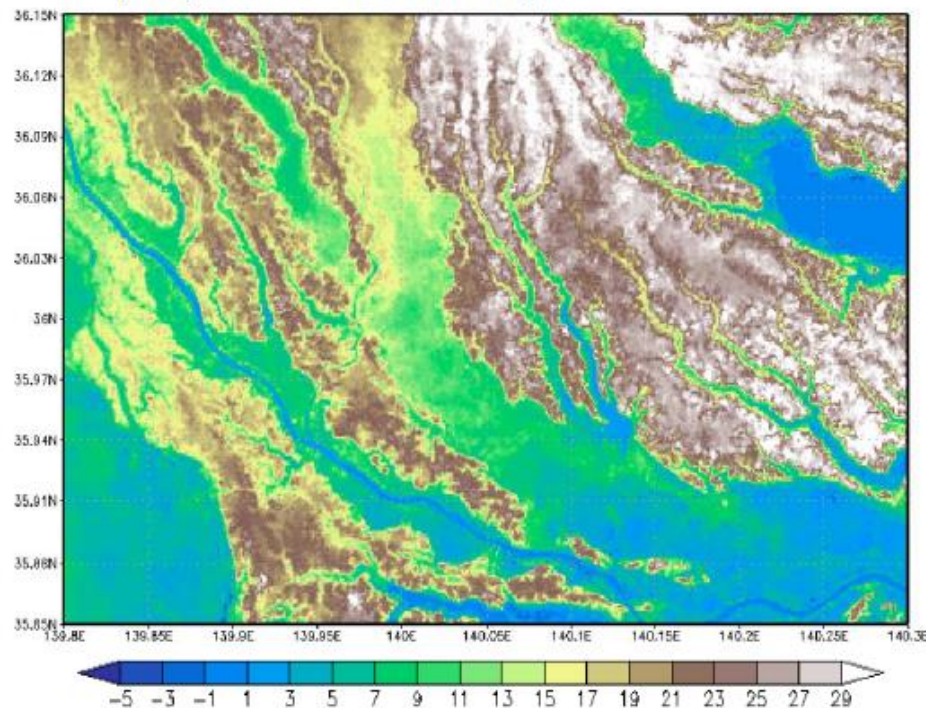
# Global Topography data



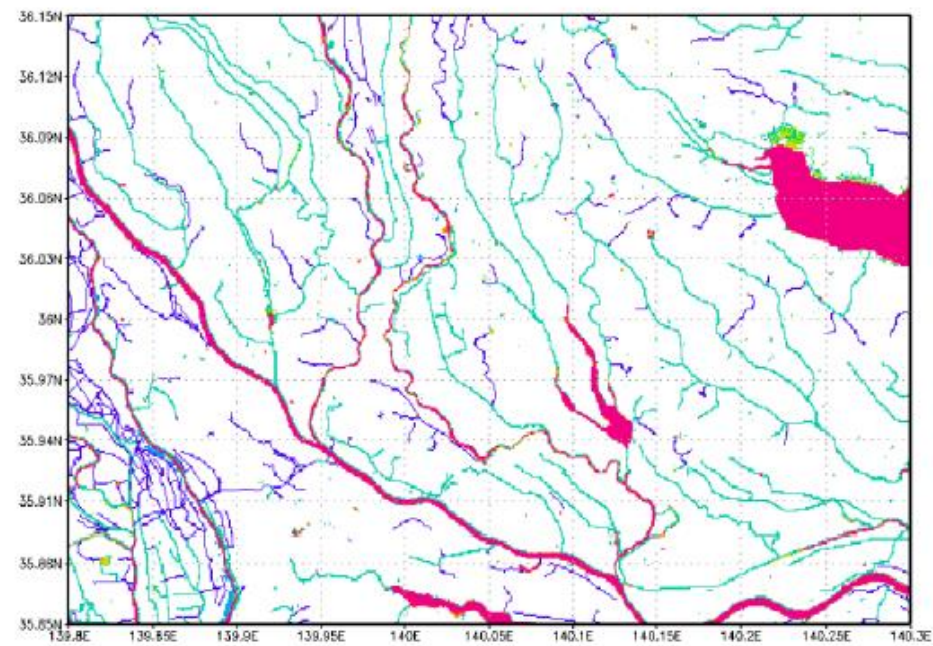
# Global Topography data

Modified elevations of DEMs using multiple water body maps to ensure river connectivity and to represent small channels

Tone, Kinu, Kokai Rivers confluence in Japan



MERIT DEM elevations



Synthetic Water Body Map

■ Landsat (Pekel et al., 2016)

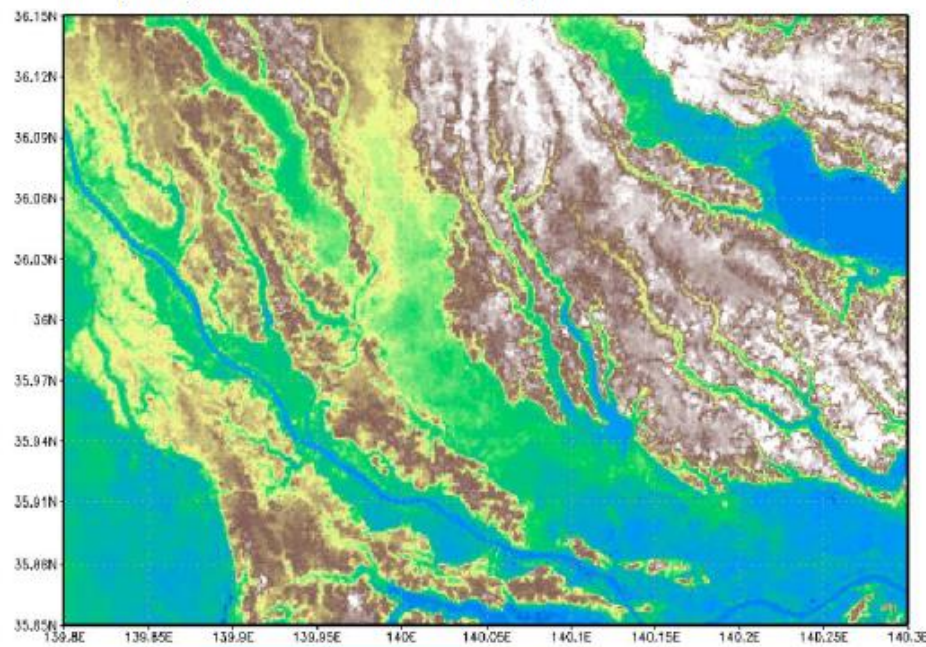
■ OpenStreetMap: River + Lake polygons

■ OpenStreetMap: Canal + stream lines

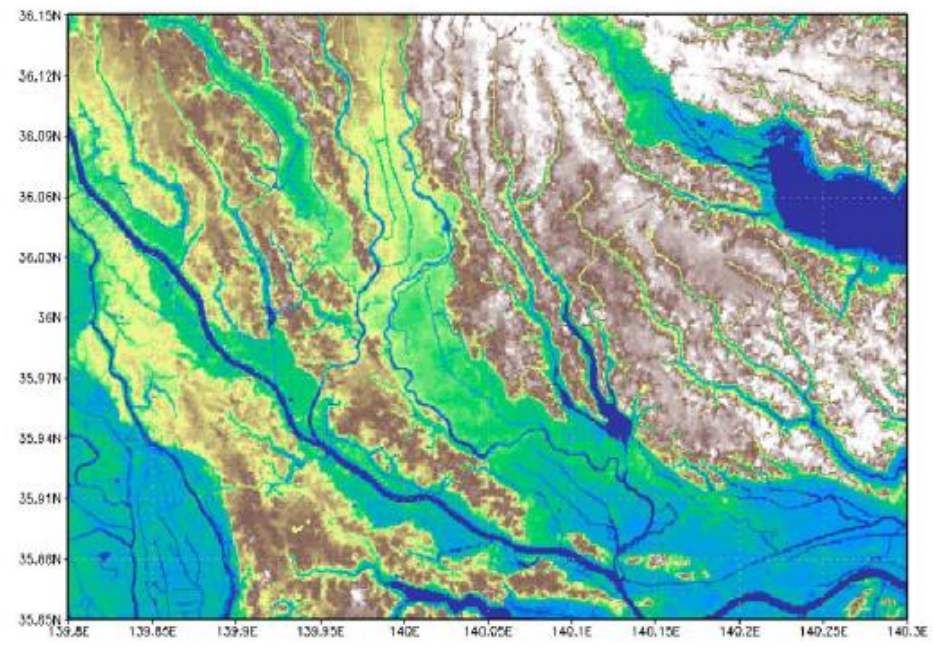
# Global Topography data

Modified elevations of DEMs using multiple water body maps to ensure river connectivity and to represent small channels

Tone, Kinu, Kokai Rivers confluence in Japan



**MERIT DEM elevation**



**Modified elevation**

*To be released  
in late 2018*

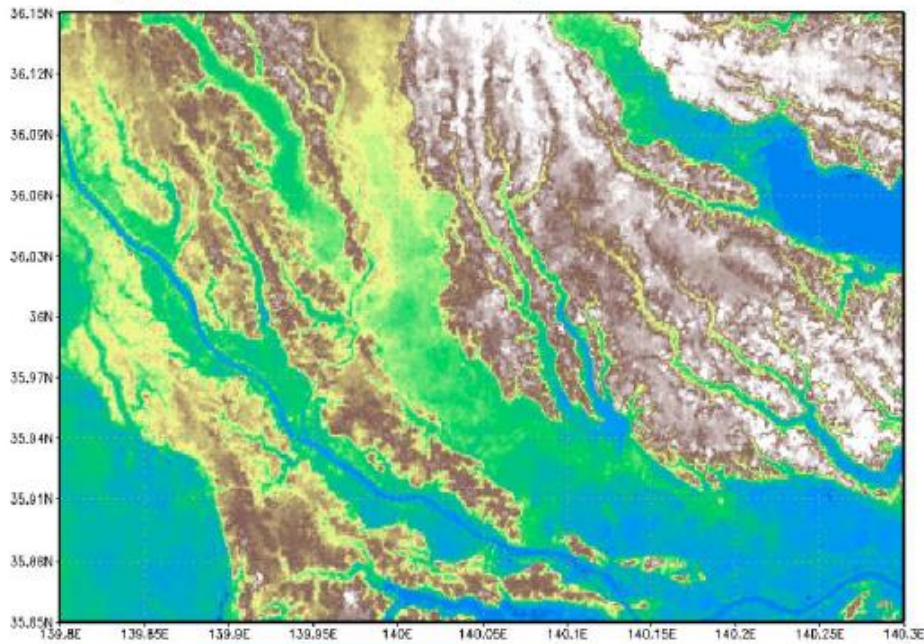
# Global Topography data

To further investigate:

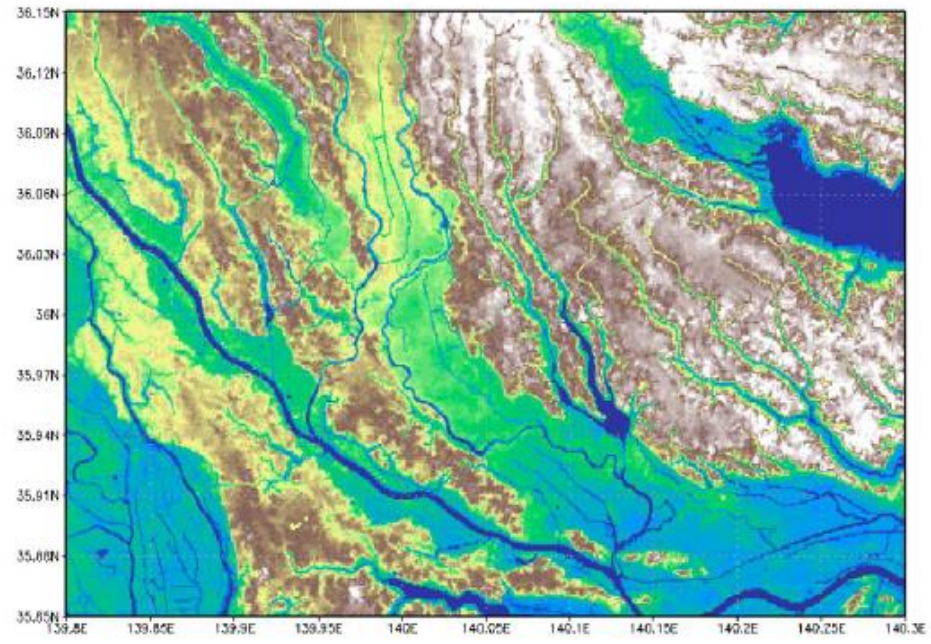
**Global Flood Partnership**

<https://gfp.jrc.ec.europa.eu/about-us>

Tone, Kinu, Kokai Rivers confluence in Japan



**MERIT DEM elevation**



**Modified elevation**

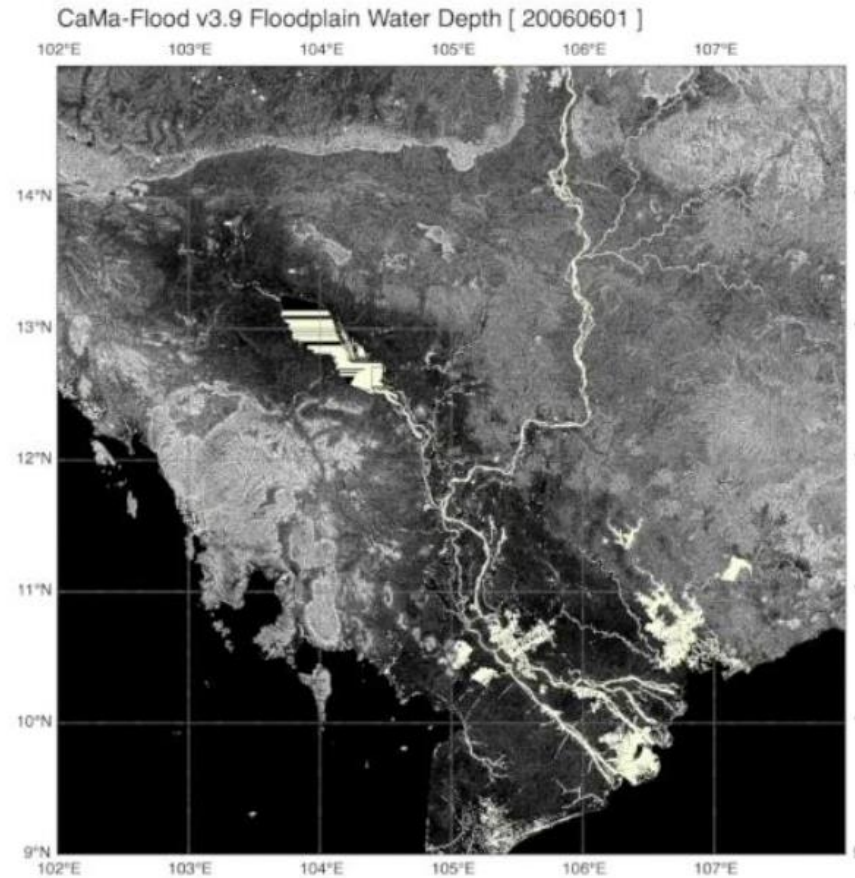
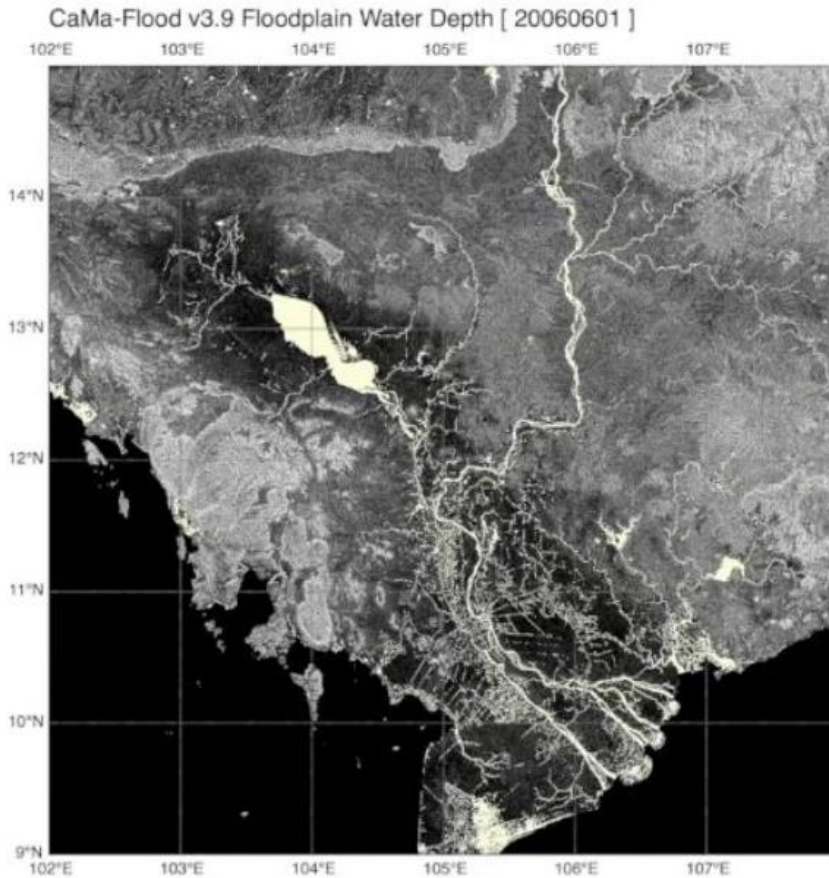
*To be released  
in late 2018*

# Global Topography data

*To be released  
in late 2018*

**[New] MERIT DEM + New hydrography  
+ Synthetic water map**

**[Old] SRTM + HydroSHEDS**



Credits to Dai Yamazaki – from his presentation at the Global Flood Partnership meeting – Delft 2018



# Global Topography data

## OPEN CHALLENGES

### - **Missing dataset to improve global flood modelling**

Global channel bathymetry

Global levee height datasets

Global reservoir, lakes datasets

### - **Local data integration**

Possible integration of high-accuracy topography available locally

### - **Validation data, assimilation**

Satellite Altimetry, multi-satellite flood extent (Landsat, MODIS, etc.)

Assimilation of these sources

# RIVER BATHYMETRY ESTIMATION

The literature reports several attempts made to handle the absence of bathymetric information:

- **Geomorphic equations** relating river discharge, depth, and water surface width as proposed by Leopold and Maddock [1953];
- Using the original **SRTM assuming the knowledge of flow rates and concurrent water depth** during the SRTM acquisition [Alfieri et al., 2013];
- Considering bathymetry as an **additional model parameter** to be calibrated (Yan et al., 2015).
- By referring to local available data
- **Data assimilation** technique combines water surface elevation,  $h$ , with hydrodynamic models in order to estimate the flow depth and the river discharge at a given section [Andreadis et al., 2007; Durand et al., 2008, 2014; Oubanas et al., 2018];
- Referring to **satellite images with the use of simplified flow resistance equation** (Flow Resistance Equation-Based Imaging of River Depths –FREEBIRD- algorithm; Legleiter, 2015)
- by considering **concurrent water surface elevation,  $h$ , and width,  $w$** , sensed from satellite [Mersel et al., 2013]

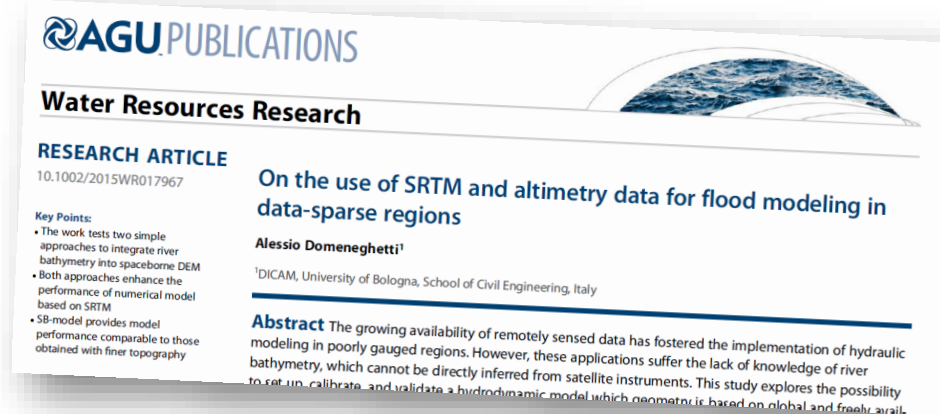
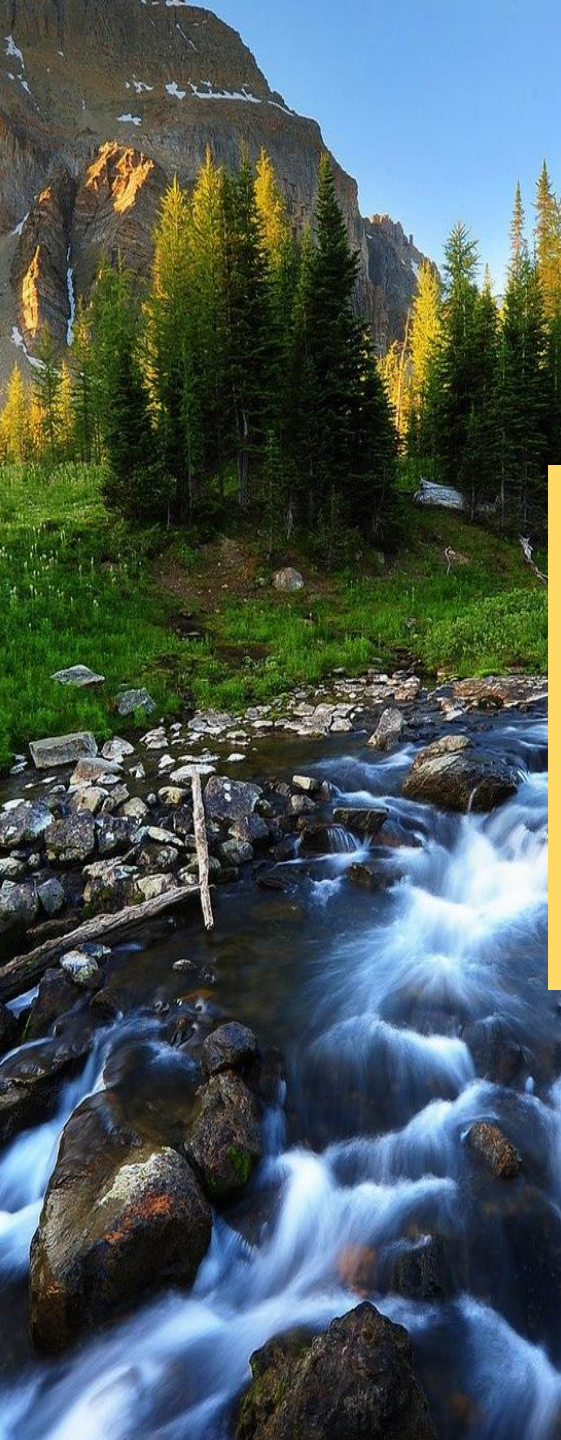
# RIVER BATHYMETRY ESTIMATION

## Channel Bankfull Method:

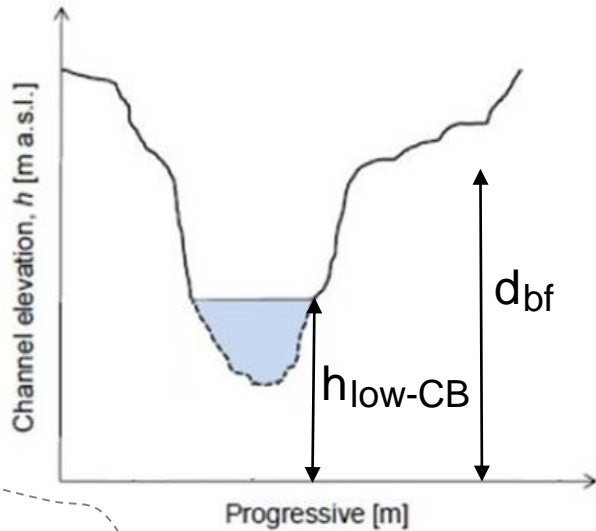
it estimates river depth using empirical relationship for a limited number of gauging stations [Leopold and Maddock, 1953]

## Slope Break Method:

it exploits the linear relationship between water surface width and water surface elevation [Mersel et al., 2013]

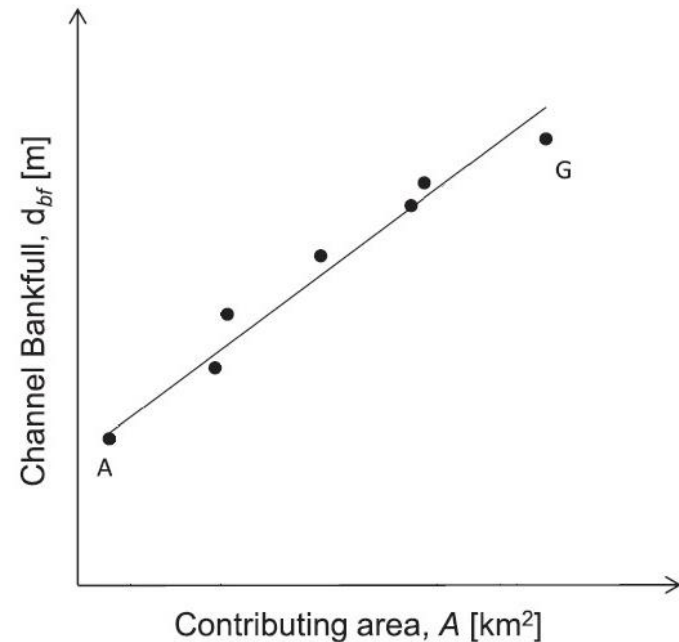
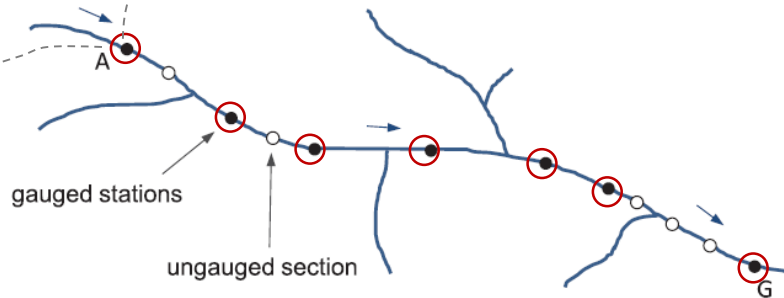


# CHANNEL BANKFULL METHOD - CB

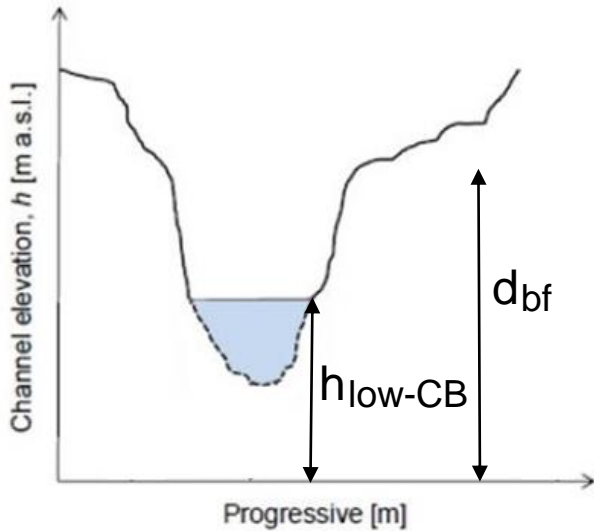


The CB approach investigates the possibility to enhance the description of the river geometry by exploiting the  $A$ - $d_{bf}$  relationship. Firstly, the  $A$ - $d_{bf}$  relationship is identified for gauged sections.

$$A \sim d_{bf}$$



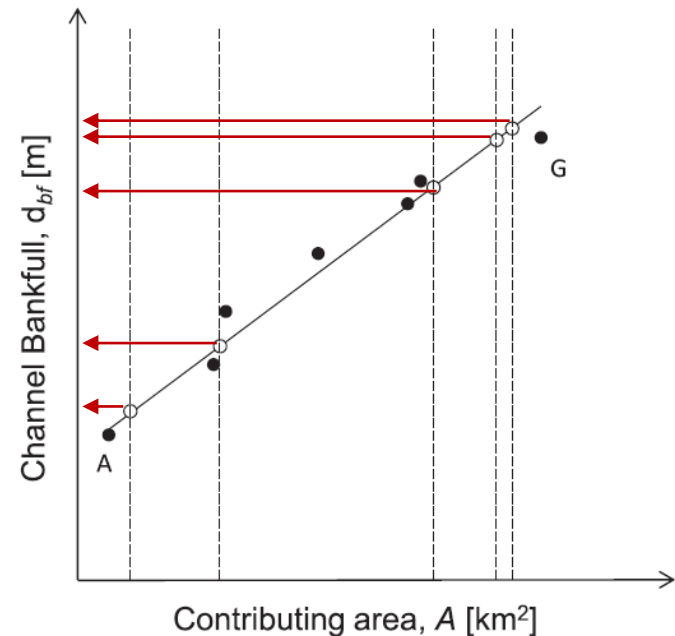
# CHANNEL BANKFULL METHOD - CB



The CB approach investigates the possibility to enhance the description of the river geometry by exploiting the  $A-d_{bf}$  relationship.

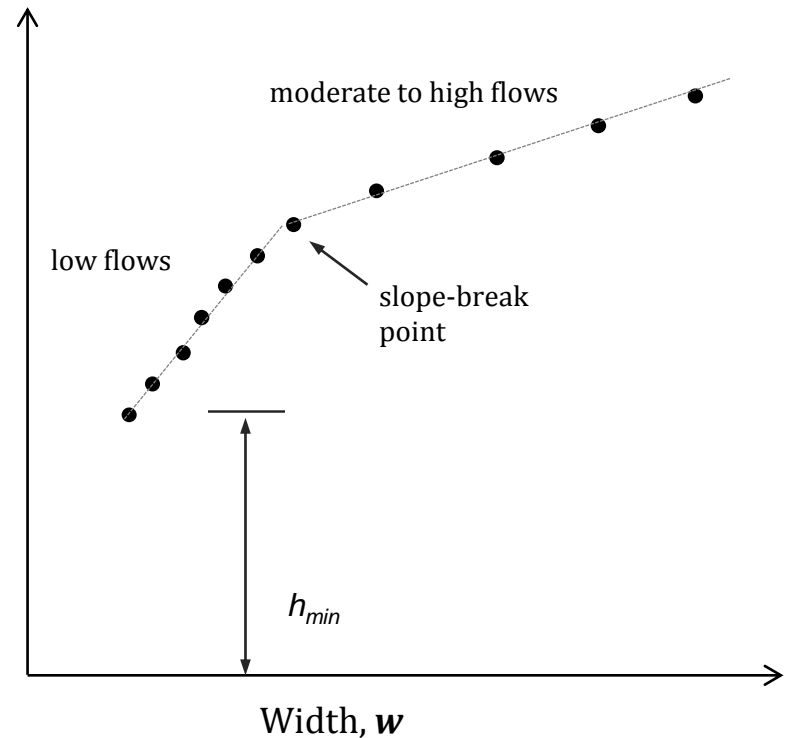
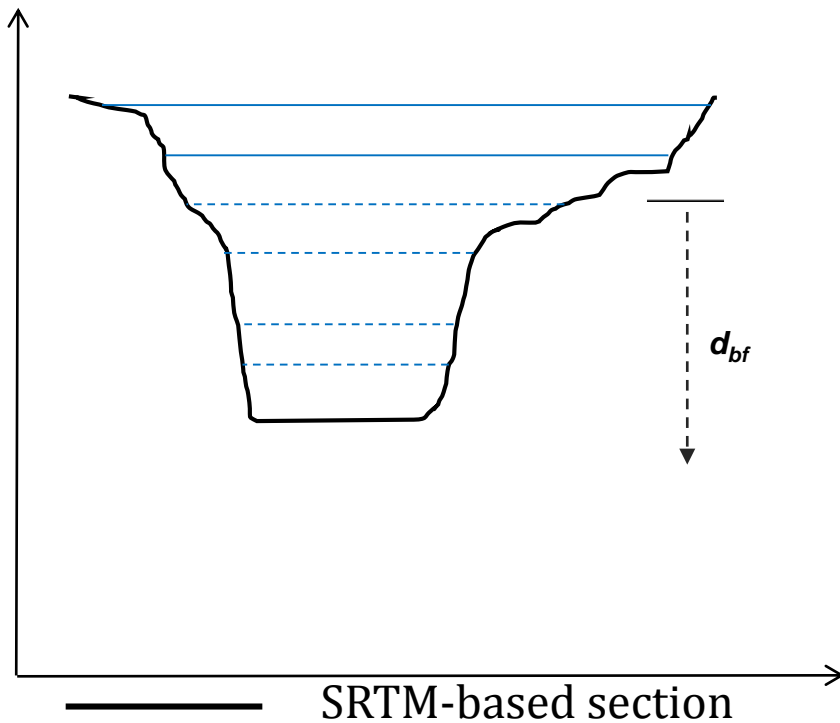
Firstly, the  $A-d_{bf}$  relationship is identified for gauged sections.

For all ungauged sections the contributing area is extracted, in order to find corresponding channel bankfull, exploiting previous linear relationship.



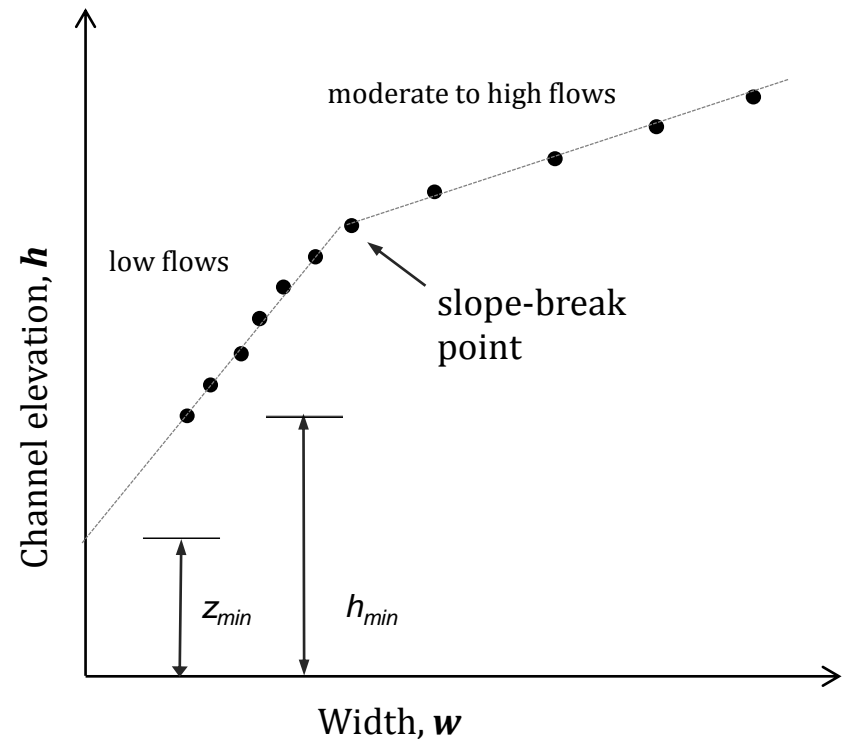
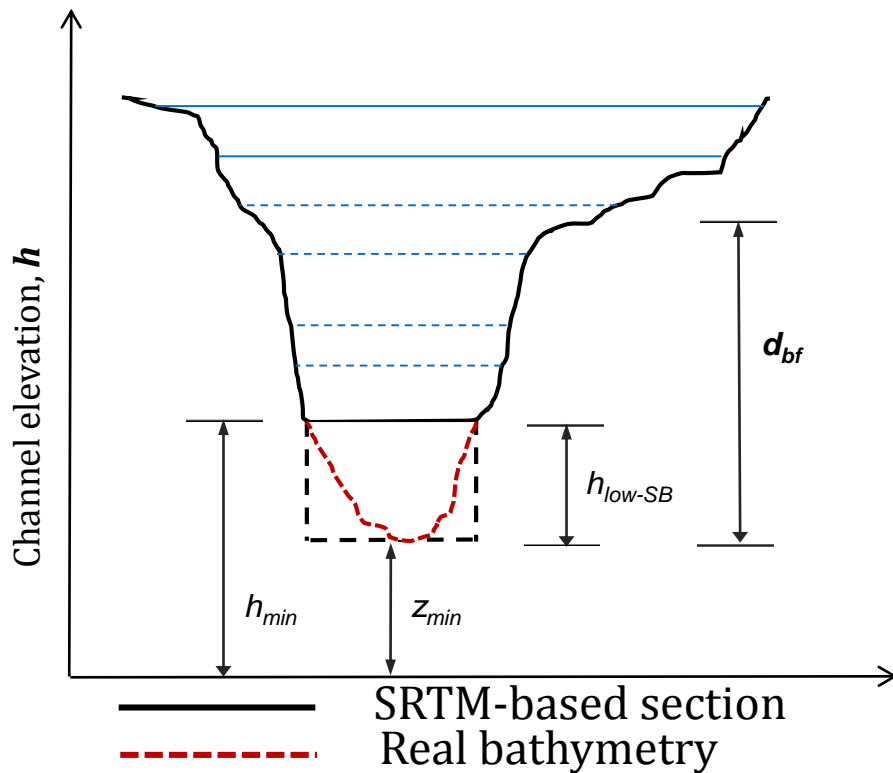
# SLOPE BREAK METHOD - SB

→ Linear relationships among the **water surface width**,  $w$ , and **water surface elevation**,  $h$



# SLOPE BREAK METHOD - SB

→ Linear relationships among the **water surface width,  $w$** , and **water surface elevation,  $h$**



# SURVEY AREAS

Po River, Italy (132 km)

Limpopo River, Mozambique (164 km)

*Case study characteristics*

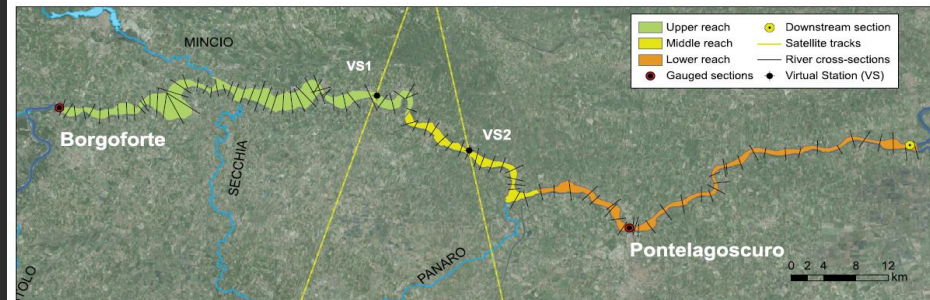
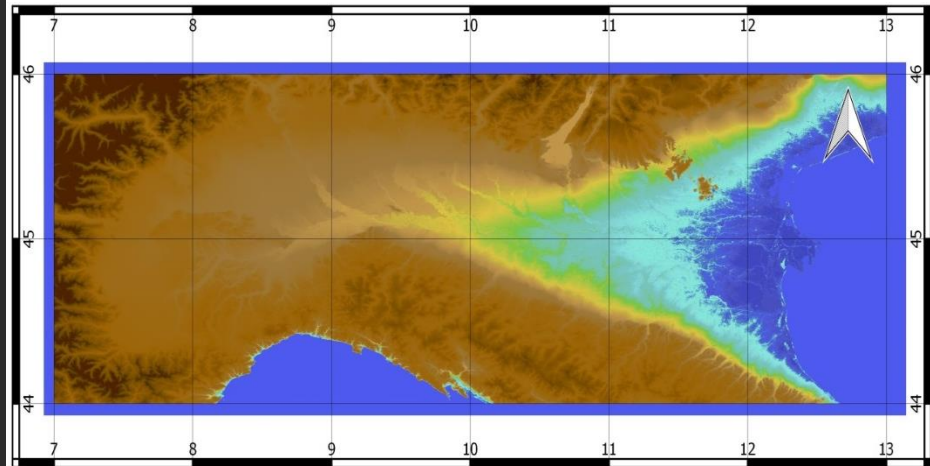
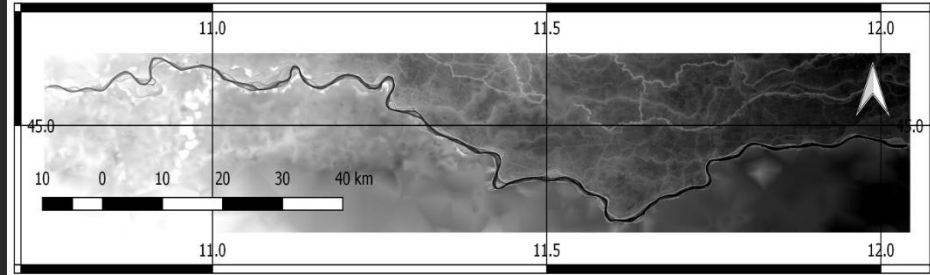
1. *Mono-corsual stretch*
2. *River width greater than DEM resolution*
3. *Availability of in-situ measurements*





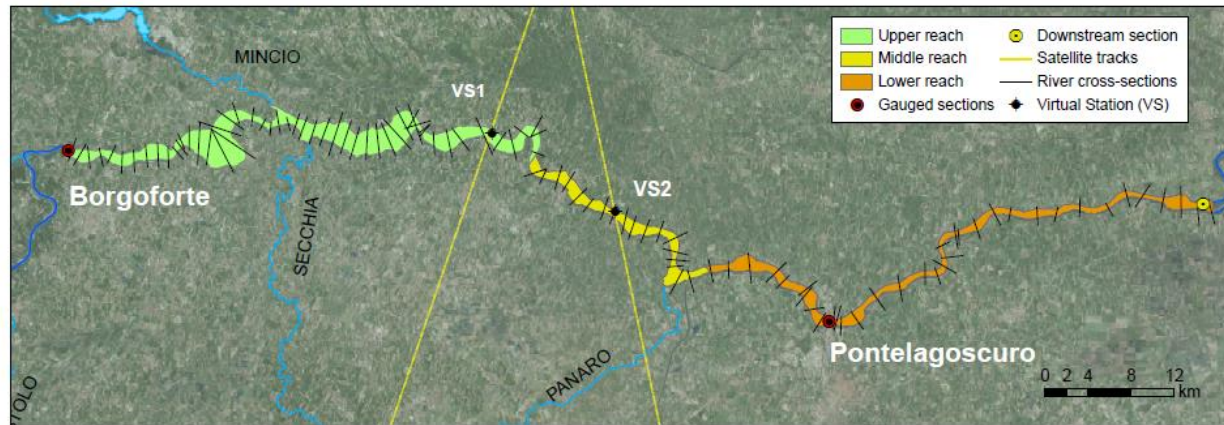
# PO RIVER: AVAILABLE DATA

- **LiDAR DEM** (resolution 2 m integrated with in-situ bathymetry measurements)
- **SRTM 90**
- Mean daily water level and discharge at **gauged stations**
- **Altimetry series** (ERS and ENVISAT)
- **Reference hydraulic model (quasi-2D)**



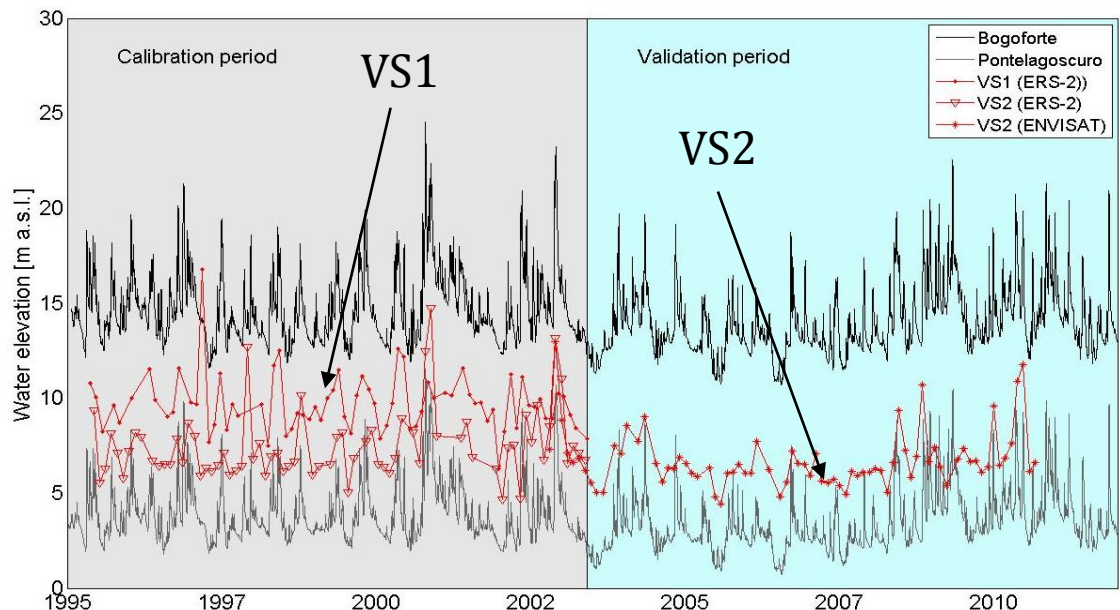
# DATA & BENCHMARK MODEL

- 2 m **LiDAR** for the overall study area
- 104 river cross-sections
- **Mean daily discharge** at the upstream section



- **Mean daily water elevation** at Pontelagoscuro

- Satellite **altimetry datasets**:



ERS-2: June 1995-May 2003

ENVISAT: Oct. 2002- Aug. 2010

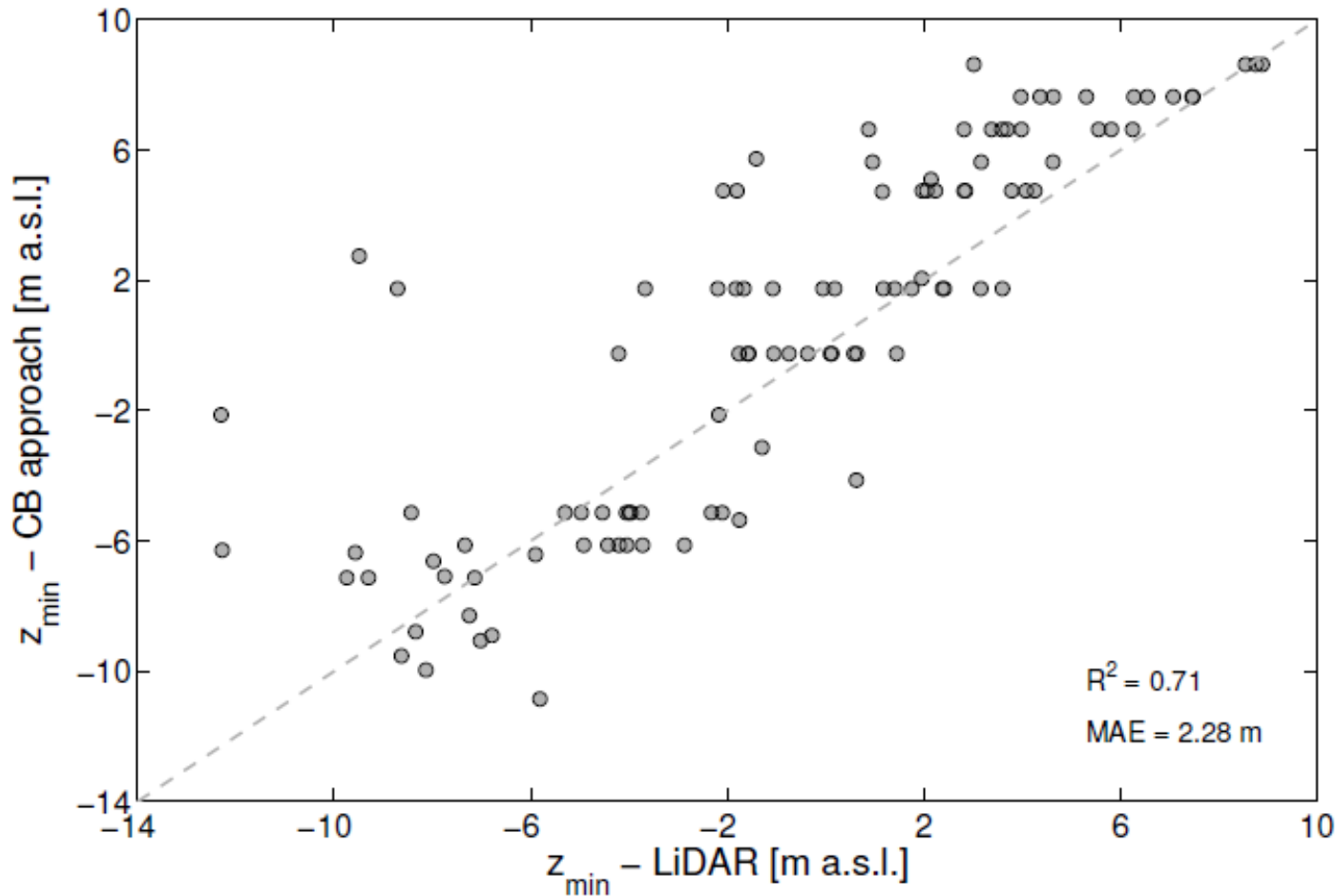
# CHANNEL BANKFULL METHOD - CB

River thalweg:  
LiDAR vs CB-approach

Linear relationship identified among

$$A \sim d_{bf}$$

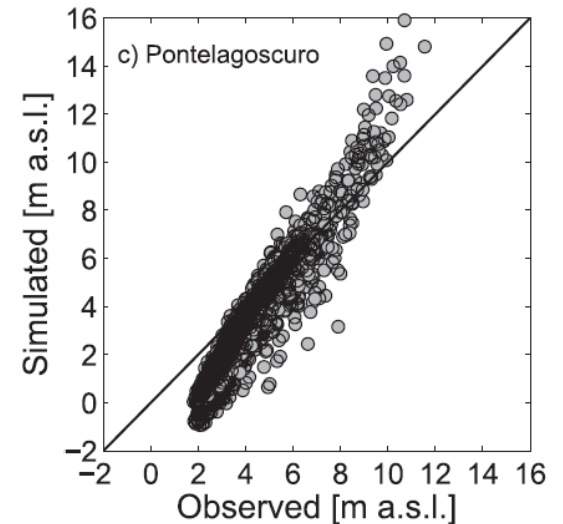
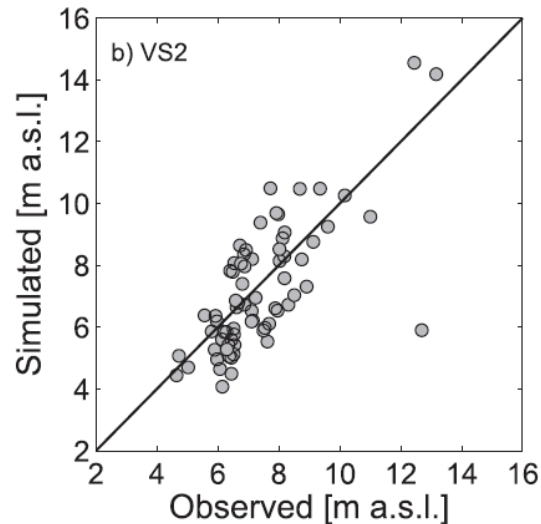
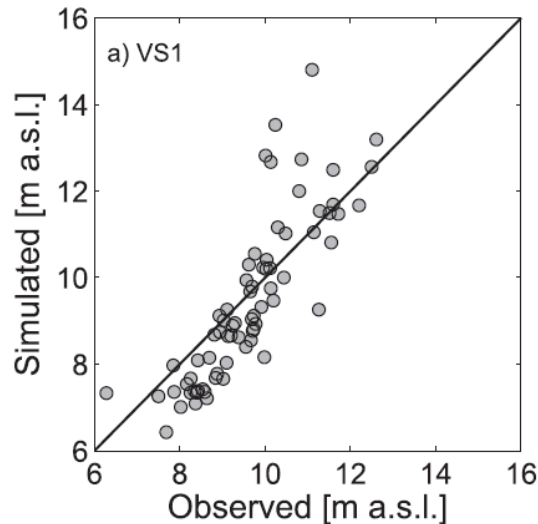
Lowering values:  $4.37 \div 7.13$  m



$R^2 = 0.71$   
ME = 1.18 m  
MAE = 2.28 m

# CHANNEL BANKFULL METHOD -CB

Configuration	River Portion	Manning's coefficient (s m <sup>-1/3</sup> )	NS	MAE (m)	RMSE (m)
<b>CB-model</b>	Upper reach (VS1)	0.049	0.23	0.86	1.09
	Middle reach (VS2)	0.045	0.34	1.10	1.44
	Lower reach (PonteLS)	0.052	0.17	1.18	1.38
<b>LiDAR-model</b>	Upper reach (VS1)	0.044	0.43	0.70	0.93
	Middle reach (VS2)	0.042	0.34	0.76	1.08
	Lower reach (PonteLS)	0.025	0.95	0.28	0.35



*The image shows the comparison between simulated water levels from CB-model and observed ones for VS1, VS2 and Pontelagoscuoro, respectively.*

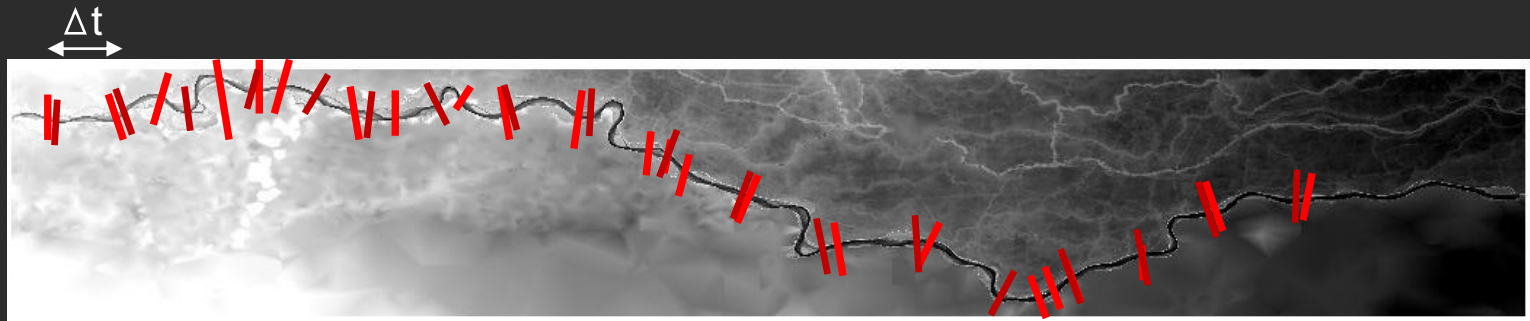
# SLOPE BREAK METHOD - SB

## River cross-sections extraction

01

- DEM reading (SRTM-MERIT)
- extract river cross sections: the user can exploit a shapefile or makes the code generate perpendicular equidistant cross sections respect with a given channel center line.

River Bathymetry Estimation from SaTellite (Ri-BEST) is a Matlab software for river bathymetry evaluation applying the Slope-Break Method

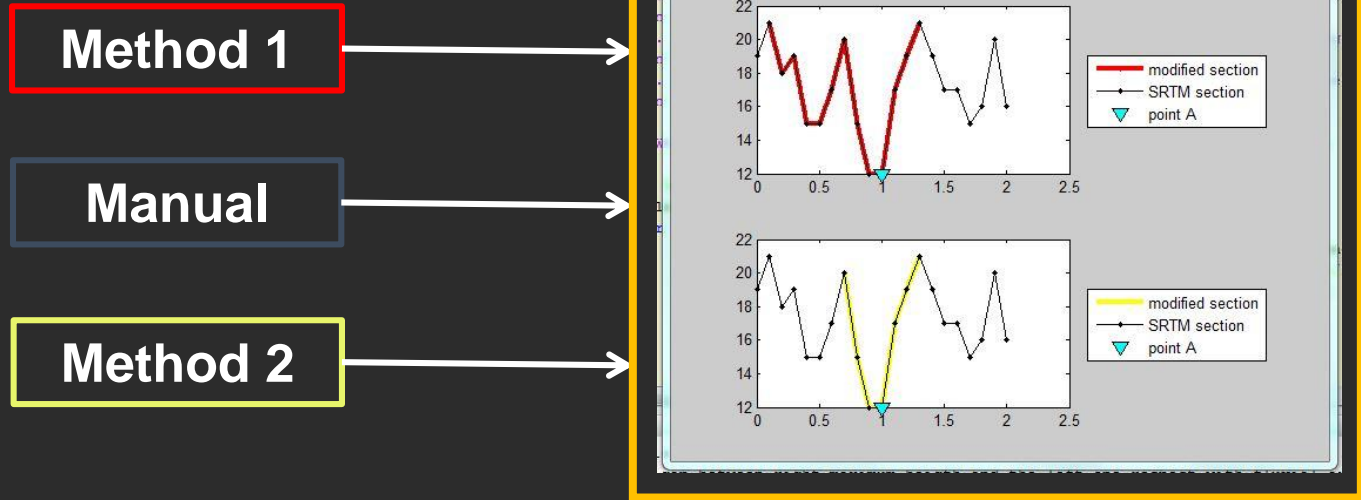


Equidistant cross sections provided by a shapefile

# 02

## River channel selection

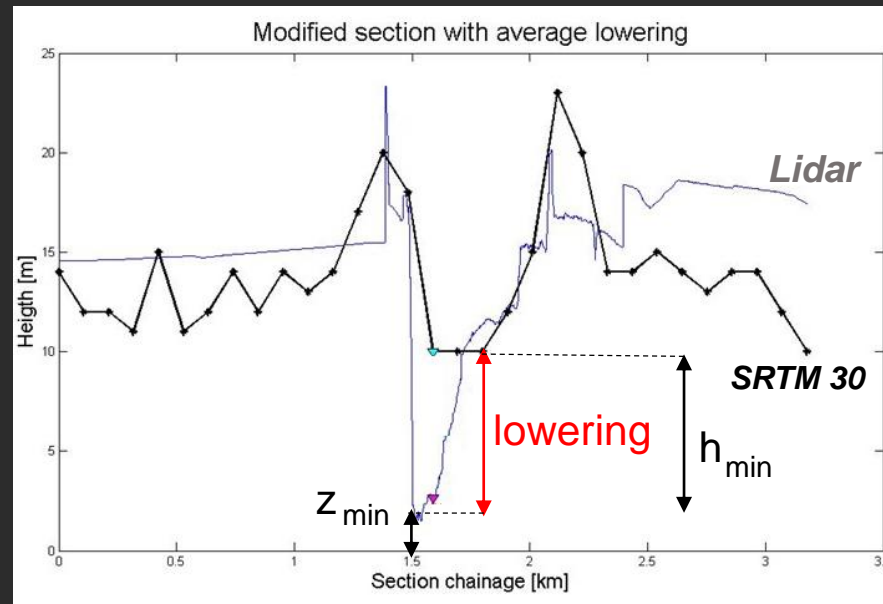
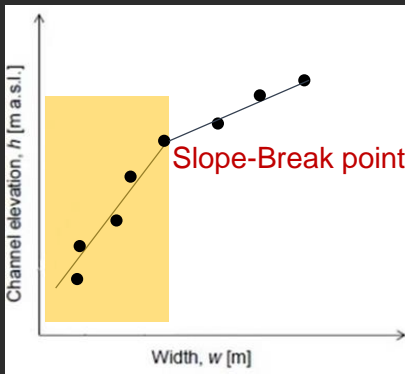
- Method 1 isolates cross section portion between left maximum height and right one;
- Method 2 identifies the part for which each point has a greater elevation than the previous one (on left and right side respectively).
- Using “Manual” method the user can see both two selections and choose the best one.



# 03

## Average lowering estimation

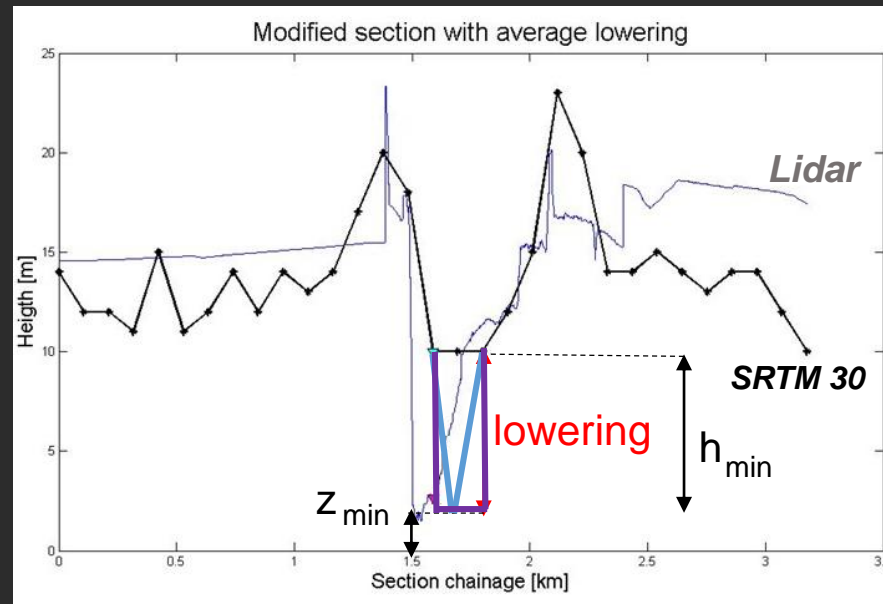
Only cross sections that have at least 5 points under slope-break point are used to estimate the river bathymetry.



# 04

## Cross section geometry modification

SRTM profile is corrected with two different approach: triangular and rectangular modification.

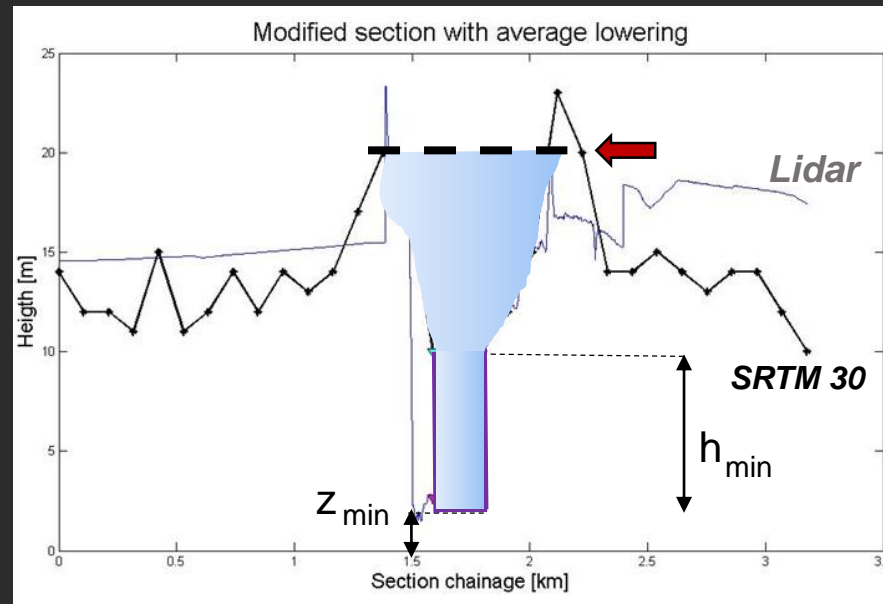




# 05

## Estimation of flow area and wetted perimeter

Imposing a water level, flow area and wetted perimeter are estimate for the new modified cross section.



# PO RIVER RESULTS:

## bathymetry

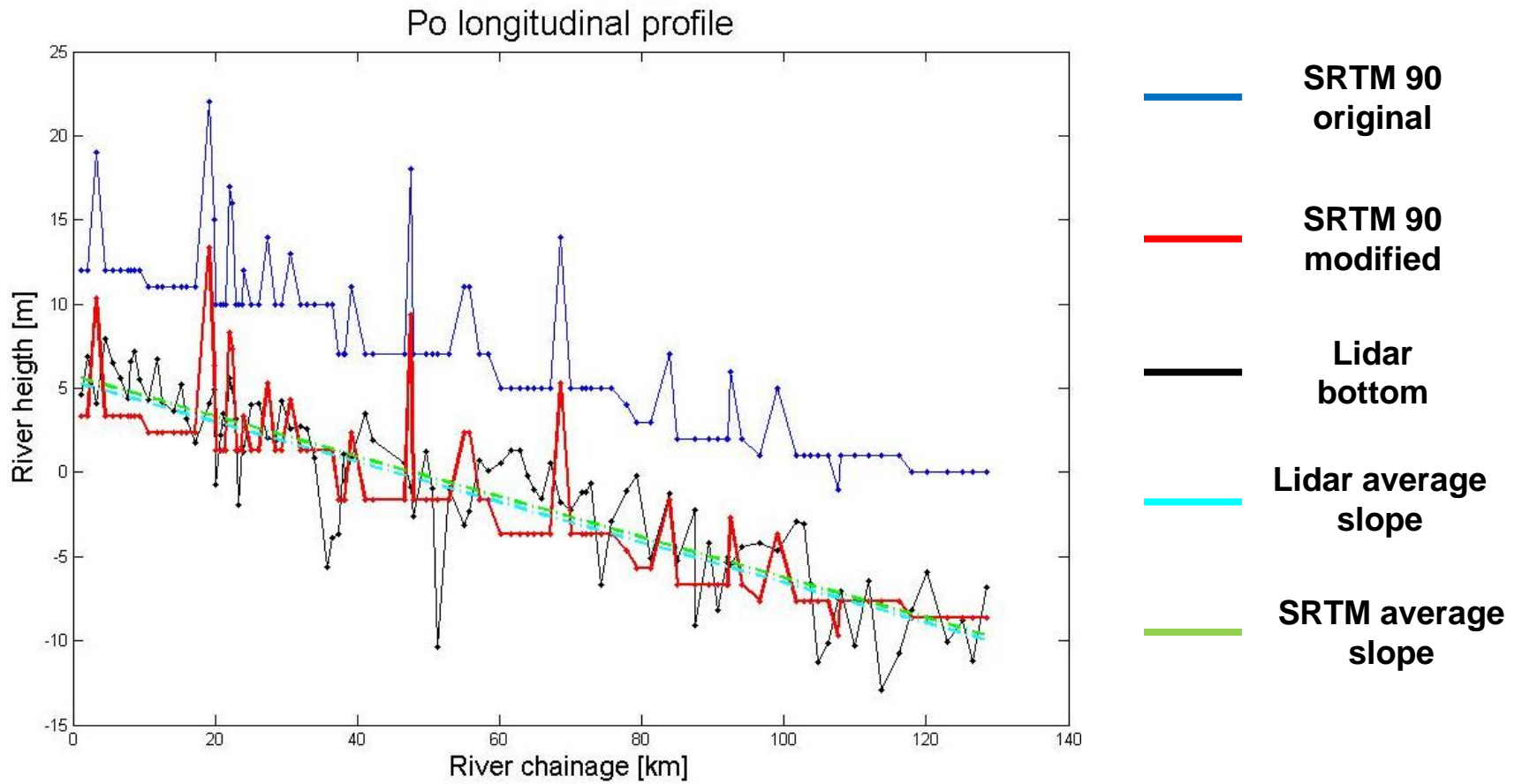
SRTM 90	Equidistant sections			Historical sections		
Channel selection method	Manual Method	Method 1	Method 2	Manual Method	Method 1	Method 2
<b>Average lowering* [m]</b>	8.3	8.8	8.9	8.7	8.5	8.6

	SRTM 90	SRTM 90 mod**		
		Manual Method	Method 1	Method 2
ME [m]	8.34	<b>-0.32</b>	<b>-0.15</b>	<b>-0.22</b>
RMSE [m]	9.02	3.45	3.44	3.44
MAE [m]	8.34	2.8	2.75	2.77

\* Average lowering is the different between LiDAR and SRTM bottoms

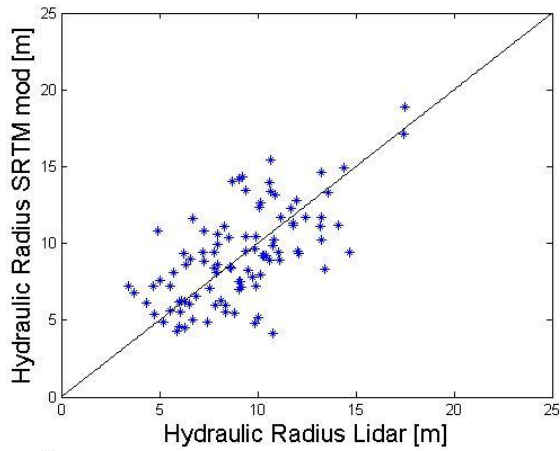
\*\* SRTM 90 mod are referred to cross sections modified with Ri-BEST tool

# PO RIVER RESULTS: Longitudinal profile

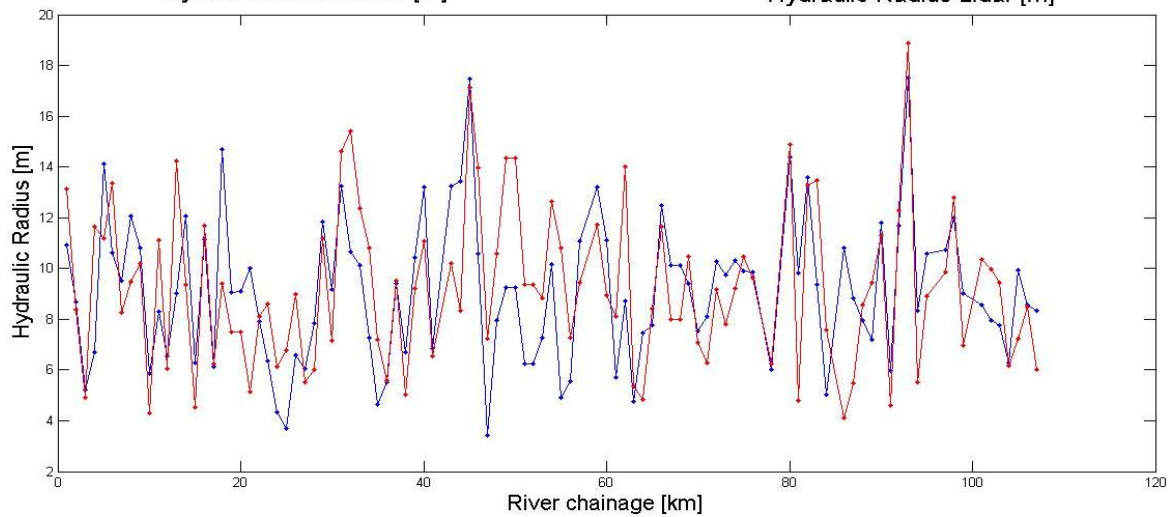
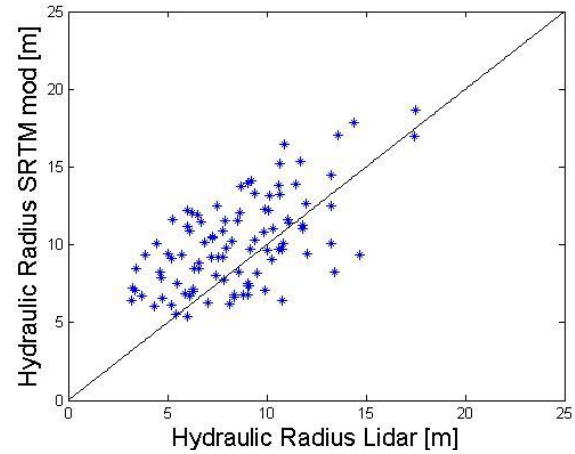


# PO RIVER RESULTS: Hydraulic radius

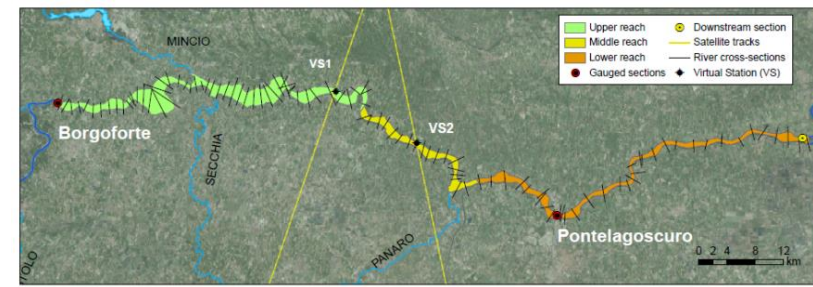
rectangular modification



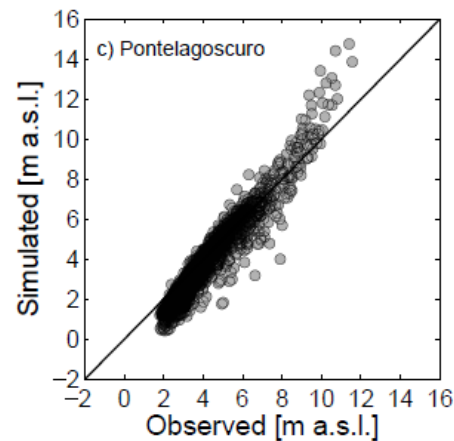
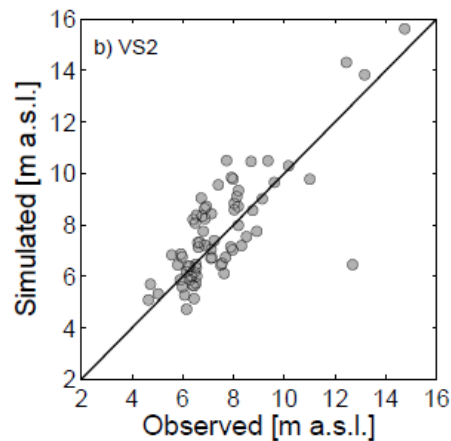
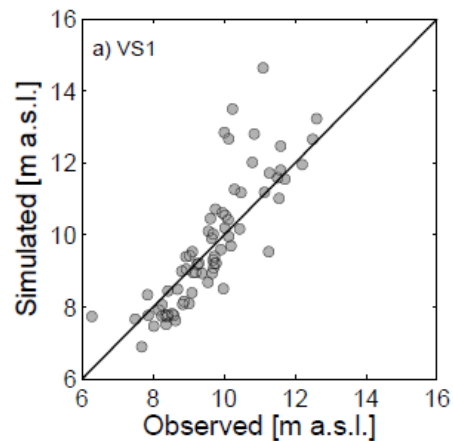
triangular modification



# PO RIVER RESULTS: Hydraulic model



Configuration	River Portion	Manning's coefficient (s m <sup>-1/3</sup> )	NS	MAE (m)	RMSE (m)
<b>SB-model</b>	Upper reach (VS1)	0.044	0.38	0.68	0.97
	Middle reach (VS2)	0.042	0.49	0.97	1.13
	Lower reach (PonteLS)	0.040	0.79	0.55	0.70
<b>LiDAR-model</b>	Upper reach (VS1)	0.044	0.43	0.70	0.93
	Middle reach (VS2)	0.042	0.34	0.76	1.08
	Lower reach (PonteLS)	0.025	0.95	0.28	0.35

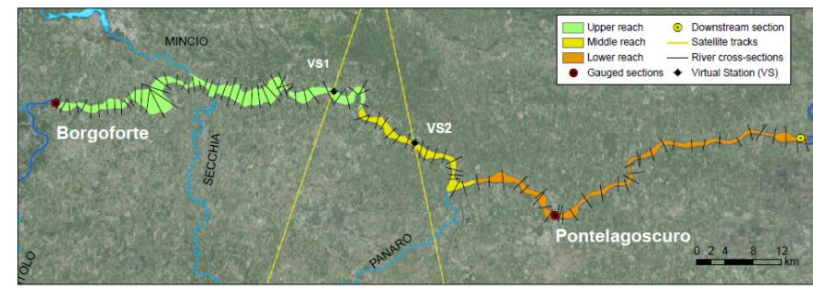


Reference model

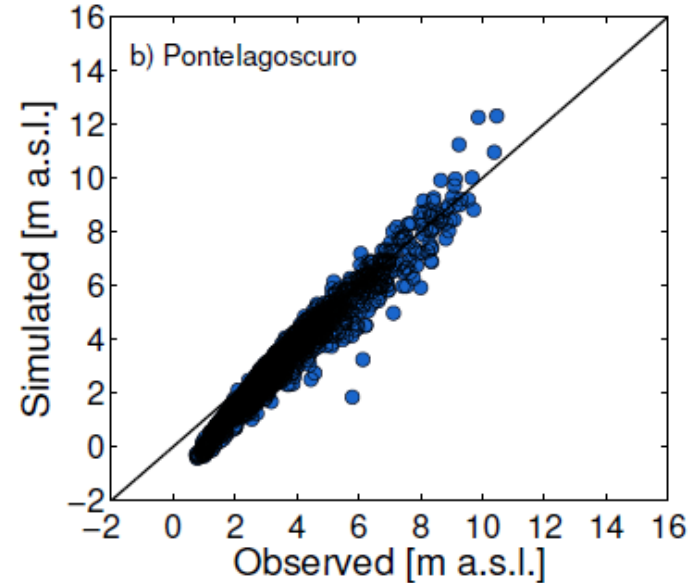
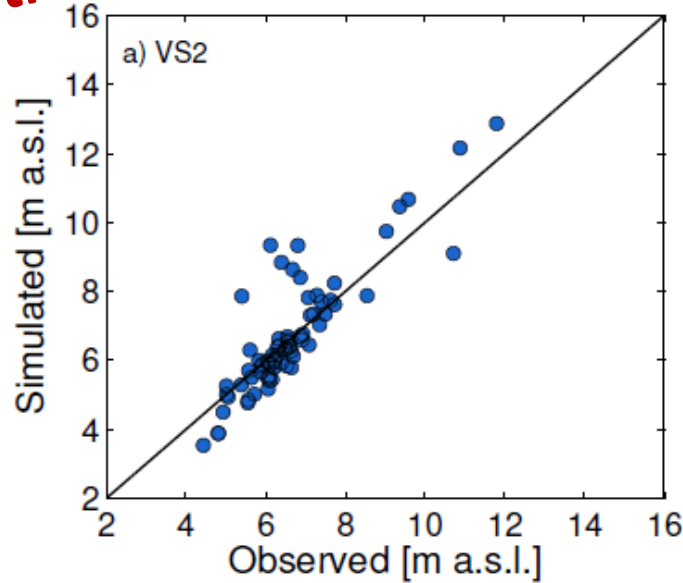
**Calibration**

$$\Delta NS = -0.16 \quad \Delta MAE = 0.27 \text{ m} \quad \Delta RMSE = 0.35 \text{ m}$$

# PO RIVER RESULTS: Hydraulic model



**Validation**



**LiDAR model**

NS = 0.76  
RMSE = 0.66 m

NS = 0.96  
RMSE = 0.32 m

**SB-model**

NS = 0.57  
RMSE = 0.87 m

NS = 0.83  
RMSE = 0.60 m

**Reference model**

# Main findings

- Both CB and SB approaches can enhance the bathymetry description of the original SRTM
- SB does not require in-situ data and is more reliable than CB approach for the reconstruction of the river geometry (MAE = 2.28 m and 1.75 m for CB and SB approach, respectively)
- Calibrated friction coeff. of the SB-model are physically meaningful and reproduce the real characteristics of the river
- SB-model performances are of the same order of magnitude of the benchmark model based on LiDAR (max  $\Delta$ MAE =  $\sim$  0.30 m)

# Next steps?

## Utilizing Flood Inundation Observations to Obtain Floodplain Topography in Data-Scarce Regions

Apoorva Shastry<sup>1,2\*</sup> and Michael Durand<sup>1,2</sup>

<sup>1</sup> School of Earth Sciences, The Ohio State University, Columbus, OH, United States, <sup>2</sup> Byrd Polar and Climate Research Center, The Ohio State University, Columbus, OH, United States



*“Spaceborne remote sensing observations of inundation extent contain indirect information about floodplain topography.”* Shastry and Durand 2019

**Main idea** → Because two-dimensional flood models encapsulate floodplain processes, it is natural to attempt to use such models to help extract topographic information from inundation. So, the idea is to infer floodplain topography using inundation maps, while flood models do the inverse: predict inundation using floodplain topography



Inverse problem solved with Data Assimilation technique

Great potential in the light of the upcoming **SWOT mission** (see later on)



# THE USE OF REMOTE SENSING-DERIVED WATER SURFACE DATA FOR HYDRAULIC MODELING



AGU PUBLICATIONS  
Water Resources Research

RESEARCH ARTICLE  
10.1002/2015WR017654

Spatiotemporal densification of river water level time series by multimission satellite altimetry  
M. J. Tourian<sup>1</sup>, A. Tarpanelli<sup>2</sup>, O. Elmi<sup>1</sup>, T. Qin<sup>1</sup>, L. Brocca<sup>2</sup>, T. Moramarco<sup>2</sup>, and N. Sneeuw<sup>1</sup>

- Key Points:**
- Temporal densification of altimetric time series over rivers (sub)monthly to ~3 day resolution
  - Dealing with spatial resolution problem of altimetry by hydrological info of river (slope and width)
  - Achieving different intersatellite bias estimates than global studies

**Abstract** Limitations of satellite radar altimetry for operational hydrology include its spatial and temporal sampling as well as measurement problems caused by local topography and heterogeneity of the reflecting surface. In this study, we develop an approach that eliminates most of these limitations to produce an

## Investigating the uncertainty of satellite altimetry products for hydrodynamic modelling

Alessio Domeneghetti,<sup>1,\*</sup> Attilio Castellarin,<sup>1</sup> Angelica Tarpanelli<sup>2</sup> and Tommaso Moramarco<sup>2</sup>

<sup>1</sup> DICAM—University of Bologna, School of Engineering, Viale del Risorgimento, 2, Bologna, Italy  
<sup>2</sup> Research Institute for Geo-Hydrological Protection, National Research Council, Via Madonna Alta 126, 06128 Perugia, Italy

Remote Sensing of Environment  
journal homepage: [www.elsevier.com/locate/rses](http://www.elsevier.com/locate/rses)

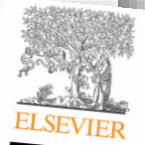
The use of remote sensing-derived water surface data for hydraulic model calibration  
Alessio Domeneghetti<sup>a,\*</sup>, Angelica Tarpanelli<sup>b</sup>, Luca Brocca<sup>b</sup>, Silvia Barbetta<sup>b</sup>, Tommaso Moramarco<sup>b</sup>, Attilio Castellarin<sup>a</sup>, Armando Brath<sup>a</sup>



Advances in Water Resources 112 (2018) 17–26  
Contents lists available at ScienceDirect

Advances in Water Resources  
journal homepage: [www.elsevier.com/locate/advwatres](http://www.elsevier.com/locate/advwatres)

Evaluation of multi-mode CryoSat-2 altimetry data over the Po River against in situ data and a hydrodynamic model  
L. Schneider<sup>a,\*</sup>, Angelica Tarpanelli<sup>b</sup>, Karina Nielsen<sup>c</sup>, Henrik Madsen<sup>d</sup>, G. Gauer-Gottwein<sup>e</sup>

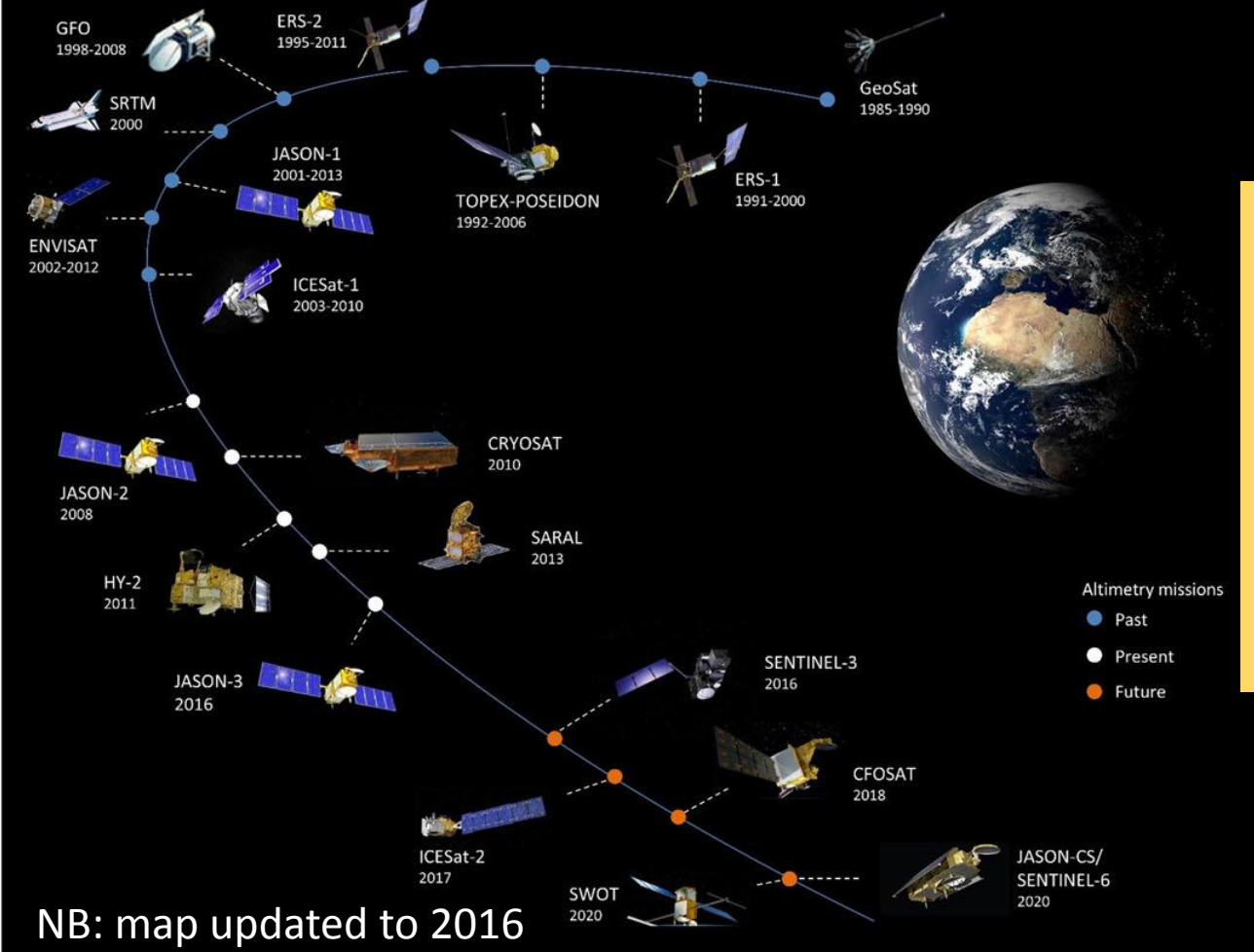


Contents lists available at ScienceDirect

Journal of Hydrology  
journal homepage: [www.elsevier.com/locate/jhydrol](http://www.elsevier.com/locate/jhydrol)

Research papers  
River discharge estimation at daily resolution from satellite altimetry over an entire river basin  
M.J. Tourian<sup>a,\*</sup>, C. Schwatke<sup>b</sup>, N. Sneeuw<sup>a</sup>





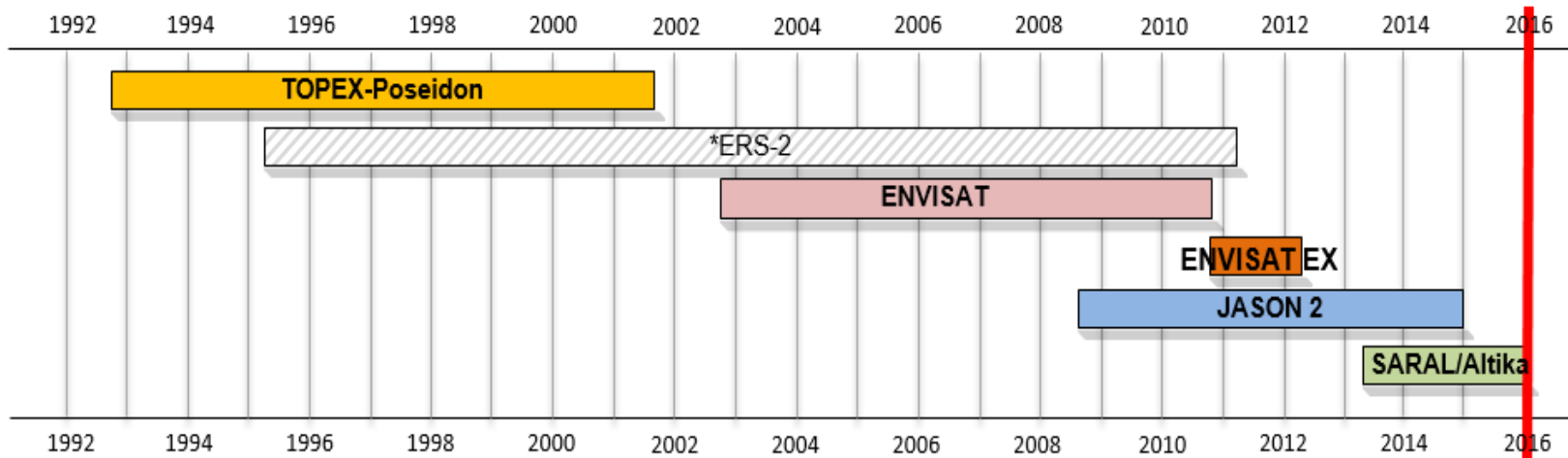
NB: map updated to 2016

Graphical illustration of past, current and future **satellite altimetry missions** for the monitoring of the world's rivers, lakes and reservoirs.

Monitoring of freshwater represents the base for the management of global water resources. However, the high cost related to the set-up and maintenance of traditional monitoring networks makes the density of observed data very limited in vast parts of the globe. On the contrary, the last decades have seen a great evolution on the capability to acquire remotely sensed observations, providing an increasing availability of spatially distributed data to be used for monitoring inland water.

## ON THE POTENTIAL OF ALTIMETRY DATA FOR THE CALIBRATION OF HYDRAULIC MODELS: A COMPARISON OF DIFFERENT PRODUCTS AND MULTI-MISSION SERIES

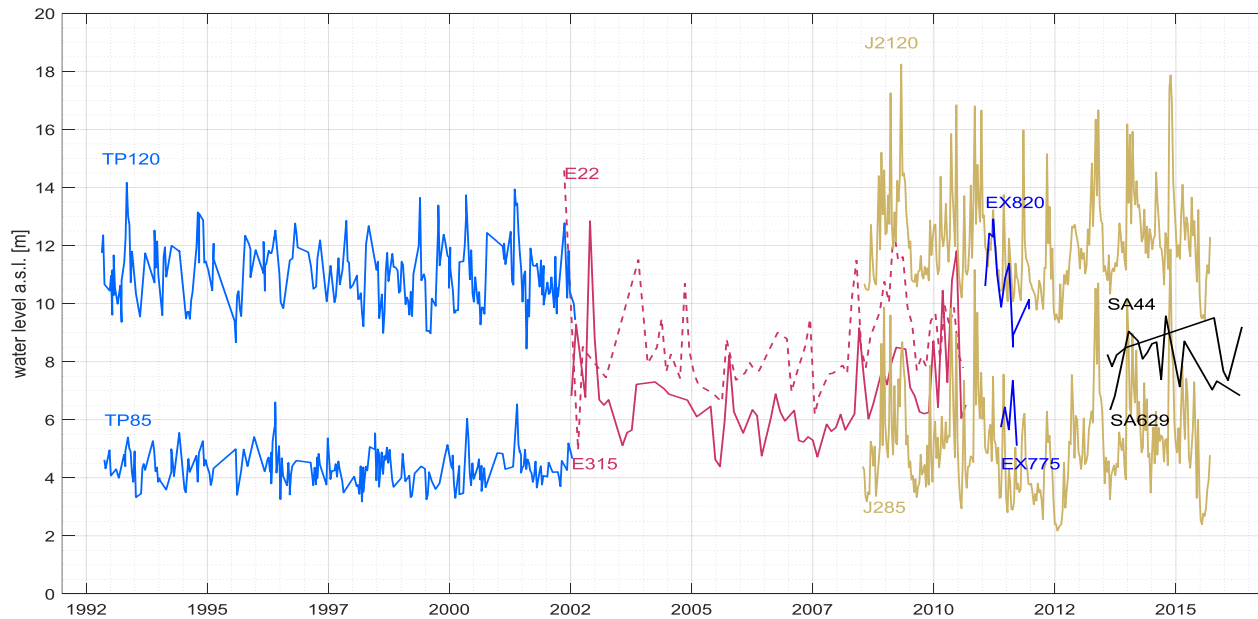
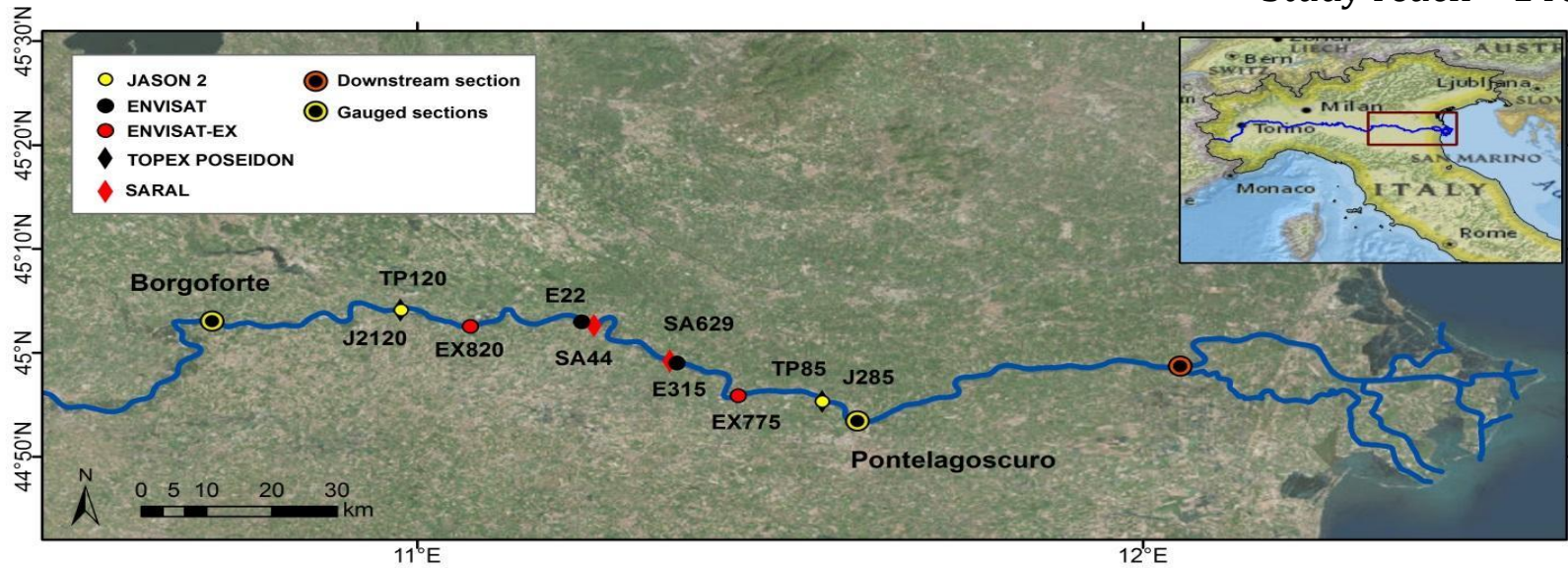
- the effect of satellite record length (i.e. number of available measurements) on the calibration of the hydraulic model;
- the impact of the uncertainty of altimetry data on the accuracy of model calibration;
- comparison of different satellite altimetry products;
- the benefit of multi-mission series, which overcome the low satellite temporal resolution.



*Temporal distribution of all satellite altimetry missions available up to 2016 (red line): TOPEX/Poseidon, Envisat, Envisat EX, JASON-2, SARAL/AltiKa (\*ERS-2 data are shown for completeness but not explicitly considered in the study).*

# CASE STUDY

Study reach ~140 km



Synoptic view of altimetry series at the virtual stations identified along the river stretch of interest

# CASE STUDY



Mission	Abbreviations	Version	Retracker	Observation period	Temporal resolution [day]
TOPEX/Poseidon	TP	MGDR-B	onboard	1992–2002	10
Envisat	E	GDR	ICE-1	2002–2010	35
Envisat XT	EX	GDR	ICE-1	2010–2012	35
SARAL/AltiKa	SA	GDR-t	onboard	2013–2016	35
JASON 2	J2	GDR	ICE-3	2008–2015	10
Multi-mission	MM			1995–2016	3

Satellite sensors and altimetry series considered in this study

# DATA ANALYSIS – Multi-mission

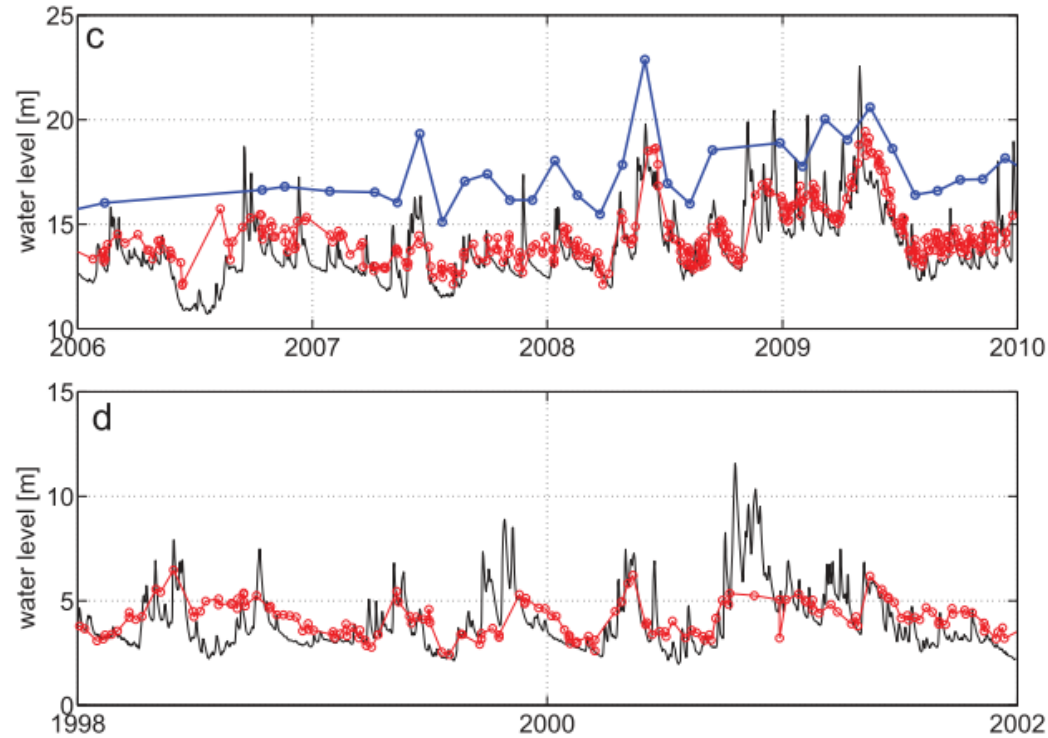
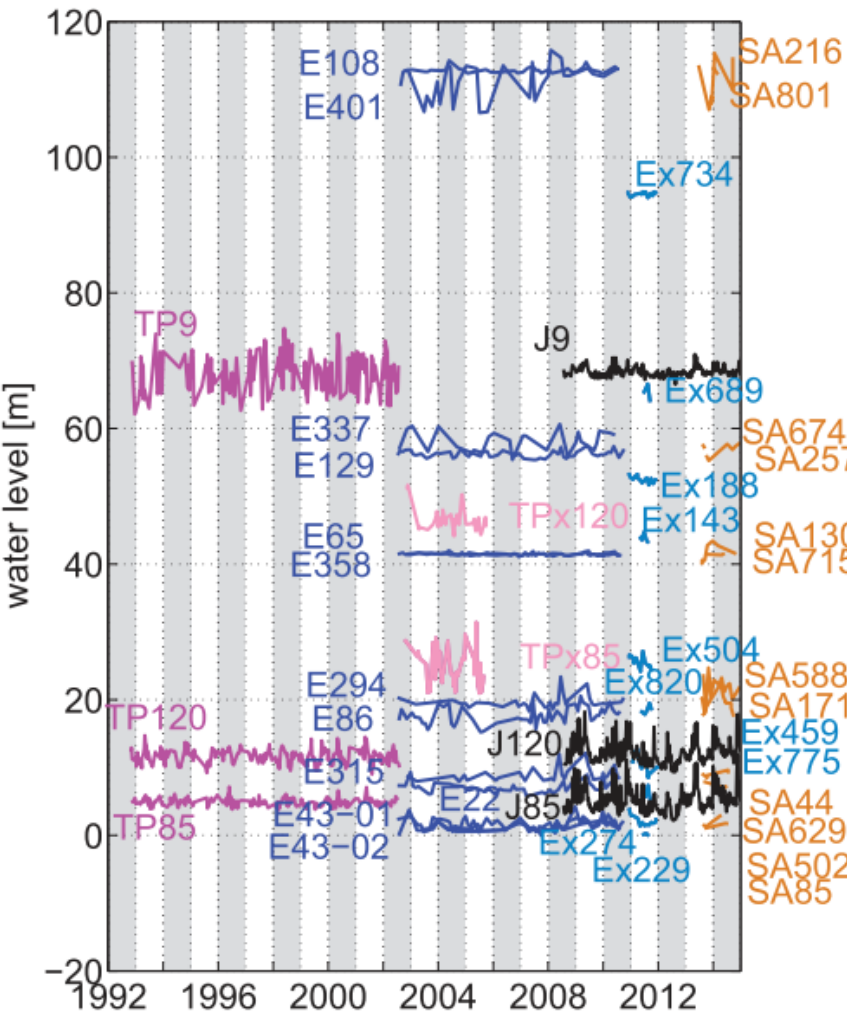


**Table 4.** Mean Water Level Time Series Obtained From Different Missions Over the Northern Part of the Adriatic Sea Against Tide Gauge

Mission	Mean Water Level (m)	Number
TOPEX/Poseidon	$0.48 \pm 0.03$	516
TOPEX/Poseidon XT	$0.41 \pm 0.05$	164
ENVISAT	$0.52 \pm 0.06$	148
ENVISAT-XT	$0.55 \pm 0.06$	21
Jason 1	$0.61 \pm 0.04$	363
Jason 2	$0.55 \pm 0.04$	255
CryoSat-2	$-1.19 \pm 0.05$	114
SARAL/AltiKa	$0.42 \pm 0.05$	22

- in situ water level
- original altimetric water level from ENVISAT
- densified altimetric water level

# DATA ANALYSIS – single mission

$$\varepsilon(x, t) = h_{sat}(x, t) - h_{obs}(x, t)$$



Estimated at VS by linearly interpolating concurrent water elevation measured at the gauging stations

EX775 and SA44 are particularly limited in the number of measurements.

Jason 2 outperforms all the other satellite products.

VS	n° data	r <sup>2</sup> [-]	μ [m]	σ [m]
TP120	174	0.77	-0.42	0.75
TP85	158	0.60	0.08	0.70
E22	61	0.85	0.05	0.87
E315	65	0.97	0.30	0.43
EX820	12	0.91	0.50	0.57
EX775	5	-0.35	1.17	1.40
J2-120	261	0.99	0.17	0.30
J2-85	259	0.98	0.19	0.37
SA44	8	0.92	0.14	0.55
SA629	15	0.96	0.40	0.30

# DATA ANALYSIS – multi-mission

$$\varepsilon(x, t) = h_{mm}(x, t) - h_{obs}(x, t)$$

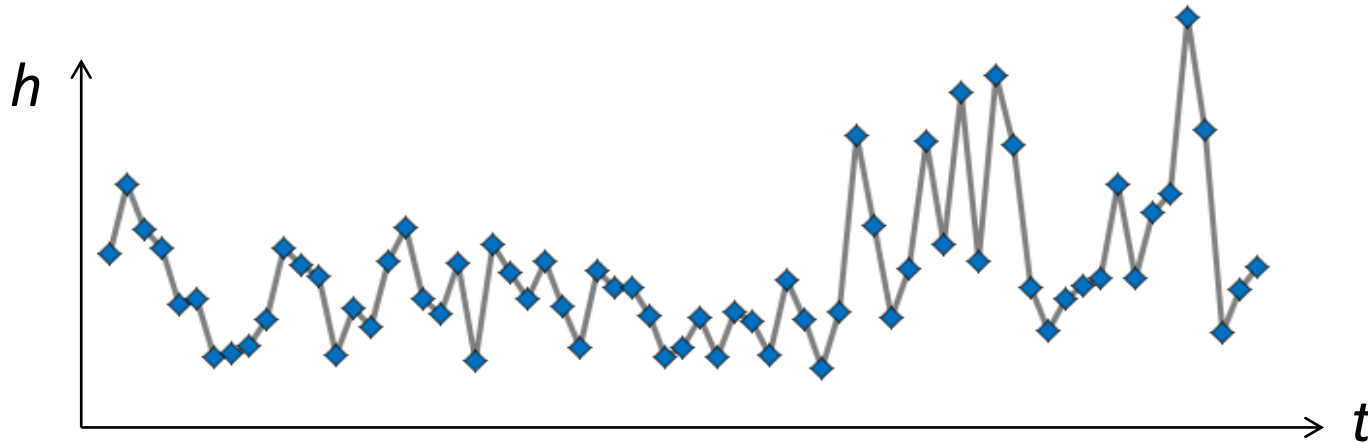
All multi-mission series reports a considerable number of observations

VS	n° data	r <sup>2</sup> [-]	μ [m]	σ [m]
MM120	1411	0.77	0.91	0.96
MM820	1237	0.77	-0.01	0.85
MM22	1235	0.78	0.20	0.89
MM44	1411	0.78	0.14	0.89
MM629	1411	0.78	0.36	0.87
MM315	1236	0.78	0.39	0.87
MM775	1236	0.77	0.79	0.93
MM85	1413	0.77	0.99	0.99

Multi-mission series (MM) algorithm connects all VSs hydraulically and statistically and densifies the water level time series obtaining a temporal density on average equal to **3 days**



# DATA ANALYSIS



$L_{tot}$  = total record length of the original satellite dataset (total number of observations)

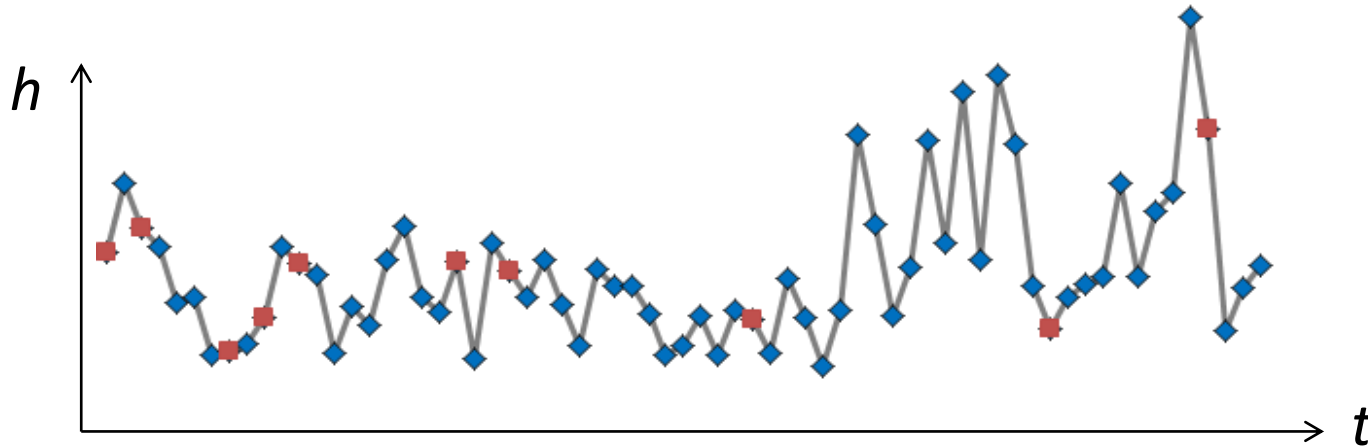
$m$  = generic record length;

$$\mathbf{h}_{sat,m}(x) = [h_{sat,m}(x, t_1), h_{sat,m}(x, t_2), \dots, h_{sat,m}(x, t_{m-1}), h_{sat,m}(x, t_m)] \quad \forall m = 3, \dots, L_{tot}$$

$$\mathbf{h}_{obs,m}(x) = [h_{obs,m}(x, t_1), h_{obs,m}(x, t_2), \dots, h_{obs,m}(x, t_{m-1}), h_{obs,m}(x, t_m)]$$

1000  $\mathbf{h}_{sat,m}(x)$  subsets for each  $m$  value

# DATA ANALYSIS



$L_{tot}$  = total record length of the original satellite dataset

$m$  = generic record length;

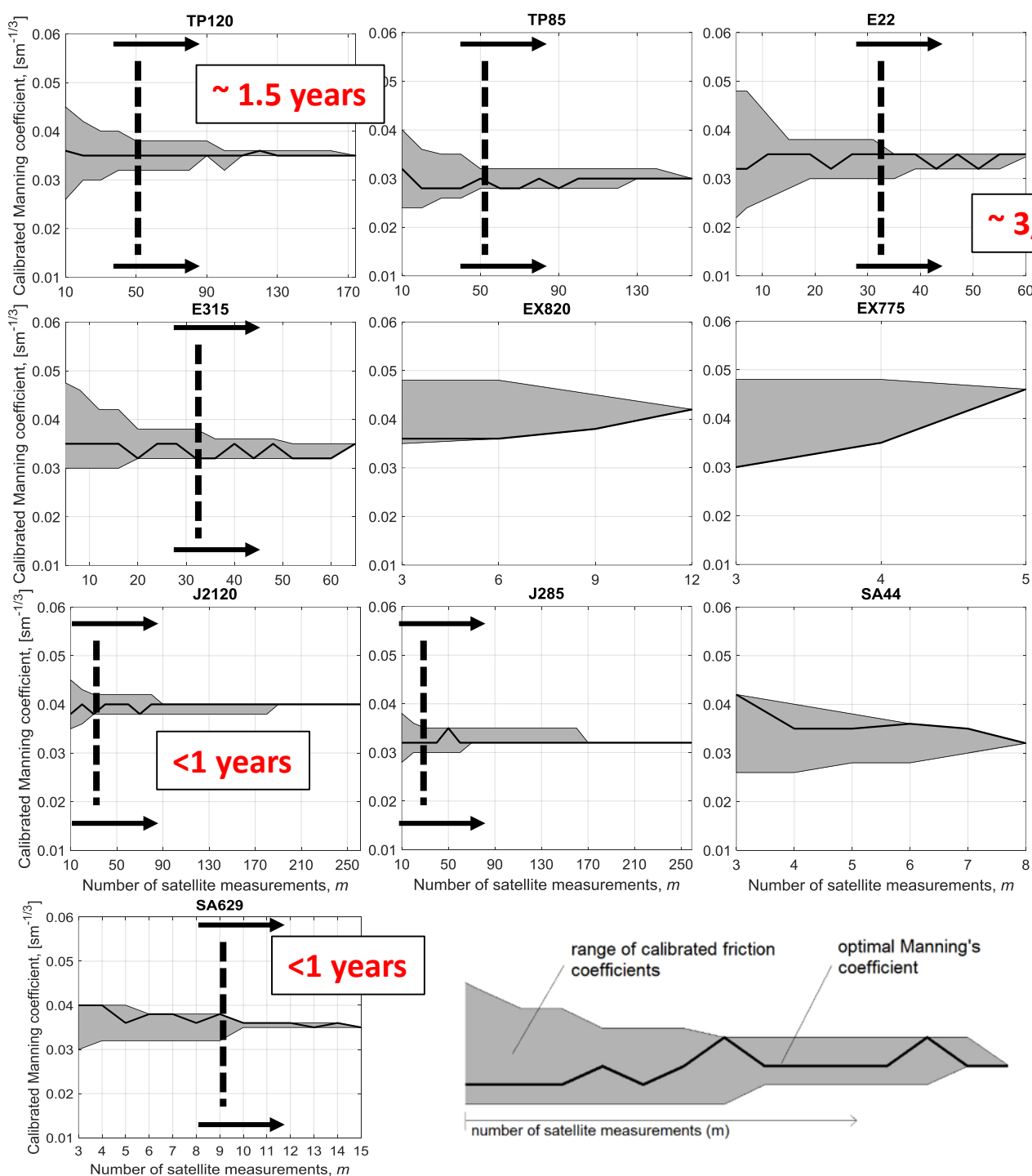
$$\mathbf{h}_{sat,m}(x) = [h_{sat,m}(x, t_1), h_{sat,m}(x, t_2), \dots, h_{sat,m}(x, t_{m-1}), h_{sat,m}(x, t_m)] \forall m = 3, \dots, L_{tot}$$

$$\mathbf{h}_{obs,m}(x) = [h_{obs,m}(x, t_1), h_{obs,m}(x, t_2), \dots, h_{obs,m}(x, t_{m-1}), h_{obs,m}(x, t_m)]$$

1000  $\mathbf{h}_{sat,m}(x)$  subsets for each  $m$  value

# RESULTS

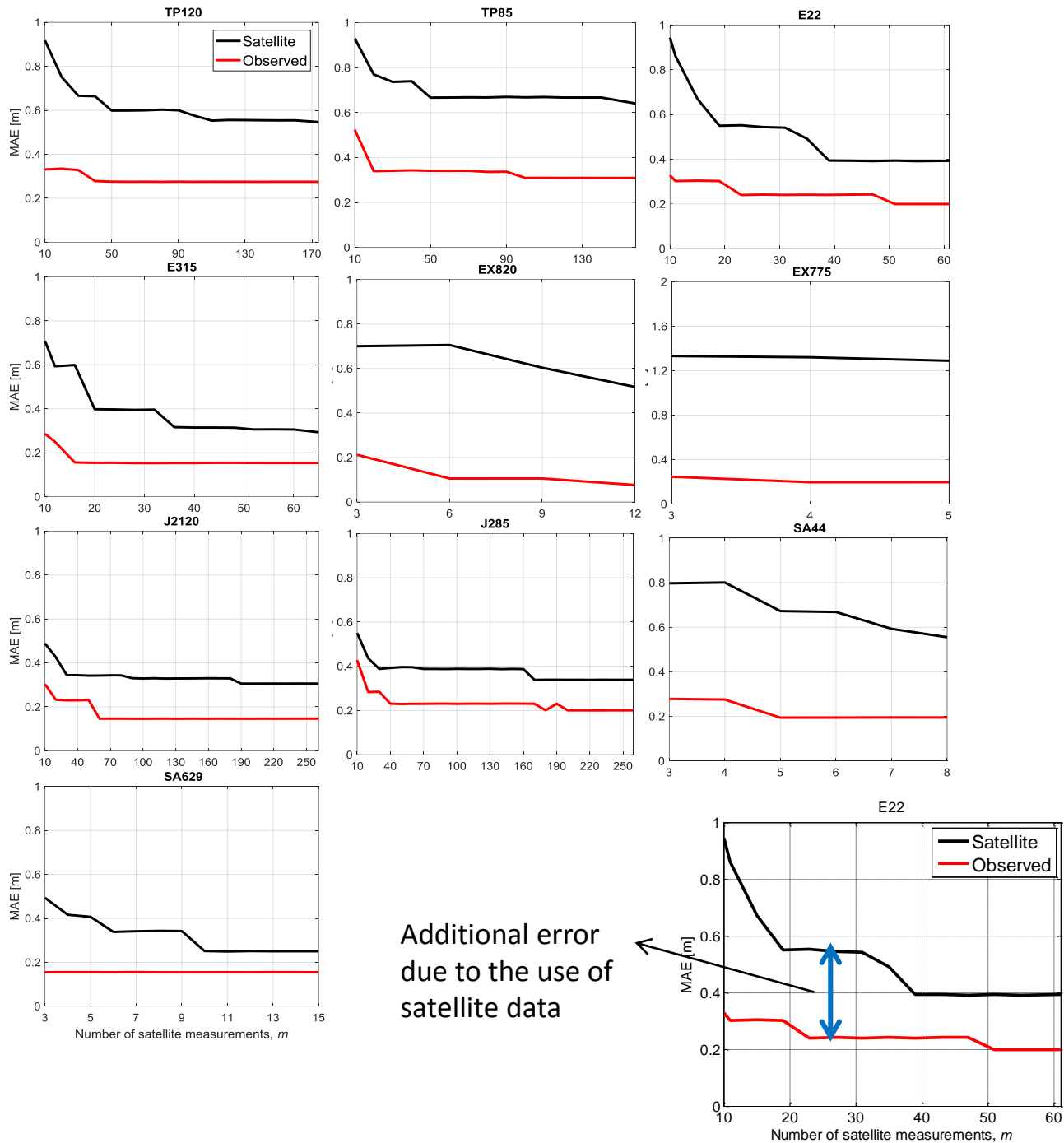
Calibration results for different altimetry series length: range of calibrated roughness coefficient (grey areas) and optimal Manning's value (black line) as a function of the number of satellite measurements,  $m$ .



Similar results using ERS-2 series

# RESULTS

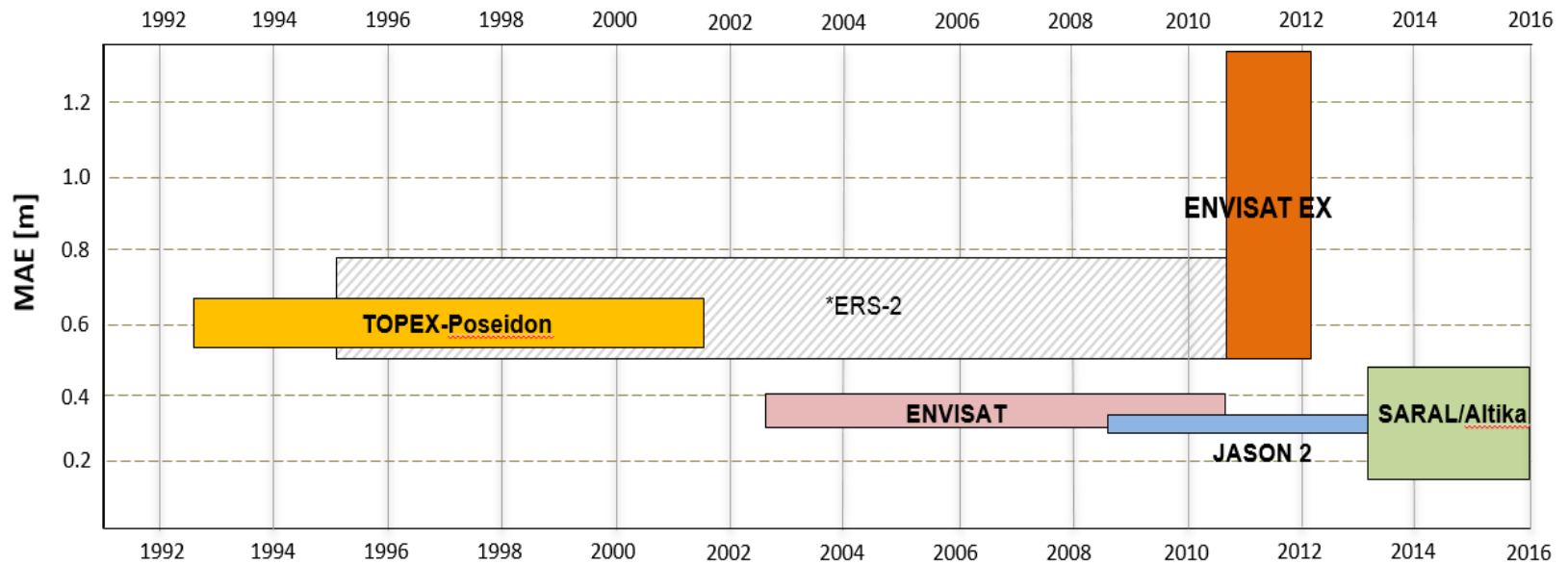
Maximum mean absolute error (MAE) obtained calibrating the numerical model with satellite altimetry data (black line) and in situ water levels (red line) as a function of data length,  $m$ .



Additional error due to the use of satellite data

# RESULTS

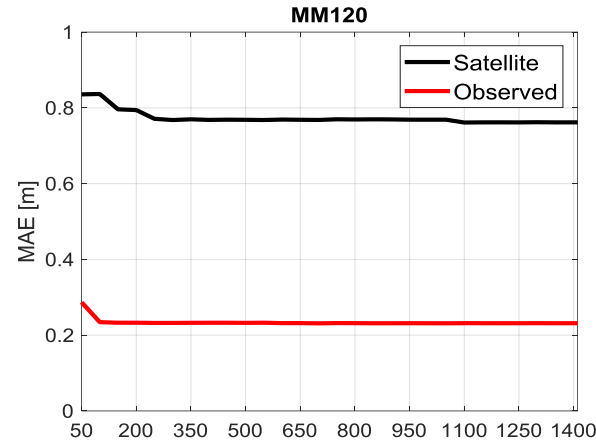
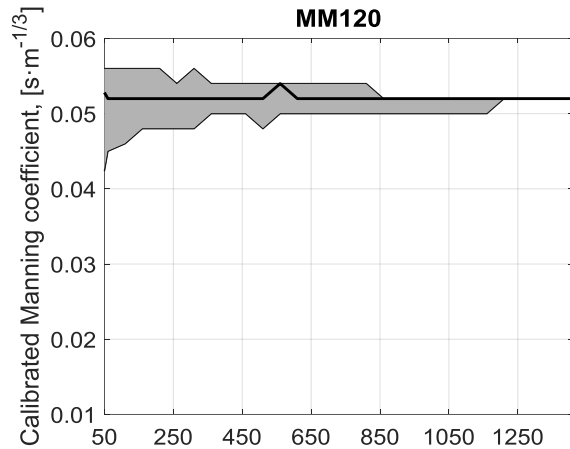
## Single mission



Synoptic view of the maximum mean absolute error (MAE) of each satellite mission in time (\*ERS-2 is a recall from a previous investigation): the vertical height of each box is defined as the range of the MAE obtained from the calibration considering  $m = L_{tot}$

# RESULTS – Multi-mission

Example of results obtained using Multi-mission series

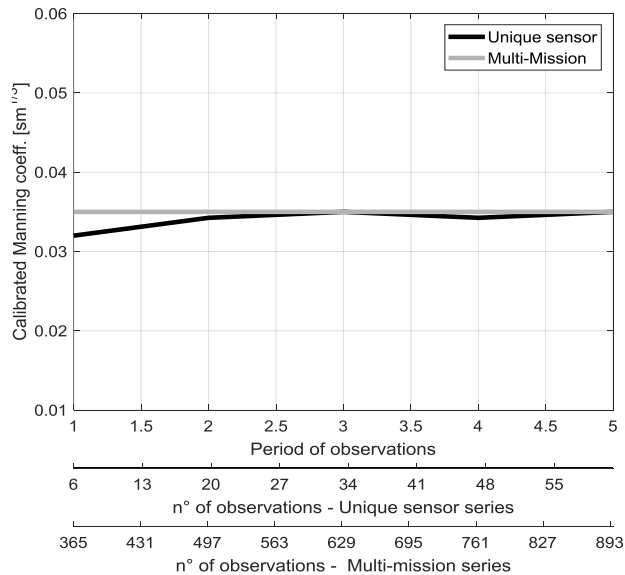
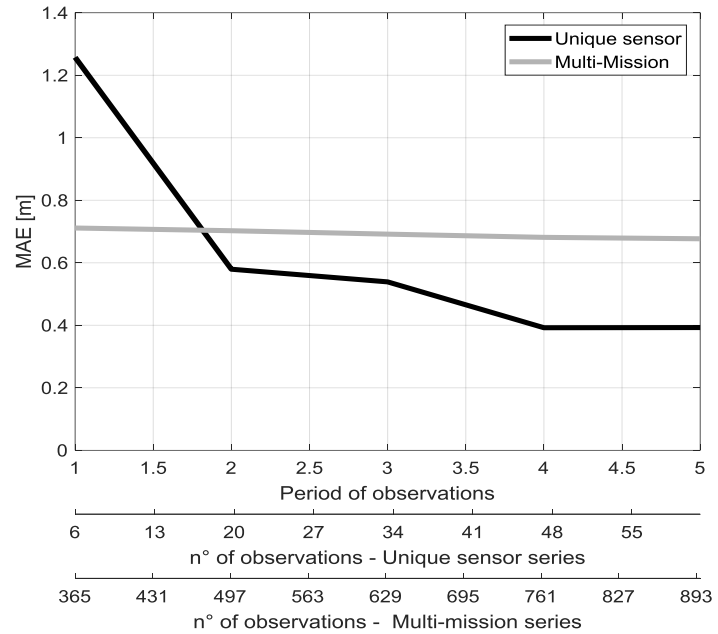
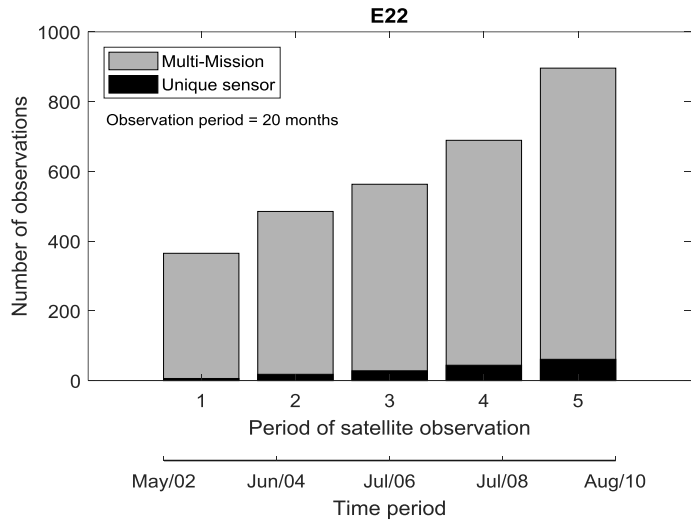


VS	MM series			Original altimetry series			$\Delta = \text{MM} - \text{Orig.}$		
	n [ $\text{m}^{1/3}\text{s}^{-1}$ ]	RMSE [m]	MAE [m]	n [ $\text{m}^{1/3}\text{s}^{-1}$ ]	RMSE [m]	MAE [m]	$\Delta n$ [ $\text{m}^{1/3}\text{s}^{-1}$ ]	$\Delta$ -RMSE [m]	$\Delta$ -MAE [m]
MM -E22	0.035	0.94	0.68	0.035	0.83	0.39	0.00	0.11	0.29
MM-E315	0.035	0.89	0.64	0.035	0.46	0.29	0.00	0.43	0.35
MM-EX820	0.038	0.92	0.65	0.042	0.61	0.52	-0.004	0.31	0.13
MM-EX775	0.043	0.96	0.70	0.046	1.53	1.29	-0.003	-0.57	-0.59
MM-TP120	0.052	1.07	0.76	0.035	0.75	0.55	0.017	0.32	0.21
MM-TP85	0.043	1.02	0.73	0.030	0.79	0.64	0.013	0.23	0.09
MM-SA44	0.032	0.96	0.69	0.034	0.72	0.56	-0.002	0.24	0.13
MM-SA629	0.035	0.90	0.65	0.035	0.29	0.25	0.00	0.61	0.4
MM-J2-120	0.052	1.07	0.76	0.040	0.40	0.31	0.012	0.67	0.45
MM-J2-85	0.043	1.02	0.73	0.032	0.48	0.34	0.011	0.54	0.39

Calibration results:  
optimal calibrated Manning's coefficient (n), root mean square error (RMSE) and mean absolute error (MAE) obtained from the calibration process performed adopting the MM and original altimetry series ( $m = L_{\text{tot}}$ ).

# RESULTS

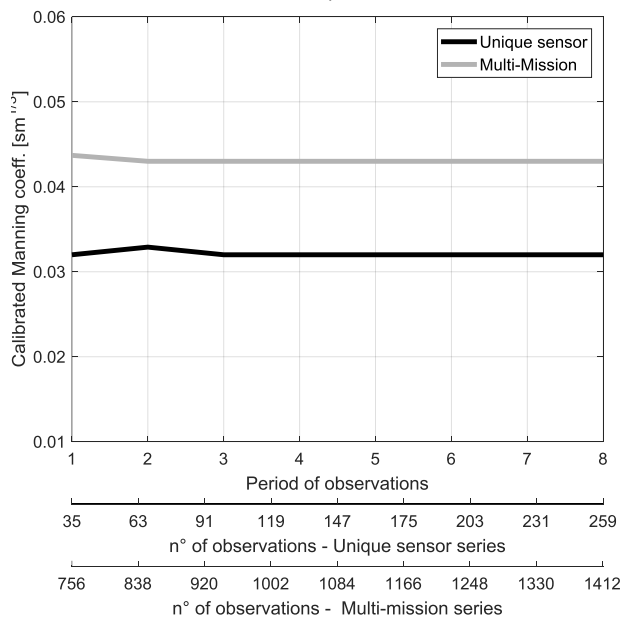
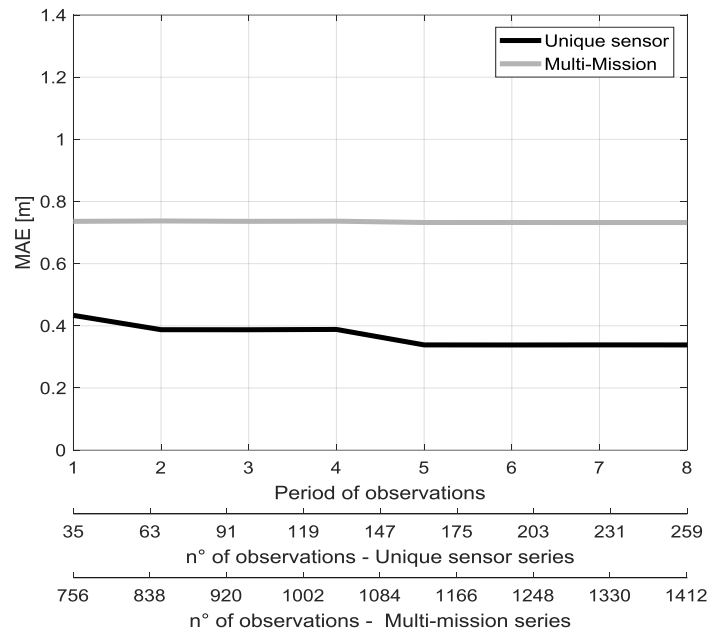
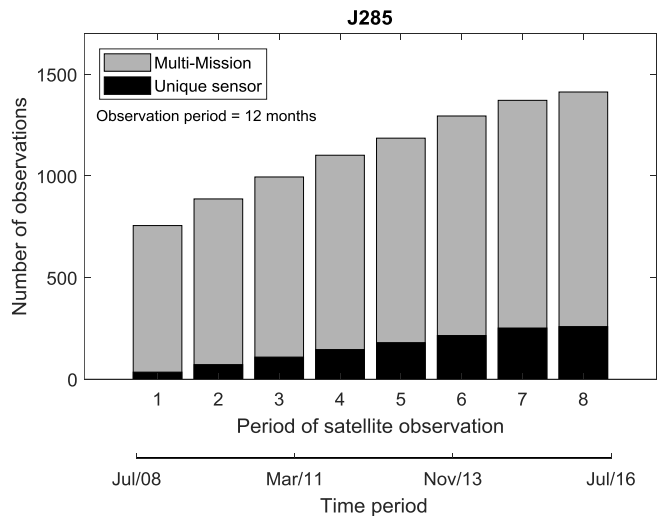
## Single Vs. Multi-mission



## ENVISAT Vs. Multi-mission

# RESULTS

## Single Vs. Multi-mission



## JASON-2 Vs. Multi-mission





# INLAND WATER MONITORING - THE **SWOT** MISSION AND ITS CAPABILITIES FOR LAND HYDROLOGY

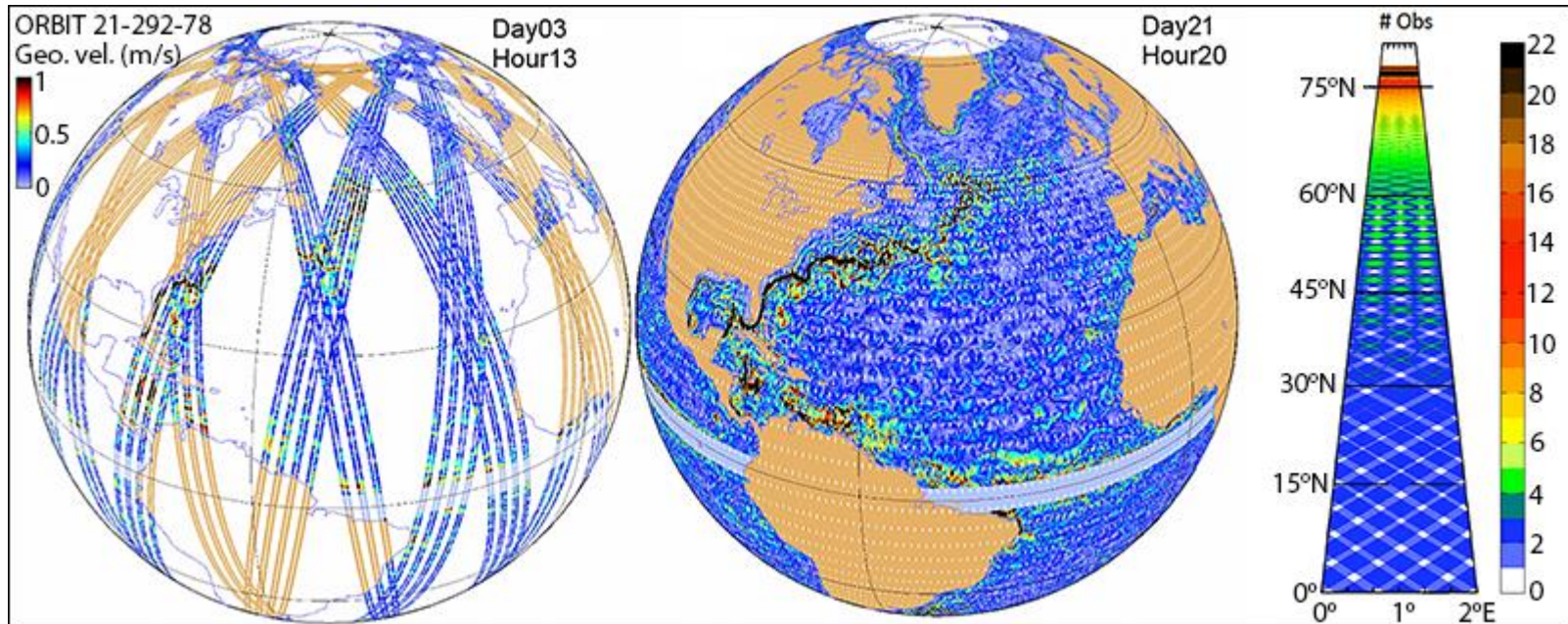
## **SWOT: Surface Water and Ocean Topography**

NASA, French, Canadian and United Kingdom  
Space Agencies

To be launched on Sept. 2021, SWOT will completely cover the world's oceans and freshwater bodies with repeated high-resolution elevation measurements.

<https://swot.jpl.nasa.gov/>

# Spatial and temporal coverage



SWOT's nominal coverage during its 3-year science orbit will include measurements between 78°N and 78°S collected over a period of 21 days. Maps show the **coverage after 3 days (left)** and the **full 21 days (center)** of a complete cycle. The graphic at the far right illustrates the number of **observations at a given latitude during the 21-day repeat period**.

Credits: C. Ubelmann, CLS (left, center) and JPL/NASA (right)

# Science requirements and goals

---

Observed areas	All observed water areas detected by SWOT will be provided to end users, but: errors will be <i>evaluated</i> for $(250 \text{ m})^2$ (= 62,500 m <sup>2</sup> ) water bodies and 100 m (width) × 10 km (long) river reaches or higher errors will be <i>characterized</i> for $(100 \text{ m})^2$ to $(250 \text{ m})^2$ <u>water bodies and 50 m to 100 m (width) × 10 km (long) river reaches</u>
Height accuracy	<10 cm when averaging over water area >1 km <sup>2</sup> <25 cm when averaging over $(250 \text{ m})^2$ <water area <1 km <sup>2</sup>
Slope accuracy	<u>1.7 cm/km</u> for evaluated river reaches when averaging over water area >1 km <sup>2</sup>
Relative errors on water areas	<15 % for evaluated water body and river reaches <25 % of total characterized water body and river reaches
Mission lifetime	3 months of fast sampling calibration orbit + 3 years of nominal orbit
Rain/layover/frozen water flag	68 % or more of the contaminated data should be correctly flagged
Data collection	>90 % of all ocean/continents within the orbit during 90 % of operational time

---

Rodriguez E. (2015) Surface Water and Ocean Topography mission (SWOT), Science Requirements Document. JPL document D-61923. [https://swot.jpl.nasa.gov/files/swot/SRD\\_021215.pdf](https://swot.jpl.nasa.gov/files/swot/SRD_021215.pdf).

Biancamaria et al., 2016 (SG)

# Science requirements and goals

---

## Orbit

Altitude	890.5 km
Inclination	77.6°
Repeat period	20.86 days

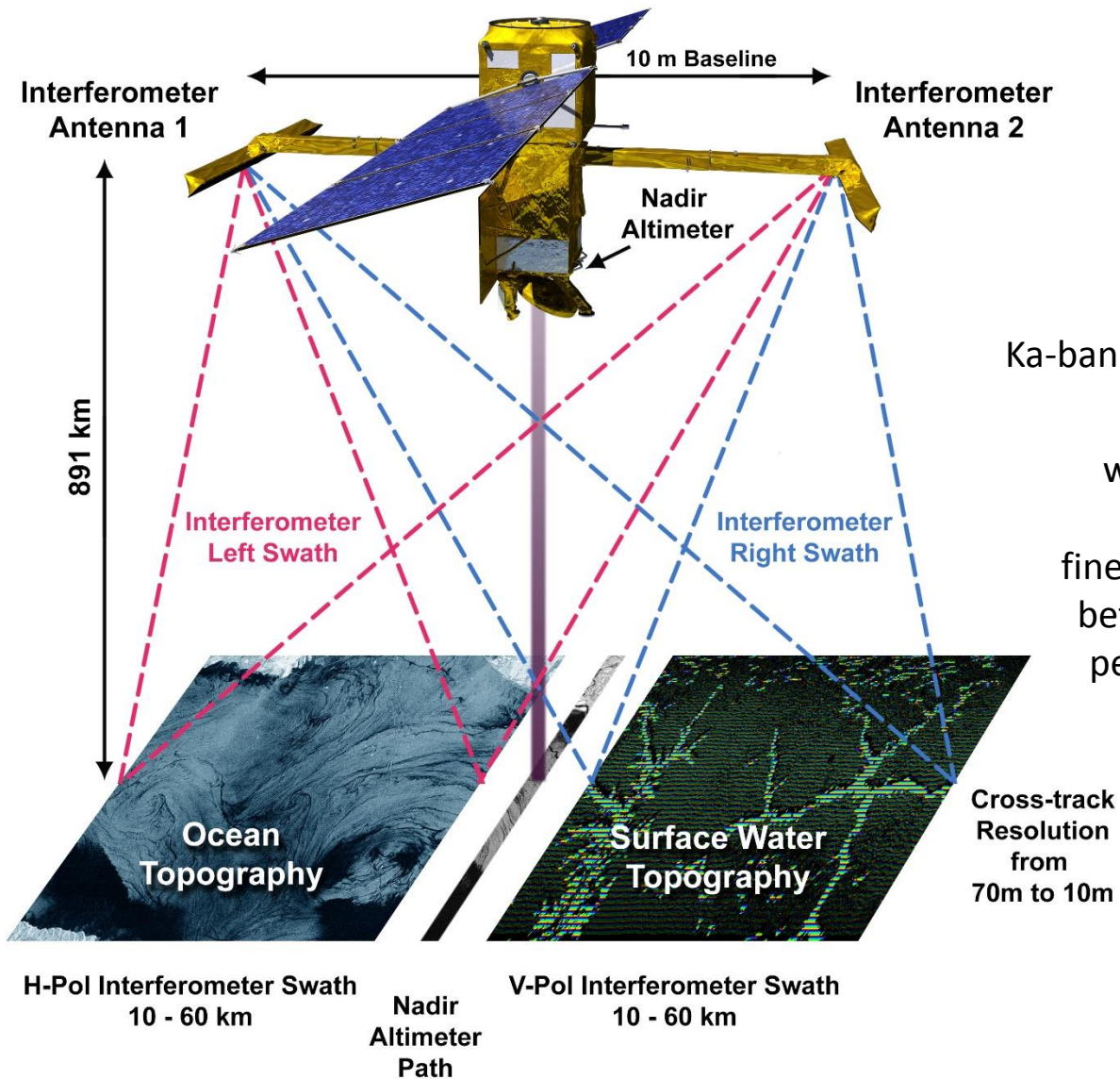
## KaRIn (core payload)

One swath extent (total swaths: 2)	50 km
Distance between the two swaths outer edges	120 km
Distance between the two swaths inner edges ("nadir gap")	20 km
Radar frequency/wavelength	35.75 GHz/8.6 mm (Ka-band)
Distance between the two antennas (baseline)	10 m
Instrument azimuth pixel size (radar projection)	6–7 m
Instrument range pixel size (radar projection)	From 60 m (near range, incidence angle $\sim 0.6^\circ$ ) to 10 m (far range, $\sim 3.9^\circ$ )

## Additional science payload

Nadir altimeter	Similar to the dual-frequency (Ku/C) Poseidon-3 nadir altimeter on Jason-2
Precise orbit determination system	Laser retroreflector DORIS receiver GPS receiver
Radiometer (usable only over oceans)	Three-frequency (18, 23 and 34 GHz) radiometer, similar to advanced microwave radiometer on Jason-2

---



Ka-band SAR interferometer (Ka-RIn)

Ka-band, instead of higher wavelength bands, has several

**advantages:**

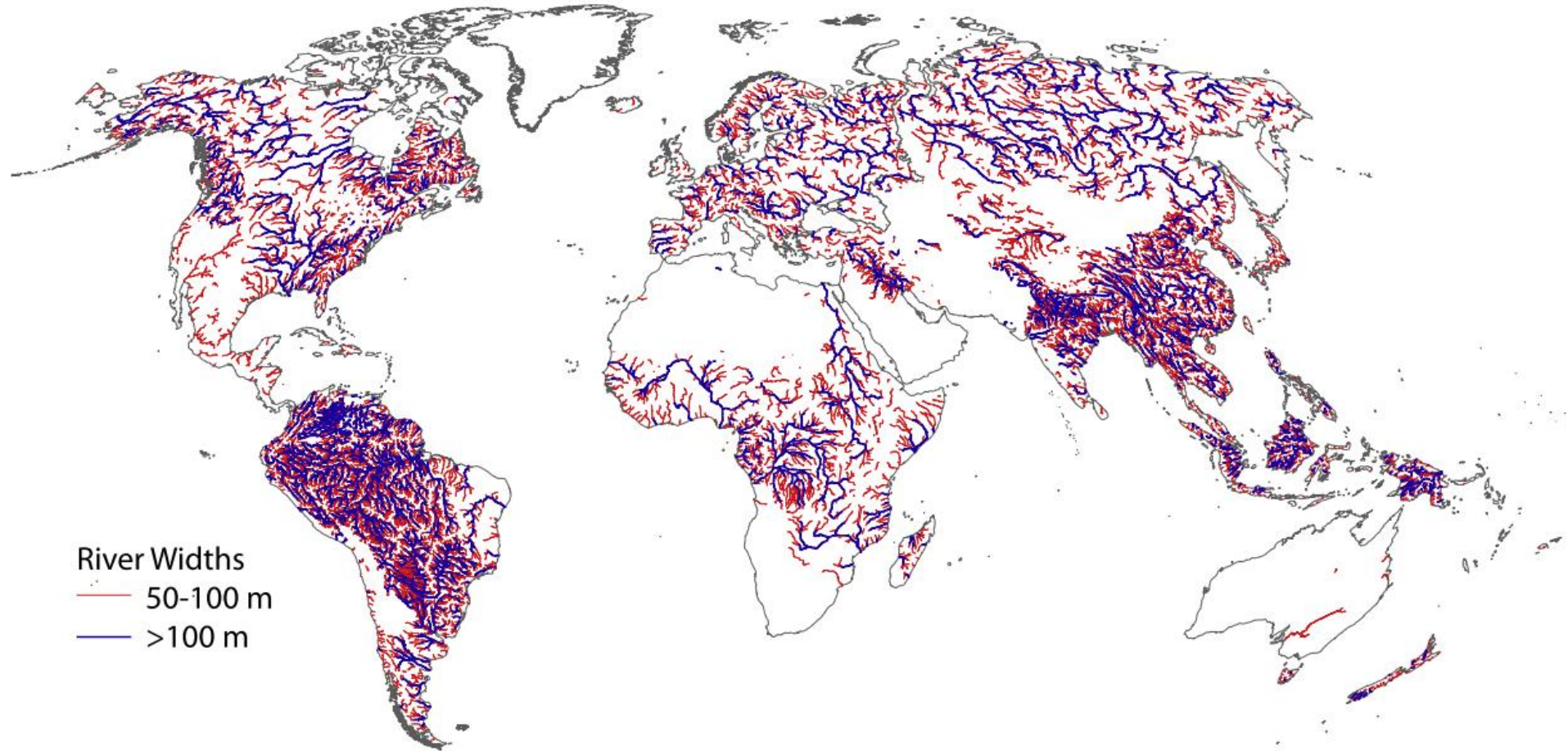
finer resolution, shorter distance between the two antennas, less penetration into soil, snow and vegetation.

**drawback:** sensitivity to rain rates > 3 mm/h

Diagram illustrating the swaths of data that SWOT will collect. The interferometer will produce two parallel tracks, with a Nadir track from a traditional altimeter in the gap between the swaths. The overall width of the swaths will be approximately 120 km.

# Global river coverage

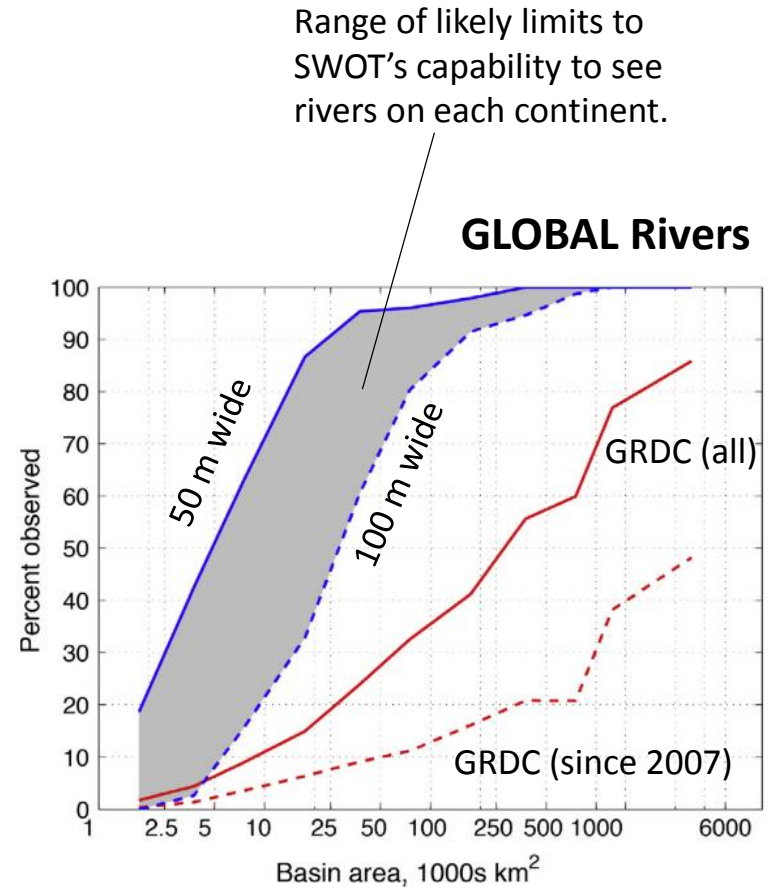
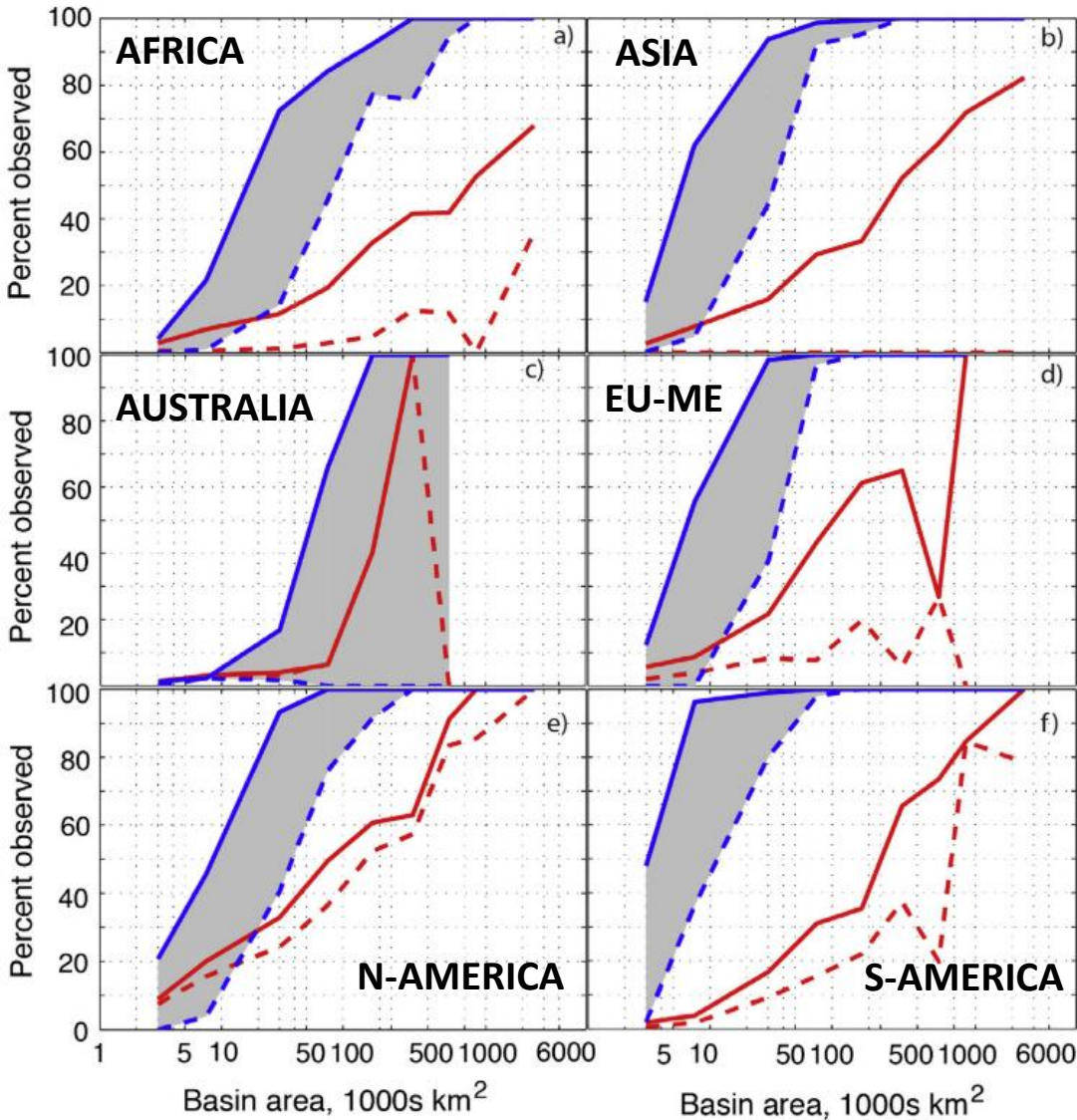
Pavelsky et al., 2014 (JH)



Map of global river database used in this study (*GRDC*).

**Allen, G. H., & Pavelsky, T. M. (2018). Global extent of rivers and streams. *Science*.**

# Global river coverage



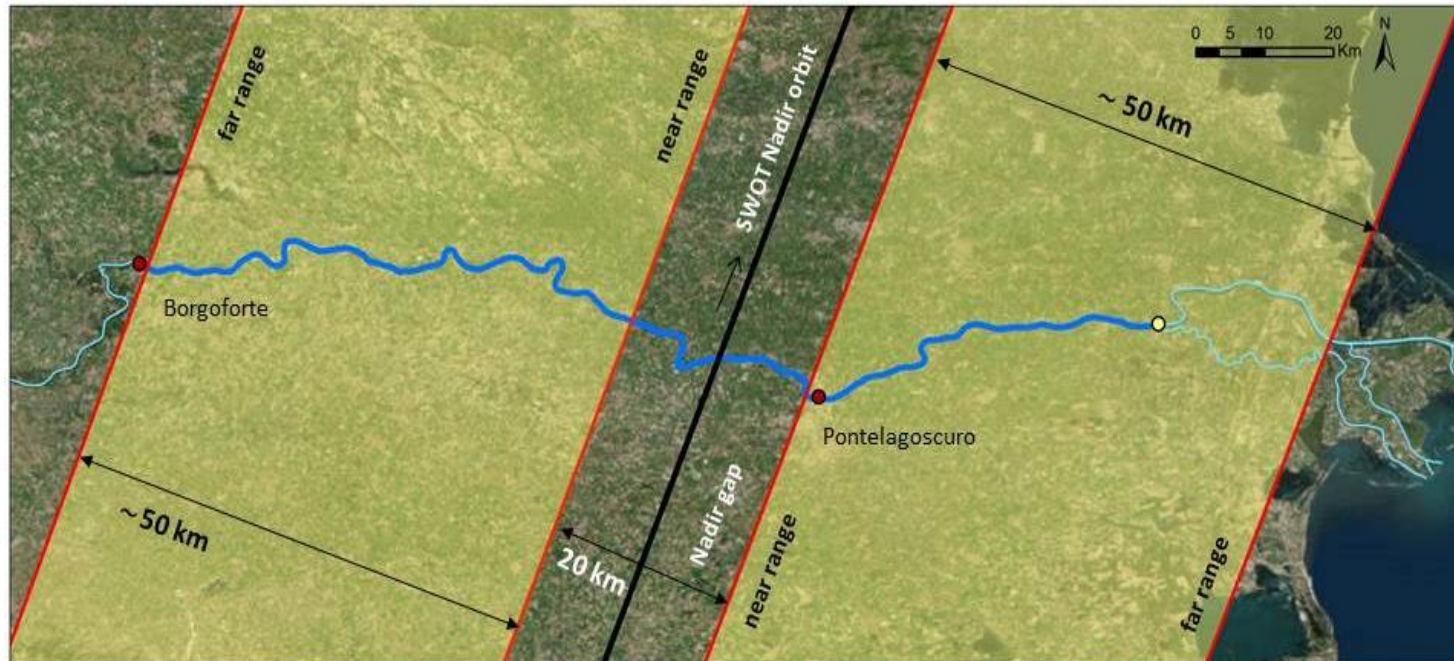
SWOT would observe more than 60 % of the global sub-basins with an area of 50,000 km<sup>2</sup> given the ability to observe rivers wider than 100 m. If SWOT can meet the goal of observing 50-m-wide rivers, more than 60 % of sub-basins with an area of 10,000 km<sup>2</sup> would be observed.

# SWOT products

Fjortoft et al., 2014 (IEEE)  
Domeneghetti et. al., 2018 (JH)

## SWOT Hydrology Simulator developed by JPL

The simulation assumes a backscatter coefficient ( $\sigma_0$ ) of -5 dB for land and 10 dB for water.

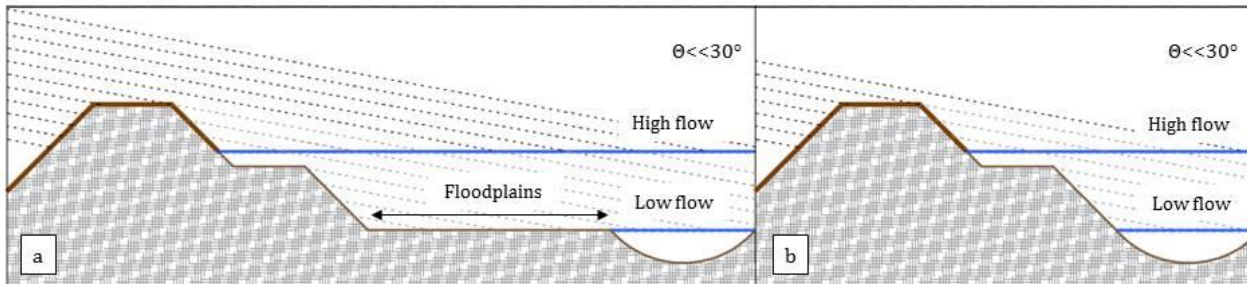
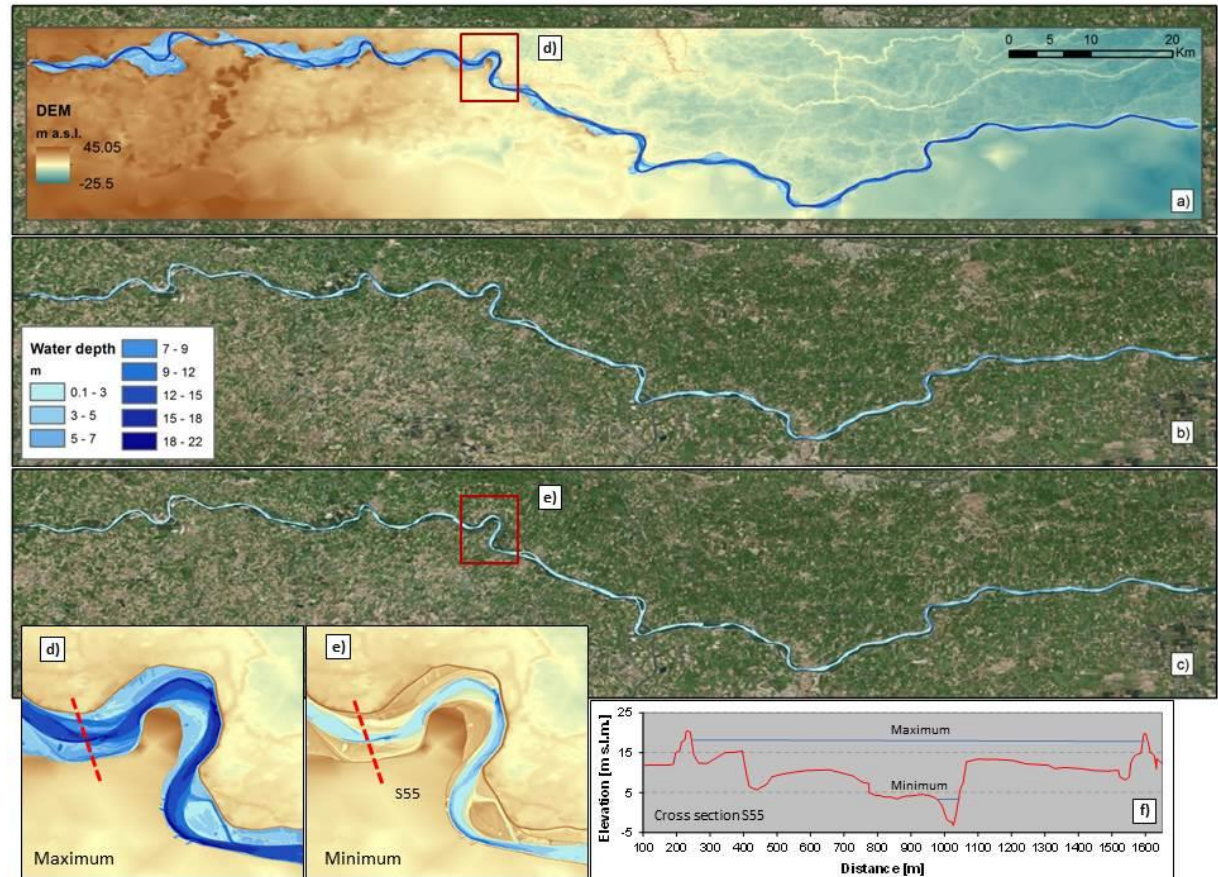


Example of a SWOT orbital pass over the study area: satellite swath (yellow areas), Po river reach considered in the study (dark blue), flowing from the gauging station (red points) of Borgoforte to the beginning of the river delta (yellow point).



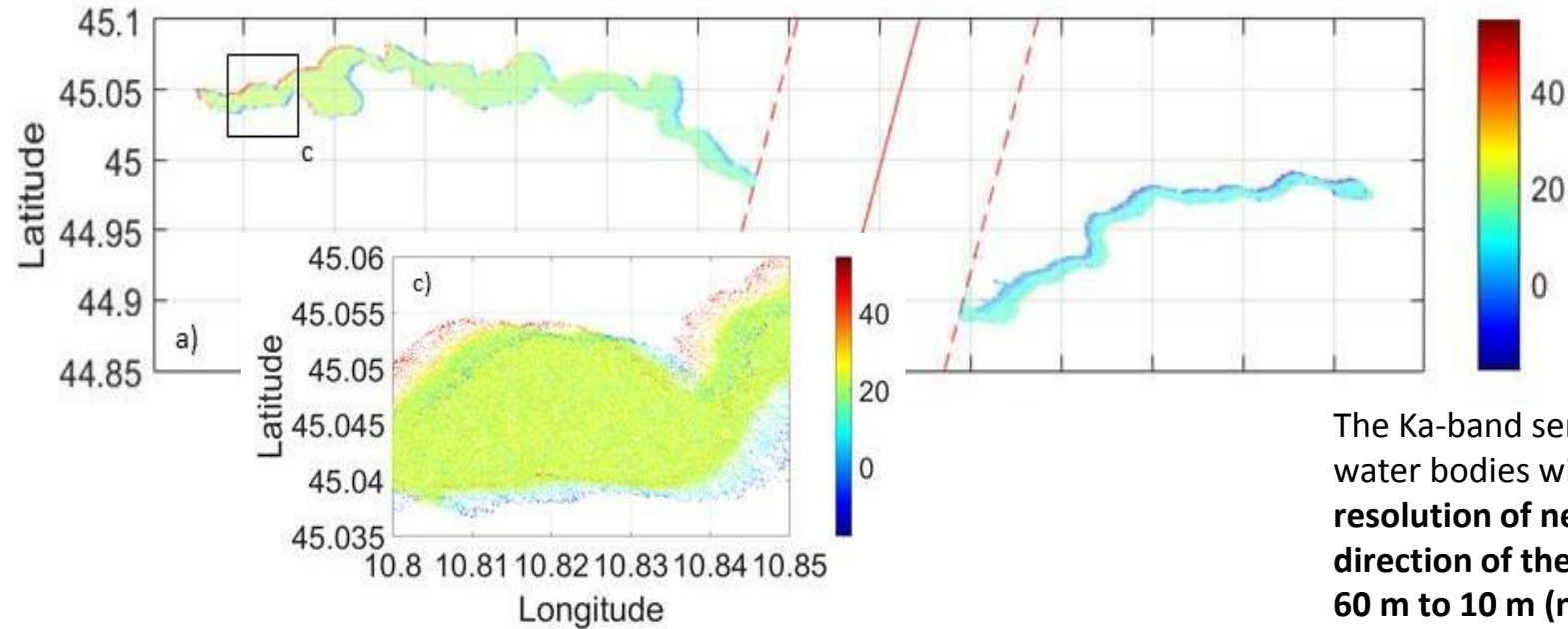
# SWOT products

Input datasets for the SWOT simulator: 2D water depth coverage simulated for (a) high, (b) mean and (c) low river flow conditions (blue scale) and 2 m resolution DEM for river bathymetry and flood prone areas (from brown to green). Red boxes identify the same area used to show the different flood extents for (d) high and (e) low flow events, which may correspond to very different water depths at a given cross-section (e.g., cross-section S55; panel (f)).



Layover illustration for embanked river in case of incidence angles  $\ll 30^\circ$  and in case of (a) large or (b) absent lateral floodplains (modified from Fjortoft *et al.*, 2014).

# SWOT products



The Ka-band sensor will observe water bodies with a **ground pixel resolution of nearly 6 m in the direction of the satellite, and from 60 m to 10 m (near and far range, respectively) in the direction perpendicular to the satellite track.**

Mean error (m) of water surface elevation for different point classifications.

	Point classification				
	All points	Interior water	Water near land edge	Land near water edge	Land
High flow	0.040	-0.0016	0.378	0.773	0.059
Mean flow	-0.354	-0.157	-1.249	-1.489	-0.197
Low flow	-0.51	-0.218	-1.365	-1.588	-0.47

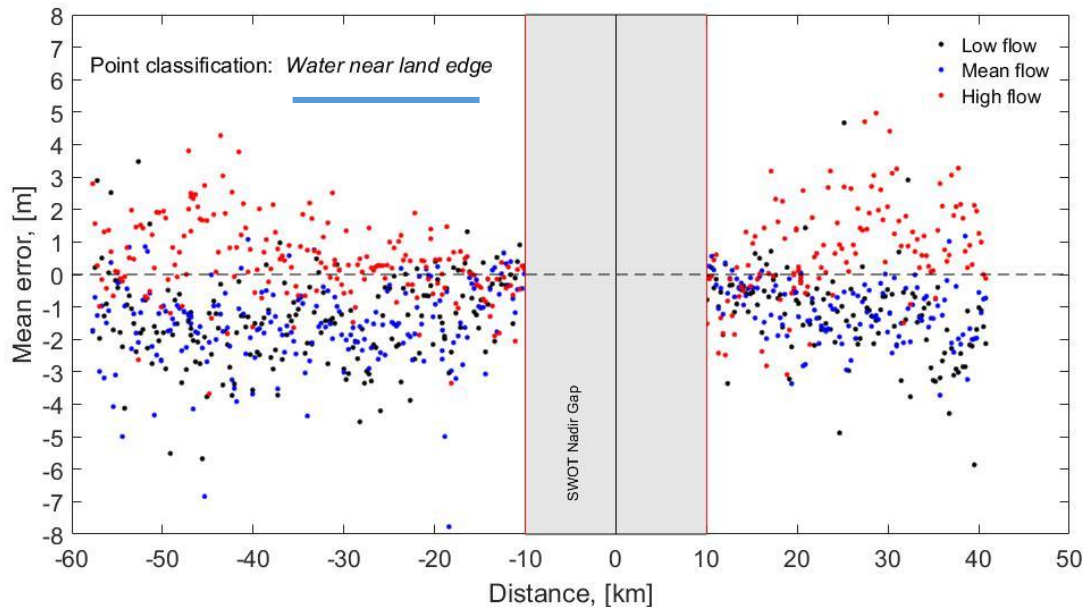
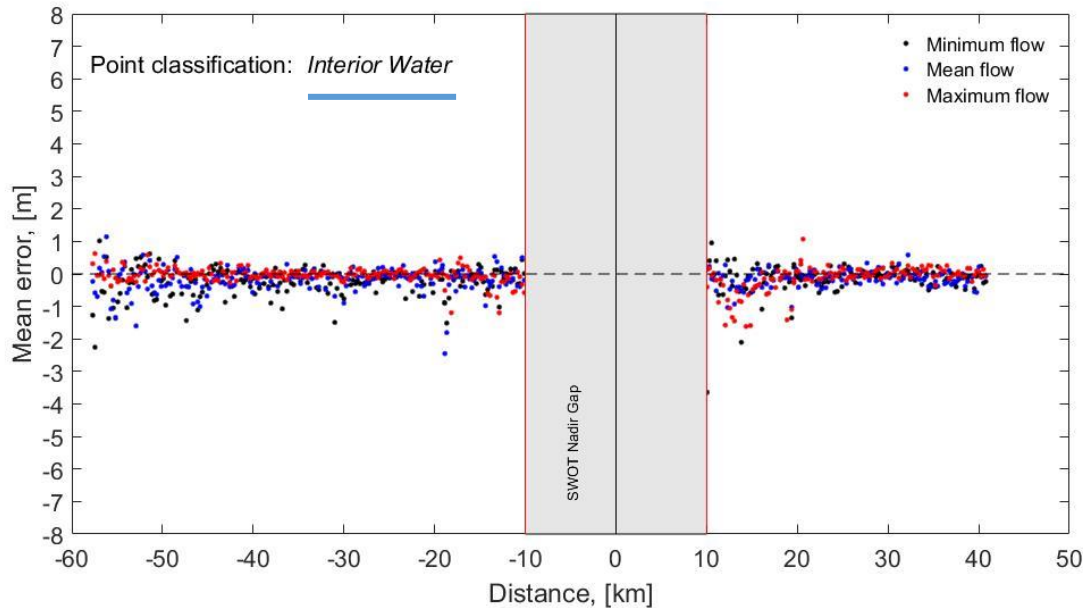
Some spatial averaging is required: **pixel cloud** → a collection of intrinsic pixels plotted with reference to a geographical coordinate system

**Mission Requirements - Height accuracy:**

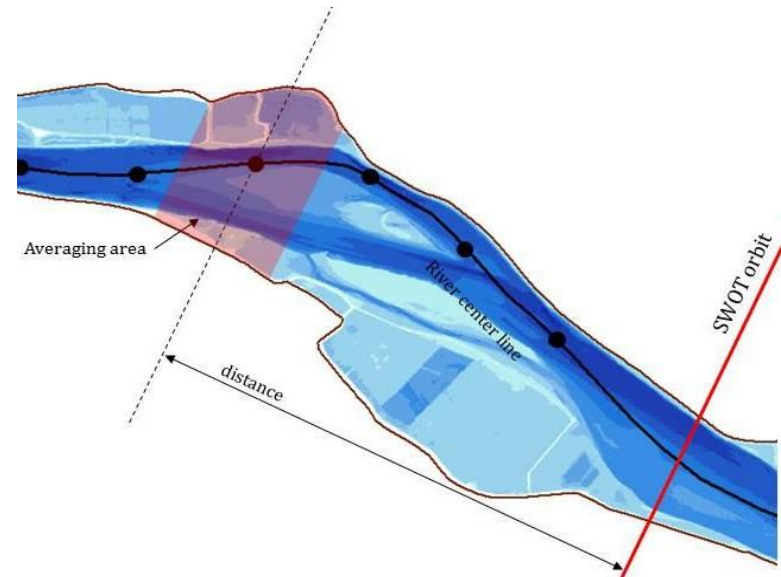
< 10 cm; area > 1 km<sup>2</sup>

< 25 cm; (250 m)<sup>2</sup> < water area < 1 km<sup>2</sup>

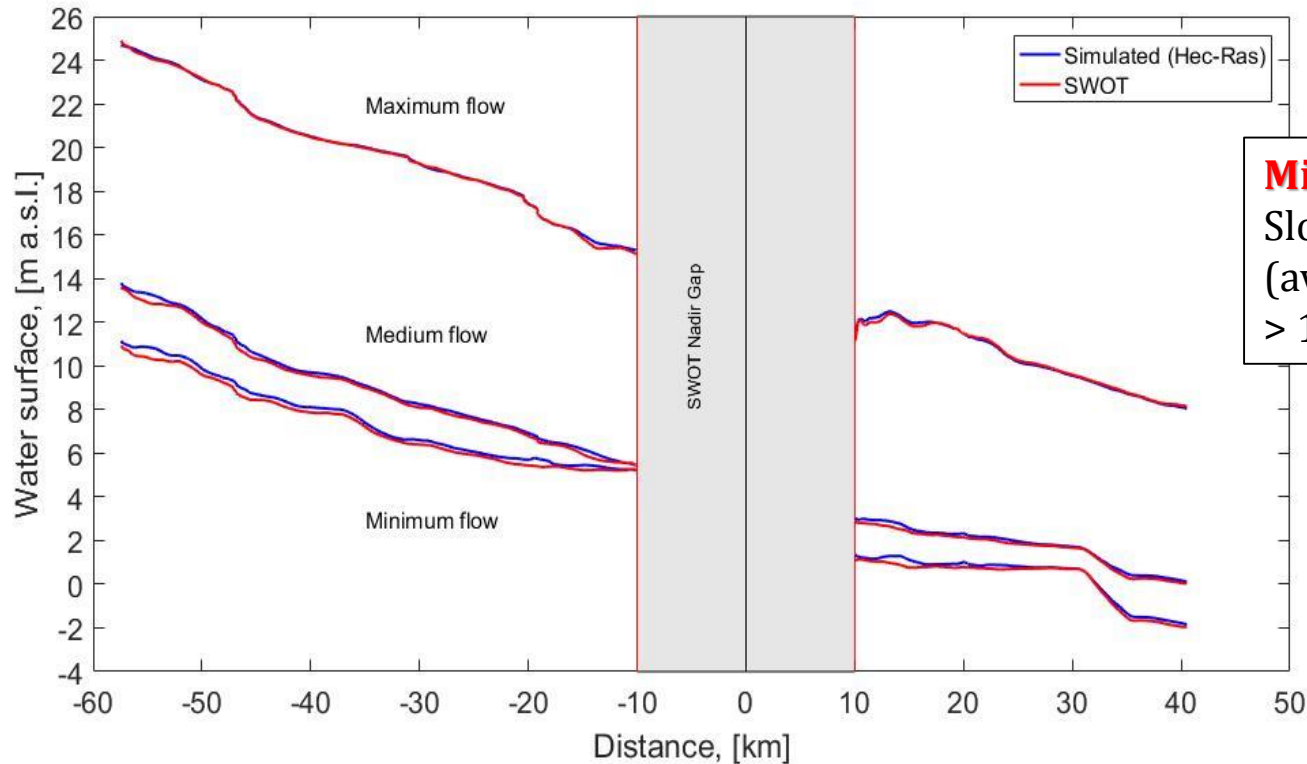
# SWOT products



Mean error (ME) on water surface elevation for interior water (upper panel) and water near land edge (lower panel) points; points are shown in relation to the distance from the Nadir orbit (negative distances indicate the left swath).



# SWOT products



**Mission requirements**  
 Slope accuracy: 1.7 cm/km  
 (averaging over water area > 1 km<sup>2</sup>)

Water surface profiles for the three considered scenarios: (blue) Hec-Ras and (red) SWOT water profiles estimated considering an averaging area of 1 km<sup>2</sup> and a ten-point moving average filter

	HR-slope (m/km)	SWOT-slope (m/km)	$\Delta$ slope SWOT-HR (cm/km)
Max flow	0.172	0.175	0.2573
Mean flow	0.0954	0.0855	0.9942
Min flow	0.0948	0.0608	3.394

# SWOT products

SWOT will provide measurements of **surface water elevation, slope, and water mask**

**SWOT level-2 data products will (likely) include:**

- For each pass a water mask with point cloud product with water elevation (and uncertainty)
- Once every repeat cycle: a global water mask following shorelines of observed water bodies in vector format (+ e.g., water elevation, wetted area, slope)
- Global one-dimensional vector product with estimated discharge along river reaches (wider than 50 m)
- Cross-sectional map of all observed water bodies derived from time-varying water elevations (yearly)

...in addition to this product SWOT will be able to characterize *changes in cross-sectional area*, as well as *channel morphology* through indices such as *sinuosity, meander length, and radius*, whereas the remaining variables, i.e., **velocity and depth, will have to be estimated.**

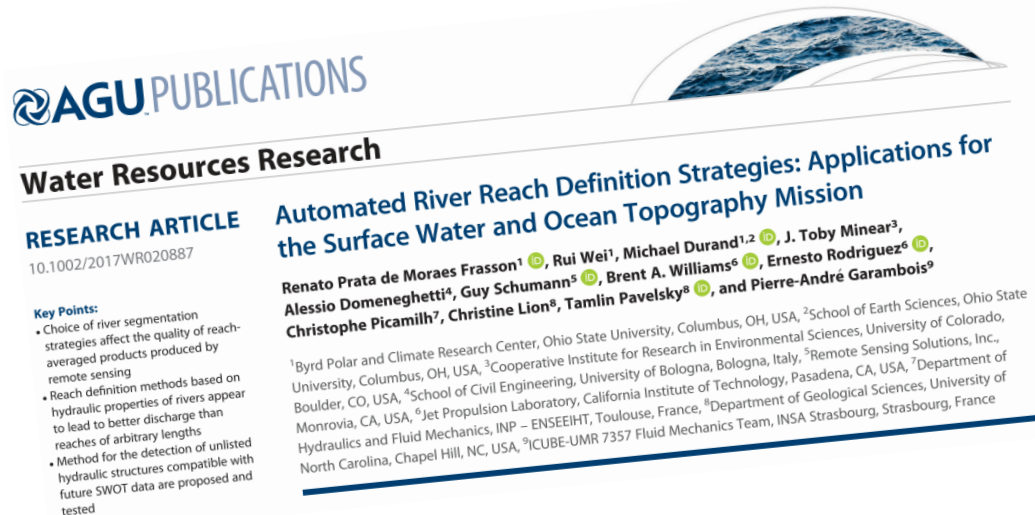
No real-time consideration for provision of SWOT data product

→ Derived product are expected to be provided within 60 days of their collection

# SWOT products

There are still many challenges regarding how to manage and process the observations.

**What is the best river reach definition strategies?**  
**How does this choice impacts on product accuracy?**  
**What is the accuracy on discharge estimation?**



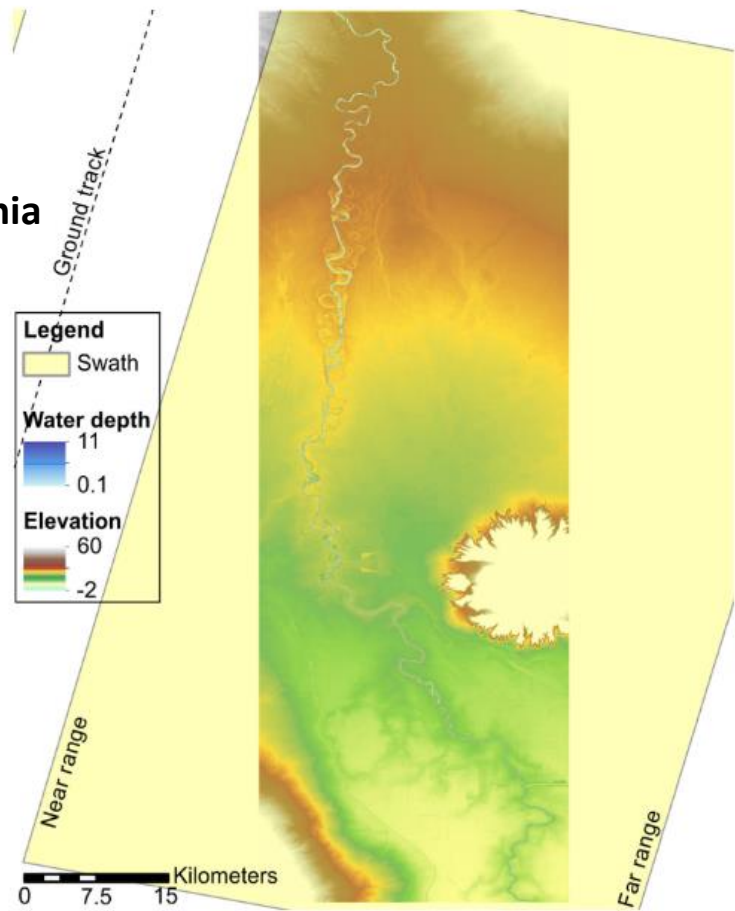
- Arbitrary lengths (es. 10km, 15km, etc.)
- River sinuosity
- Inflection points on the water surface profile

**How do height, width and slope errors propagate to discharge estimation?**

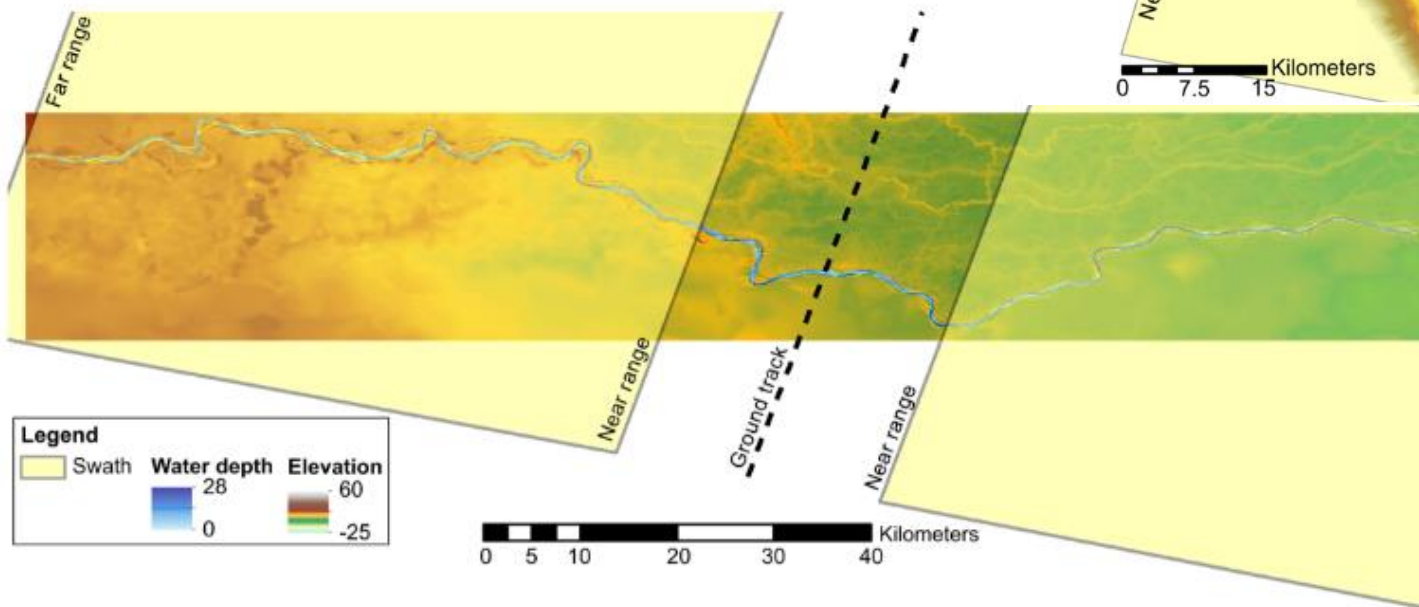
# SWOT products

## SACRAMENTO river - California

1-D hydraulic model ran for **6 months**, simulating discharges from 118 to 510 m<sup>3</sup>/s



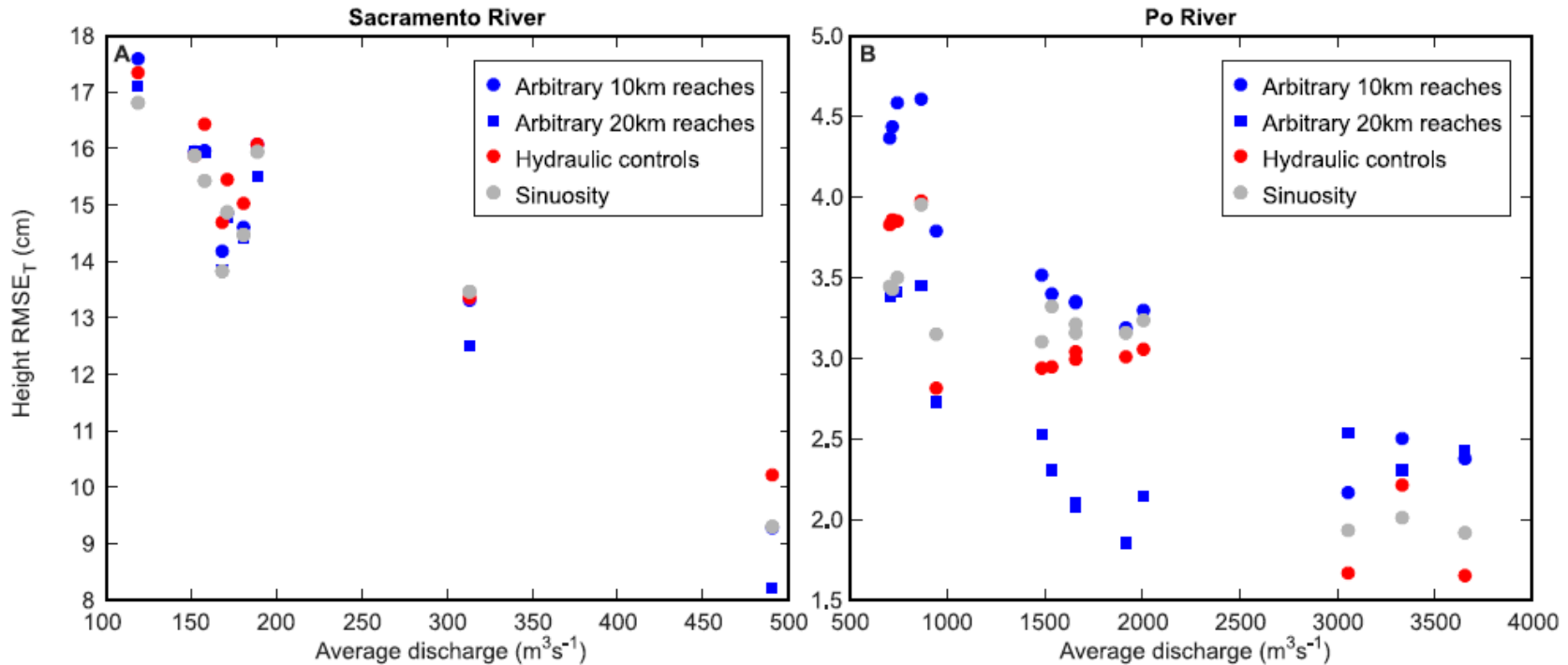
The hydraulic model of the Po River ran for **12 months**, simulating discharges from 711 to 4.770 m<sup>3</sup>/s



Po river - Italy

# SWOT products

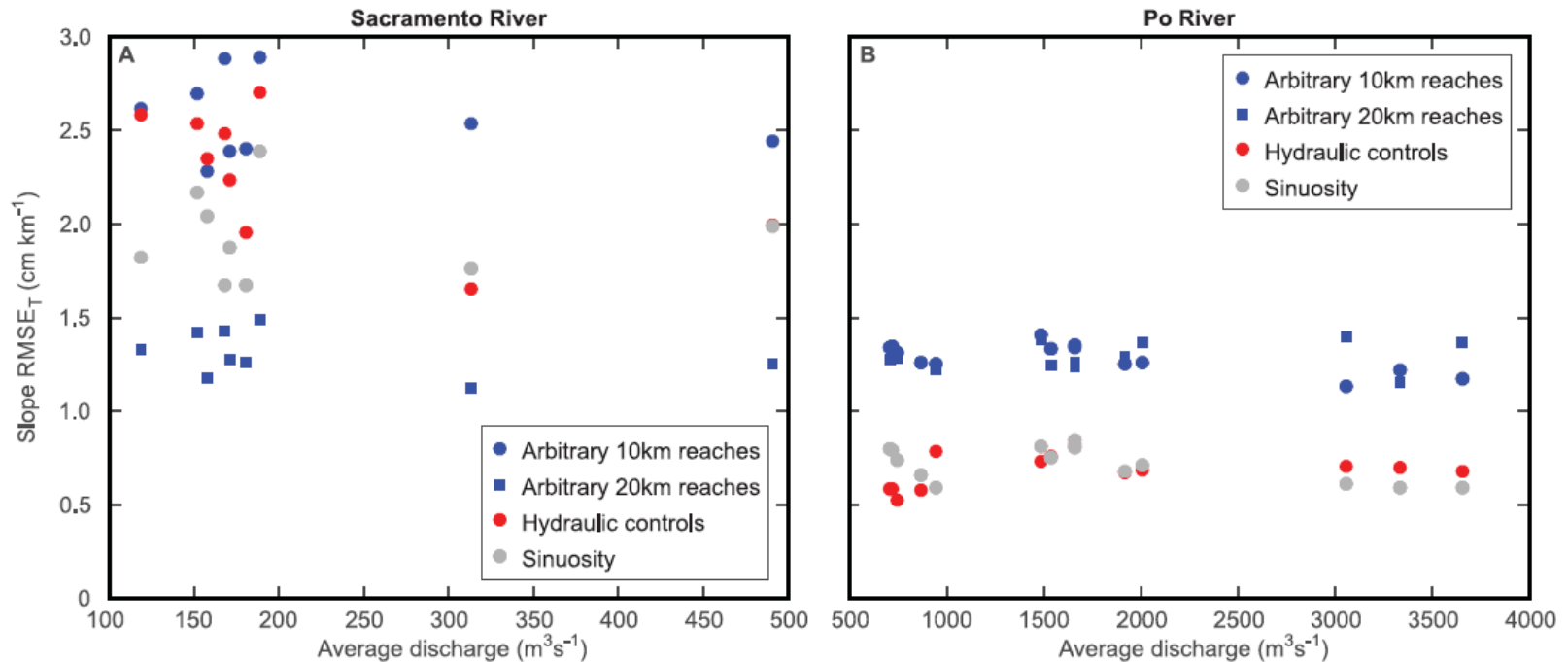
SWOT will provide an estimate of discharge by means of slope, river width and height





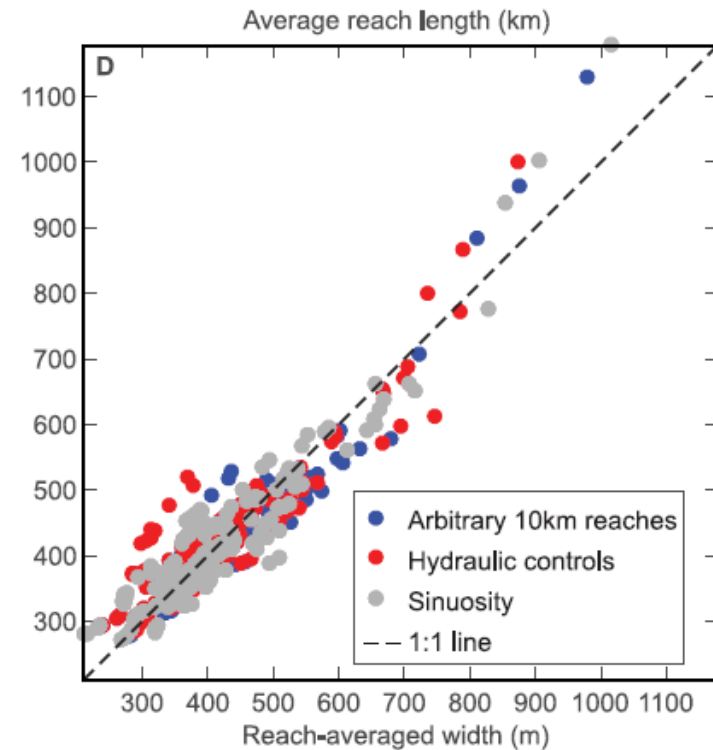
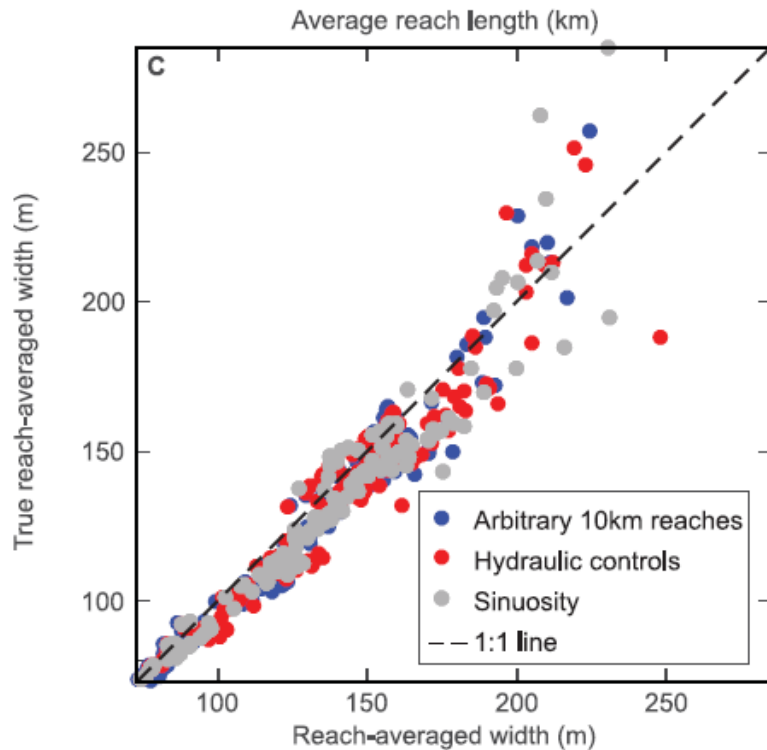
# SWOT products

SWOT will provide an estimate of discharge by means of slope, river width and water surface elevation



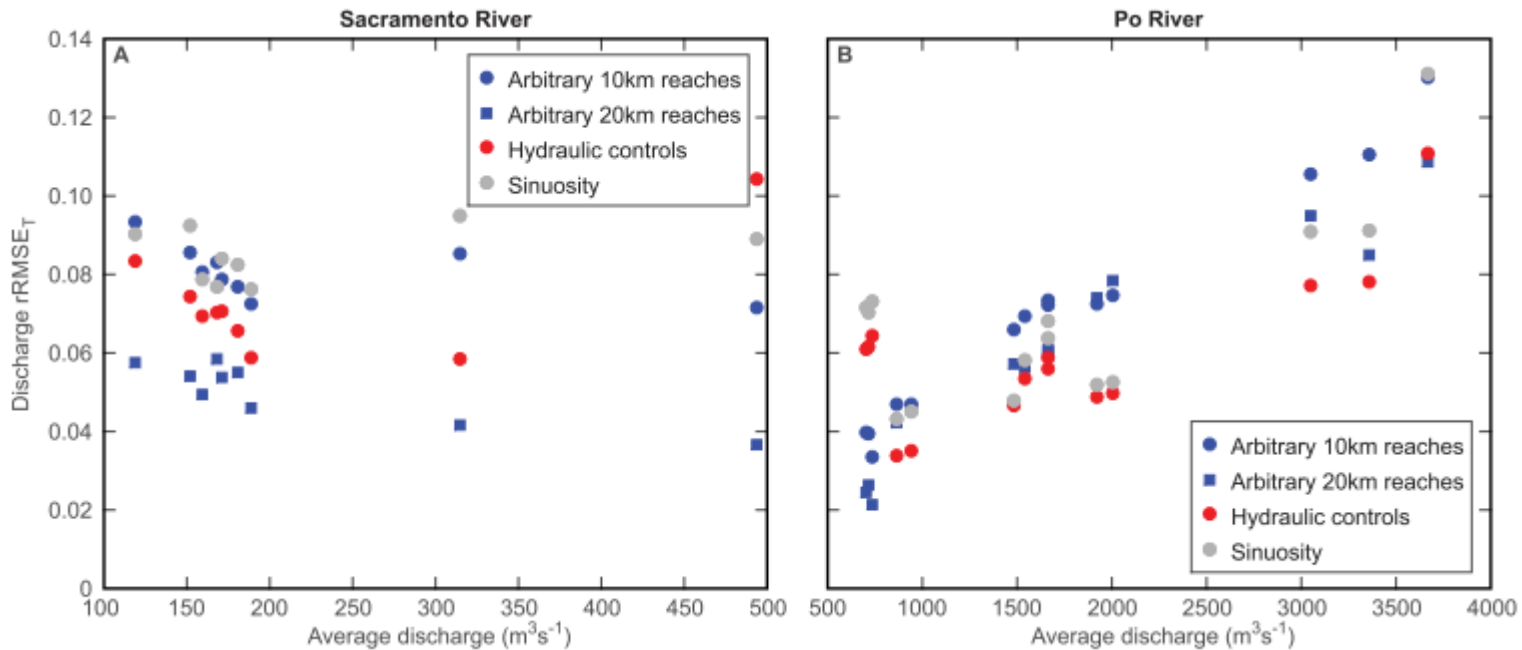
# SWOT products

SWOT will provide an estimate of discharge by means of slope, river width and water surface elevation



# SWOT products

Estimated discharge errors caused by the propagation of height, width, and slope errors through the discharge equation were often smaller for sinuosity (on average 8.5% for the Sacramento and 6.9% for the Po) and hydraulic control (Sacramento: 7.3% and Po: 5.9%) reaches than for arbitrary reaches of comparable lengths (Sacramento: 8.6% and Po: 7.8%).

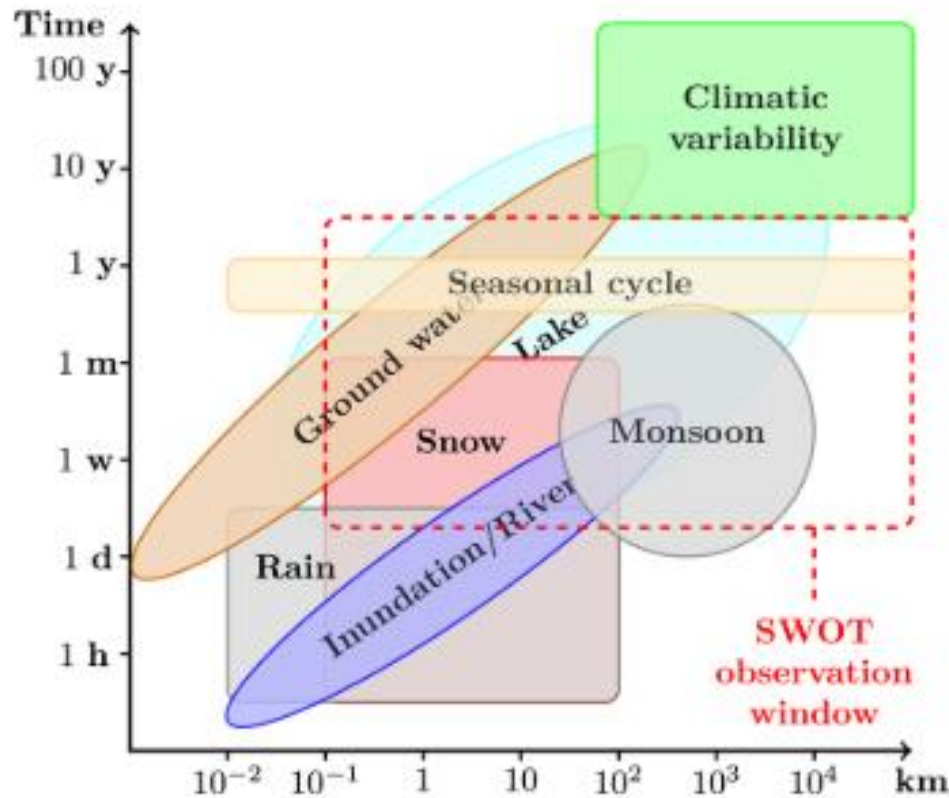


Hydraulic control method often leads to smaller discharge errors than arbitrary 10 km reaches, whereas the sinuosity method, despite its shorter reach lengths, led to discharge errors that were comparable to the arbitrary 10 km reaches.

For the Po River, both sinuosity and hydraulic control methods outperformed the arbitrary 20 km reaches in 9 out of the 14 evaluated overpasses

# APPLICATIONS

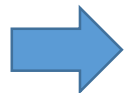
Biancamaria et al., 2016 (SG)



“Time–space diagram of continental water surface processes and SWOT observation window.”

- Discharge
- lakes and reservoirs
- Transboundary rivers
- Impact of human activities on hydrological cycle.
- Data for calibration and validation
- Stream-aquifer interactions
- Estuaries dynamics

To further investigate



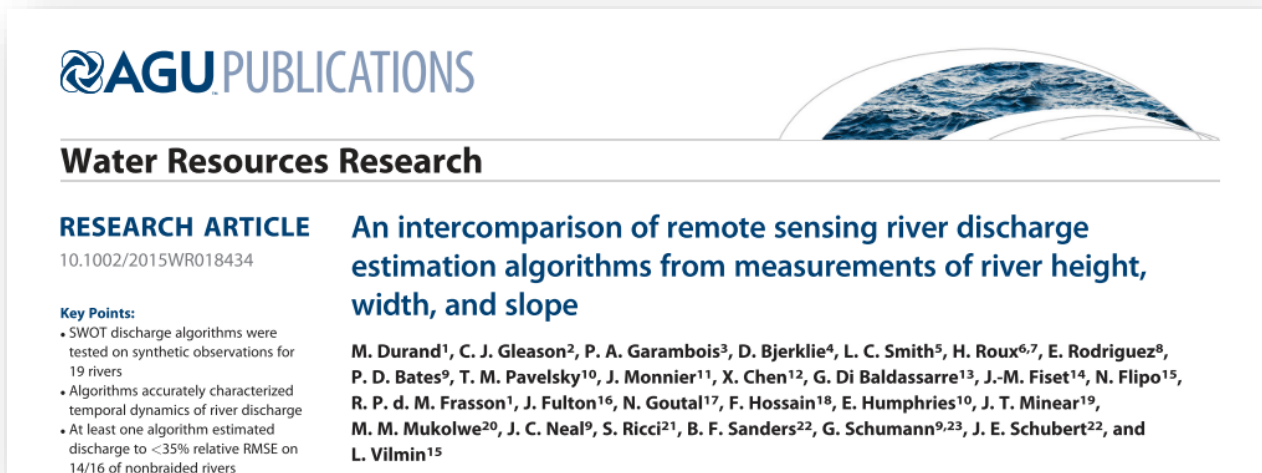
Algorithm Development for SWOT River Discharge Retrievals

<https://swot.jpl.nasa.gov/project-wood.htm>

# APPLICATIONS

## Discharge estimation

The literature provides a number of different methodologies to estimate the river discharge using different variables combinations and assumptions...few examples: Smith et al., 1996; Smith, 1997; Bjerklie et al., 2003, 2005; Kouraev et al., 2004; Dingman and Bjerklie, 2006; Bjerklie, 2007; Birkinshaw et al., 2010; Michailovsky et al., 2012, Durand et al, 2016, Hagemann et al., 2017, ...



Durand et. al., 2016 (WRR)

**Other methodologies (not considered here) are available.** Among those: Data-Assimilation (DA) [Oubanas et al., 2018 (WRR)], «inverse routing» [Pan and Wood, 2013 (HESS)], Bayesian AMHG [Hagemann et al., 2017 (WRR)].

**1)** at-many-stations hydraulic geometry (AMHG) method [Gleason and Smith, 2014; Gleason et al., 2014]; **2)** GaMo [Garambois and Monnier, 2015], **3)** MetroMan [Durand et al., 2014], and **4)** the novel mean flow and geomorphology (MFG) and **5)** the mean flow and constant roughness (MFCR) algorithms, in addition to **6)** an ensemble median product.

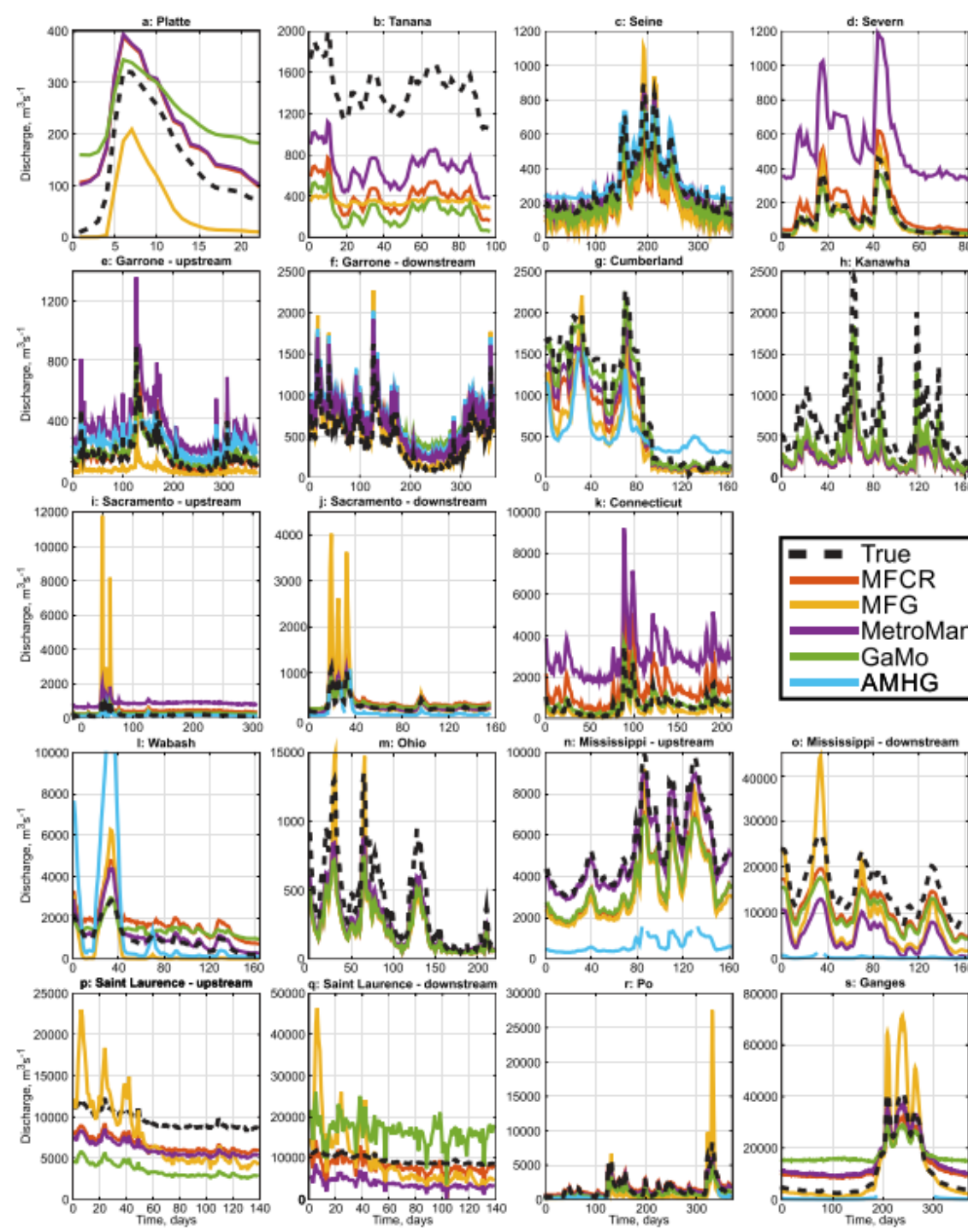
# APPLICATIONS

**Table 3.** Summary of Discharge Algorithms

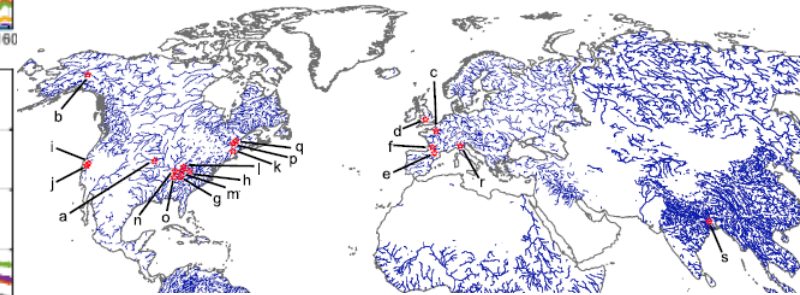
Algorithm	Theoretical Basis	Applied Variables From Observation	Estimated Variables	Variable Estimation Method
AMHG	At-many-stations hydraulic geometry	Water surface width ( $W$ )	$a, b$	$a$ and $b$ are optimized to preserve continuity between stations using a genetic algorithm
GaMo	Manning flow resistance equation (equation (4))	Change in cross-sectional area of flow ( $\delta A$ ) computed from the mean width and change in water surface height ( $\delta H$ , stage), water surface slope ( $S$ ) for several reaches	Flow resistance ( $n$ ) and cross-sectional area of channel at zero flow ( $A_0$ )	$A_0$ and $n$ are both optimized to preserve continuity between the observed reaches using a constrained, nonlinear steepest-descent optimization
MetroMan	Manning flow resistance equation (equation (4))	Change in cross-sectional area of flow ( $\delta A$ ) computed from the mean width and change in water surface height ( $\delta H$ , stage), water surface slope ( $S$ ) for several reaches	Flow resistance ( $n$ ) and cross-sectional area of channel at zero flow ( $A_0$ )	$A_0$ and $n$ are both optimized to preserve continuity between the observed reaches (must be three or more) using the Metropolis algorithm
MFG	Manning flow resistance equation (equation (5))	Water surface width ( $W$ ), water surface slope ( $S$ ), and water surface height ( $H$ , stage) for the reach	Flow resistance ( $n$ ) and height (stage) of zero flow ( $B$ )	$n$ is estimated from an empirical relation between its mean value and slope, and then adjusted based on an empirical relation between the change in river cross section. $B$ is calibrated to an estimate of the mean annual discharge for the time series
MFCR	Manning flow resistance equation (equation (4))	Water surface width, water surface slope, water surface height (stage) for the reach	Cross-sectional area of channel at zero flow ( $A_0$ )	Flow resistance is assumed constant at 0.03, an estimate of the mean annual discharge is used to calibrate $A_0$ for the time series

Tested on 19 rivers worldwide spanning a range of hydraulic and geomorphic conditions (data extracted from hydraulic models)

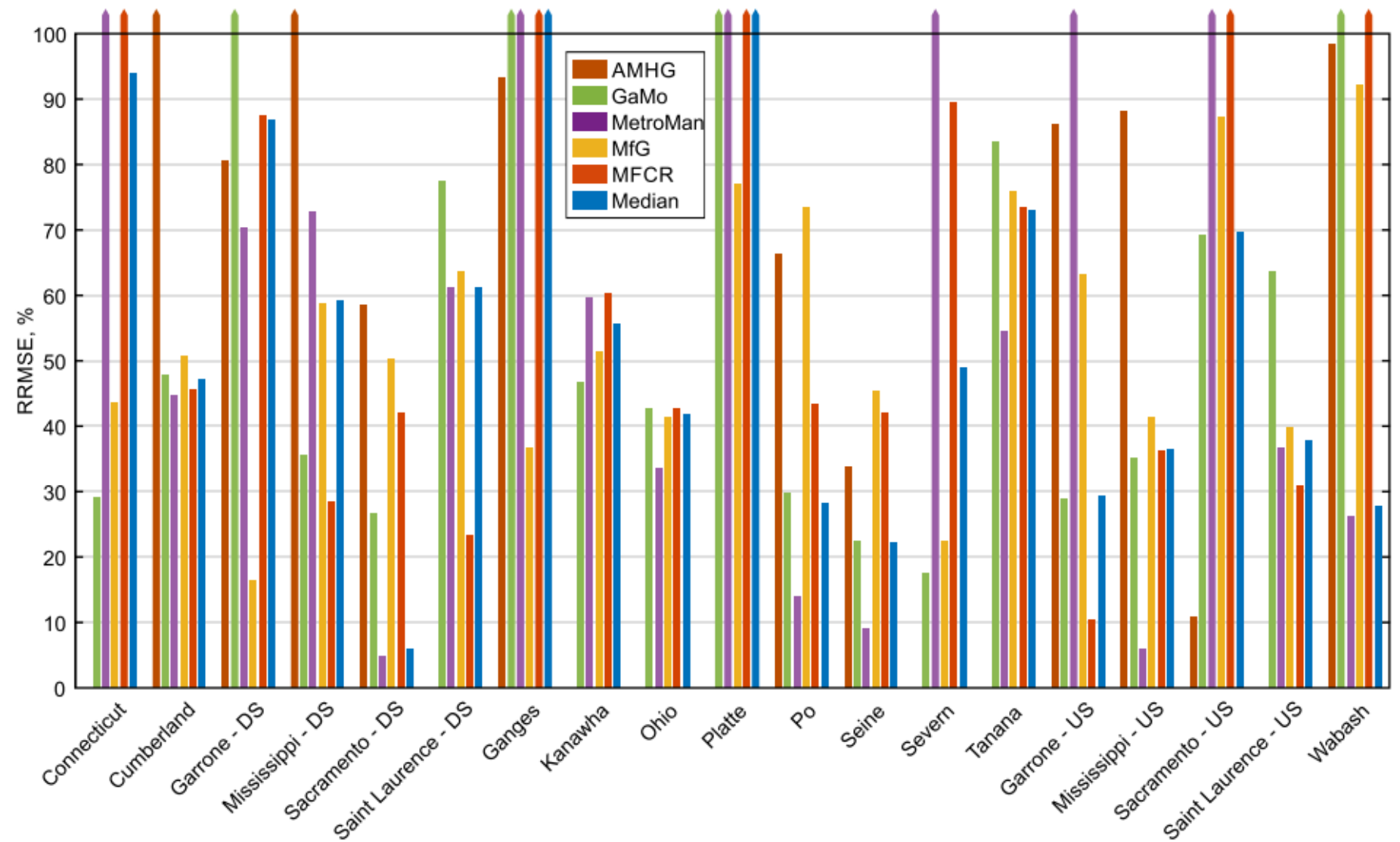
# APPLICATIONS



They found at least one algorithm able to estimate instantaneous discharge to within 35% relative root-mean-squared error (RRMSE) on 14/16 non-braided rivers despite out-of-bank flows, multichannel planforms, and backwater effects.



# APPLICATIONS





# Flow Duration Curve from Satellite: Potential of a Lifetime SWOT Mission

Alessio Domeneghetti <sup>1,\*</sup>, Angelica Tarpanelli <sup>2</sup>, Luca Grimaldi <sup>3</sup>, Armando Brath <sup>1</sup> and Guy Schumann <sup>3,4</sup>

<sup>1</sup> DICAM—University of Bologna, Viale del Risorgimento, 2, 40136 Bologna, Italy; luca.grimaldi@studio.unibo.it (L.G.); armando.brath@unibo.it (A.B.)

<sup>2</sup> Research Institute for Geo-Hydrological Protection, National Research Council, Via Madonna Alta 126, 06128 Perugia, Italy; angelica.tarpanelli@irpi.cnr.it

<sup>3</sup> School of Geographical Sciences, University of Bristol, University Road, Bristol BS81SS, UK; gjschumann@gmail.com

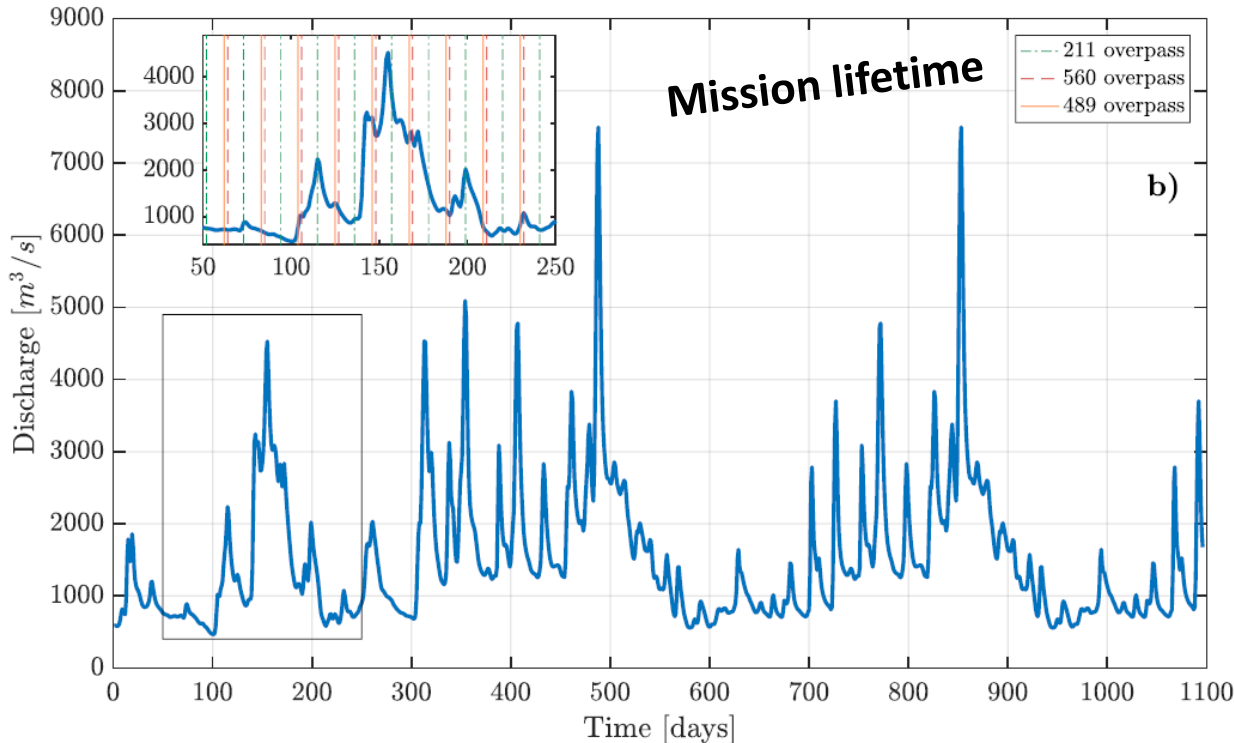
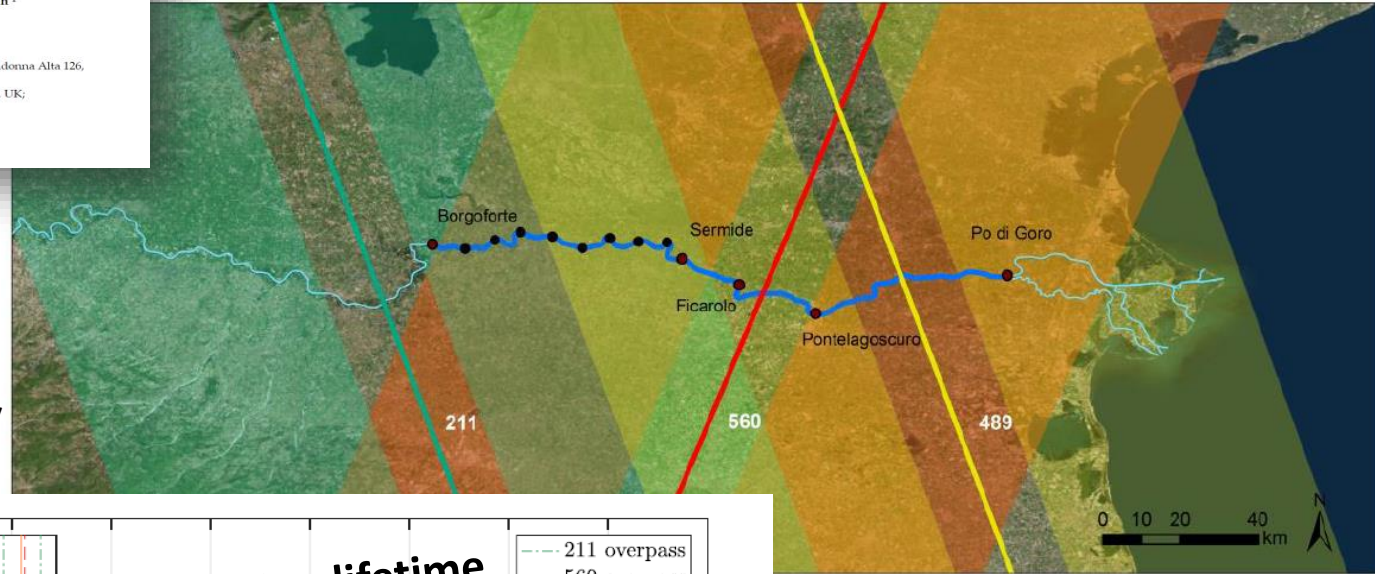
<sup>4</sup> Remote Sensing Solutions Inc., 248 E. Foothill Blvd, Monrovia, CA 91016, USA

\* Correspondence: alessio.domeneghetti@unibo.it; Tel.: +39-051-209-3355

Received: 1 June 2018; Accepted: 10 July 2018; Published: 11 July 2018

# APPLICATIONS

total number of satellite overpasses: 52, 53, and 52 referring to orbit 489, 560 and 211, respectively



Flow hydrograph at the gauging station of Sermide (blue lines) in the period 2008–2010: vertical lines represent an example of the timing of the SWOT overpasses during a short period.

# APPLICATIONS

## Discharge estimation

$$Q_{ij} = \frac{1}{n} A_{ij}^{5/3} w_{ij}^{-2/3} S_{ij}^{1/2}$$

### Manning equation

- J (friction slope) = S (surface slope)
- Large rectangular shape
- j = j-th day of SWOT pass
- i = i-branches of length  $\Delta x$

average value of the minimum wet areas recorded for the i-th branch during the entire period of study

Wetted Area, A

$$A_{ij} = A_{i0} + \delta A_{ij}$$

$$\delta A_{ij} = \frac{w_{i0} + w_{ij}}{2} (y_{ij} - y_{i0})$$

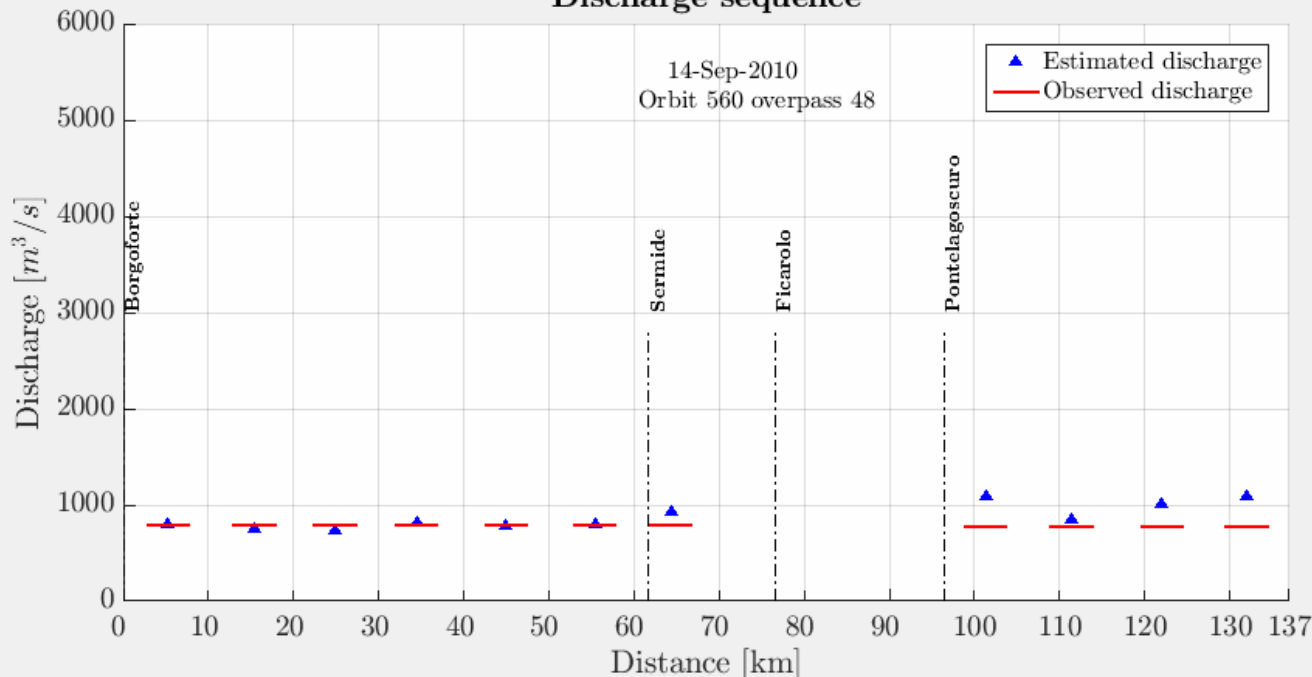
Surface Slope, S

$$y = S \cdot x + x_0$$

$$\hat{Q}_{ij} = \frac{1}{n} (A_{i0} + \delta \hat{A}_{ij})^{5/3} \hat{w}_{ij}^{-2/3} \hat{S}_{ij}^{1/2}$$

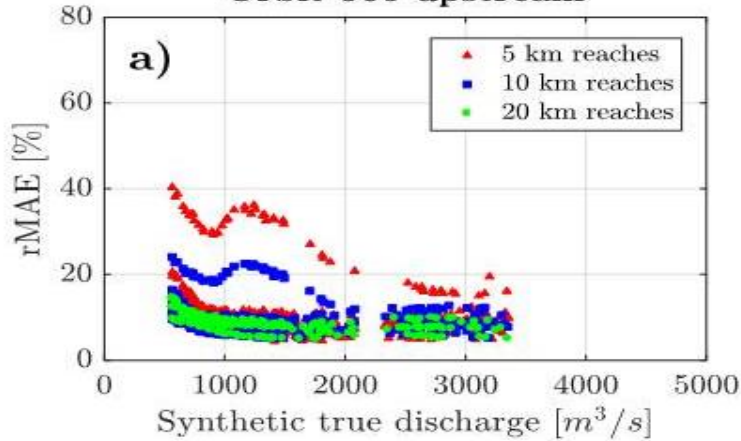
Values corrupted with Gaussian random errors (mission requirements)

Discharge sequence

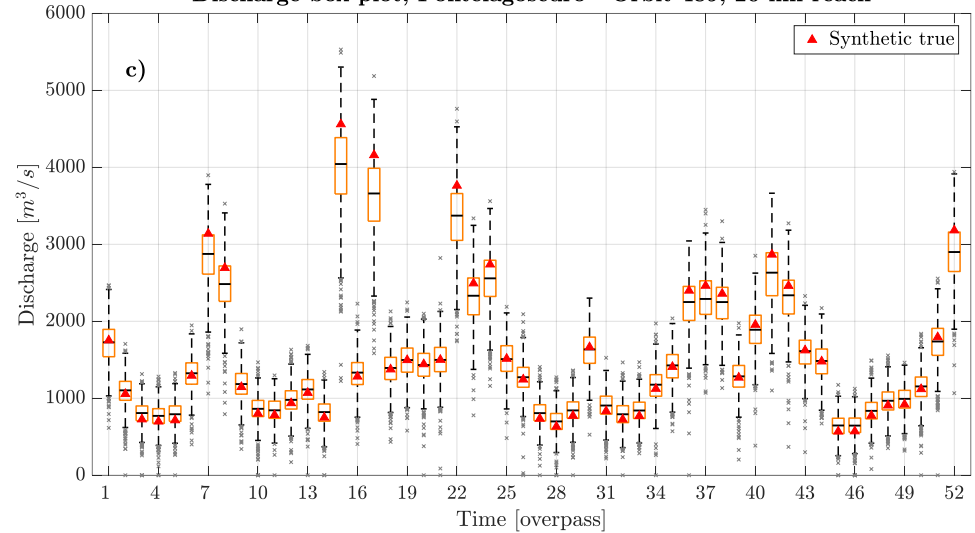


# APPLICATIONS

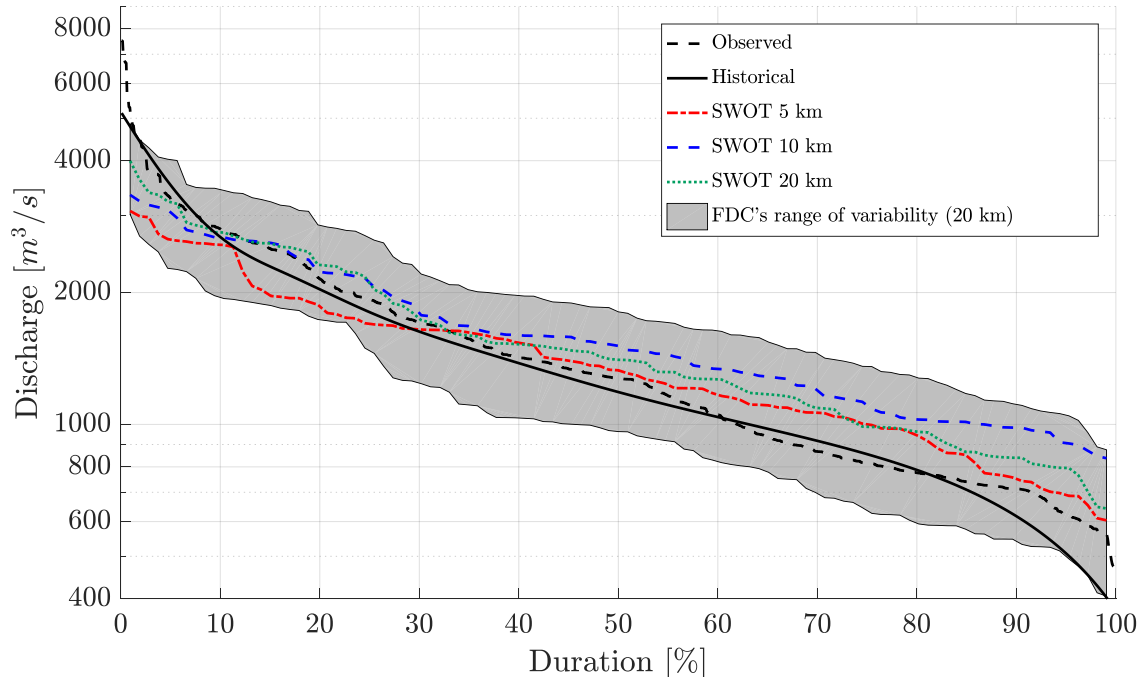
Orbit 560 upstream



Discharge box plot, Pontelagoscuro - Orbit 489, 20 km reach



Flow Duration Curve (Pontelagoscuro)



FDCs at the gauging station of Pontelagoscuro for the three-year period based on observed daily data (black dashed line) and estimated from SWOT-like observations, considering different river discretizations; grey area represents the 90% confidence interval of streamflow estimation with  $\Delta x = 20$  km; black solid lines show FDCs based on historical data recorded at the gauging stations.

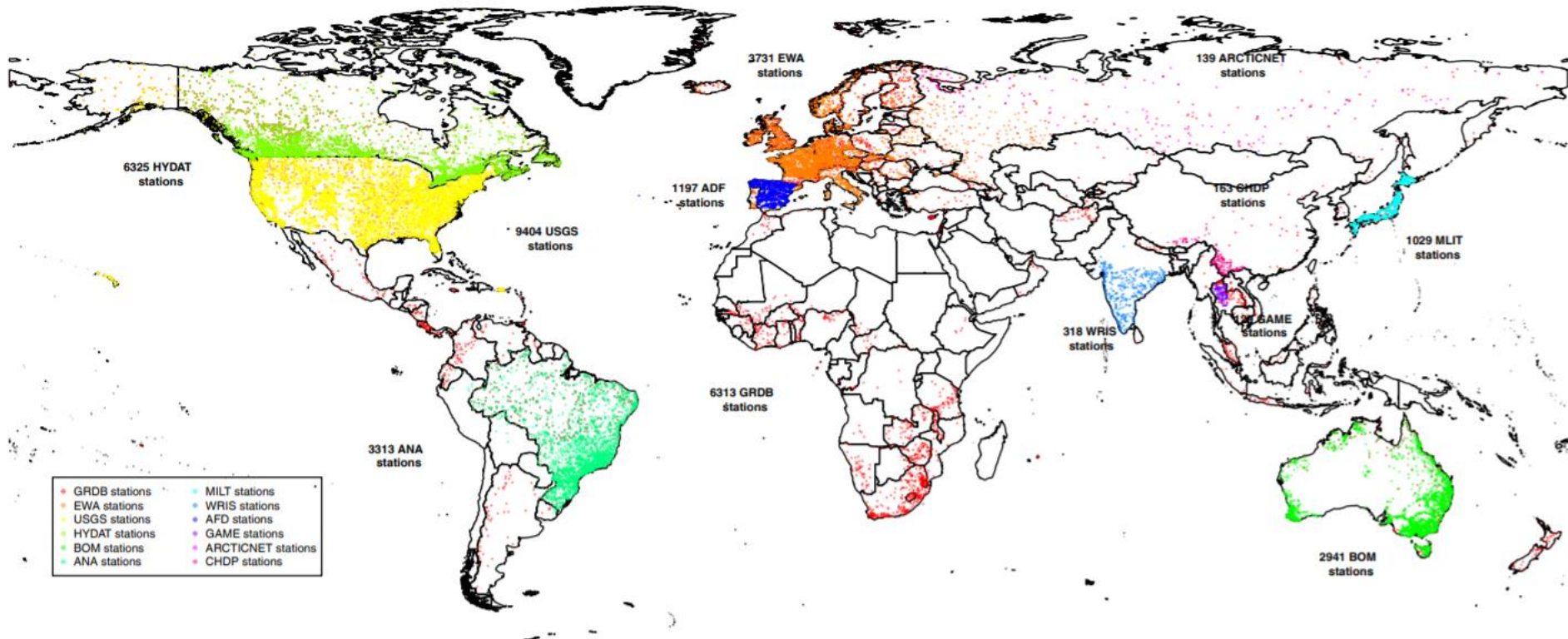


# **(NO) CONCLUSIONS**

**Many hydrologic dataset (global or nearly global) are getting available**

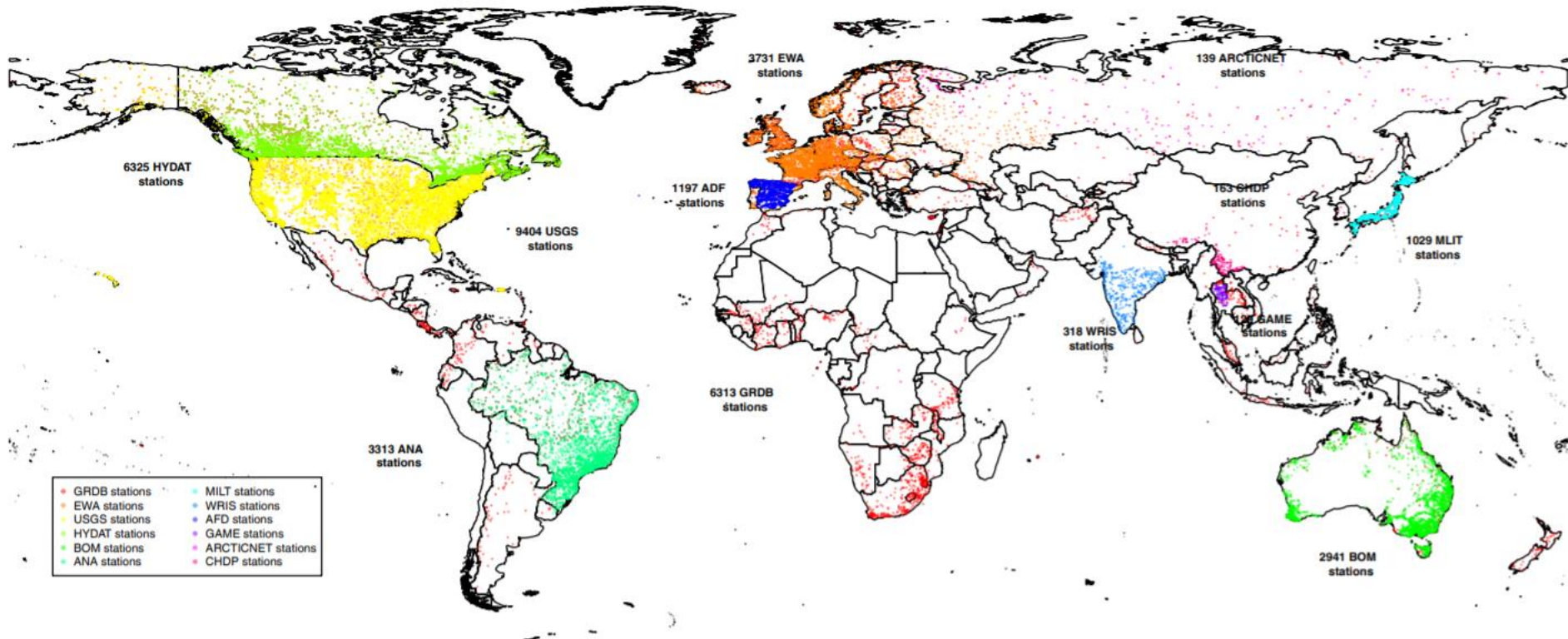
Global Streamflow Indices and Metadata Archive (GSIM) – Part 1 and Part 2

# (NO) CONCLUSIONS



PART 1: station name, river name, coordinates, elevation, drainage area, catchment boundary, catchment metadata such as land cover type, soil type, and climate and topographic characteristics

# (NO) CONCLUSIONS



PART 2: a collection of daily streamflow observations at more than 30000 stations around the world. Part 2 introduces a set of quality controlled time-series indices representing (i) the water balance, (ii) the seasonal cycle, (iii) low flows and (iv) floods

# (NO) CONCLUSIONS

**Many hydrologic dataset (global or nearly global) are getting available**

Global Streamflow Indices and Metadata Archive (GSIM) – Part 1 and Part 2

Global extent of rivers and streams (Allen, G. H., & Pavelsky, T. M., 2018).

Global river slope: A new geospatial dataset and global-scale analysis (Cohen et al., 2018 JH)

**More accurate and “hydrologically meaningful” topographic data are coming out (see MERIT and HydroMERIT)**

...the same for observations useful for model calibration and validation (see e.g., rainfall patterns, altimetry, satellite-derived inundation extent...)

...new models with higher computational efficiency

**But with some drawbacks... in terms of uncertainties and accuracy in both data and large scale model results**



# THANKS FOR YOUR ATTENTION



ALMA MATER STUDIORUM  
UNIVERSITÀ DI BOLOGNA

Alessio Domeneghetti

[alessio.domeneghetti@unibo.it](mailto:alessio.domeneghetti@unibo.it)

DICAM - Dipartimento di Ingegneria Civile, Chimica,  
Ambientale e dei Materiali

*[www.dicam.unibo.it](http://www.dicam.unibo.it)*